



# THE UNIVERSITY *of* EDINBURGH

This thesis has been submitted in fulfilment of the requirements for a postgraduate degree (e.g. PhD, MPhil, DClinPsychol) at the University of Edinburgh. Please note the following terms and conditions of use:

- This work is protected by copyright and other intellectual property rights, which are retained by the thesis author, unless otherwise stated.
- A copy can be downloaded for personal non-commercial research or study, without prior permission or charge.
- This thesis cannot be reproduced or quoted extensively from without first obtaining permission in writing from the author.
- The content must not be changed in any way or sold commercially in any format or medium without the formal permission of the author.
- When referring to this work, full bibliographic details including the author, title, awarding institution and date of the thesis must be given.

**Polymer Microarrays for Cell  
Based Applications**

by

Anne Hansen

Thesis for the Degree of Doctor of Philosophy

The University of Edinburgh

2012

## ***Abstract***

The development and identification of new biomaterials that can replace specific tissues and organs is desirable. In the presented PhD thesis polymer microarrays were applied for the screening of polyacrylates and polyurethanes and evaluation for material discovery for applications in the life sciences.

In the first part of the thesis, the largest polymer microarray ever made with more than 7000 features was fabricated and subsequently used for the screening of polyacrylates that can control the fate of human embryonic stem cells. As stem cells have unique properties that offer the potential of replacing damaged or diseased tissue in future, the identification of cultivation substrates that can replace current biological and animal derived products was desirable. The water contact angle, roughness and cell doubling time of the cells on the identified polymers was determined and the stem cells characterised after 5 passages and compared to the currently most widely used animal derived substrate Matrigel<sup>TM</sup>.

In the second part of the thesis, the development of a new polymer gradient microarray is presented. Initial studies involved the optimisation of printing parameters for the generation of linear polymer gradient lines and confirmed by XPS analysis. Cellular binding studies with the suspension cell line K562 and the adherent cell line HeLa were carried out and compared to previous binding studies to confirm the success of the concept. In further studies, the polymer gradients were functionalised with small molecules and proteins, allowing the generation of a protein gradient microarray with Semaphorin 3F. In binding studies with neuron cells it could be shown that the binding of the cells was concentration-dependent.

The identification of polyacrylates for the effective and rapid activation and aggregation of platelets is described in the third part of the presented thesis. Here, polymer microarrays were applied for the binding of platelets in human blood samples. The amount of bound platelets as well as their activation state was compared to the natural agonist collagen by employing fluorescence intensity studies and scanning electron microscopy. In shear studies, the activation of the platelets by the polymers was evaluated under physiological conditions. The mechanism by which the polymer triggered the activation was further explored by protein binding studies. It was shown that the initial adsorption of fibrinogen and von Willebrand factor on the polymers lead to the adherence and aggregation of platelets.

In the final part of the presented thesis, polymer microarrays were used to identify polymers that can sort and collect the precursor cells of platelets (megakaryocytes). For this purpose, the cell lines K562 and MEG-01 were used as cellular models. The identified polymers and the effect on the immobilised cells was further investigated by scanning electron microscopy, flow cytometry and miRNA studies. The adsorbed proteins on the different polymers were found to influence the cellular morphology on the different substrates.

# ***Table of Contents***

<b>ABSTRACT .....</b>	<b>I</b>
<b>TABLE OF CONTENTS.....</b>	<b>II</b>
<b>DECLARATION OF AUTHORSHIP.....</b>	<b>VI</b>
<b>ACKNOWLEDGEMENTS.....</b>	<b>VII</b>
<b>ABBREVIATIONS .....</b>	<b>IX</b>
<b>CHAPTER 1: INTRODUCTION .....</b>	<b>1</b>
1.1 BIOMATERIALS AND BIOCOMPATIBILITY .....	1
1.2 HIGH-THROUGHPUT SCREENING OF BIOMATERIALS .....	3
1.2.1 <i>Microarrays as Tool for HTS</i> .....	4
1.3 PRINTING TECHNIQUES.....	5
1.3.1 <i>Contact Printing Approach</i> .....	5
1.3.2 <i>Inkjet Printing Approach</i> .....	9
1.4 TYPES OF MICROARRAYS .....	11
1.4.1 <i>DNA Microarrays</i> .....	11
1.4.2 <i>Protein Microarrays</i> .....	12
1.4.3 <i>Polymer Microarrays</i> .....	12
<b>AIM OF THE THESIS .....</b>	<b>15</b>
<b>CHAPTER 2: HIGH-DENSITY POLYMER MICROARRAYS: IDENTIFYING SYNTHETIC SUBSTRATES TO CONTROL STEM CELL FATE .....</b>	<b>16</b>
2.1 TYPES OF POLYMER MICROARRAYS .....	16
2.2 STEM CELLS .....	17
2.3 EMBRYONIC STEM CELLS.....	18
2.4 CURRENT SUBSTRATES FOR STEM CELL CULTIVATION WITHOUT FEEDER LAYER CELLS .....	20
2.5 FABRICATION OF HIGH-DENSITY POLYMER MICROARRAYS .....	22

2.6 CONCLUSION .....	34
<b>CHAPTER 3: FABRICATION OF ARRAYS OF POLYMER GRADIENTS USING INKJET PRINTING.....</b>	<b>35</b>
3.1 CURRENT GRADIENT FABRICATIONS VIA PRINTING TECHNIQUES .....	36
3.2 CELLULAR MIGRATION .....	39
3.3 SEMAPHORINS AS CHEMOATTRACTANTS/CHEMOREPELLENTS IN CELLULAR MIGRATION .....	41
3.4 GENERATION OF MICROARRAYS WITH POLYMER GRADIENT LINES (COMPOSITION GRADIENTS) .....	43
3.5 CELLULAR BINDING STUDIES ON POLYMER GRADIENT ARRAYS .....	50
3.6 GENERATION OF MOLECULE GRADIENTS (CONCENTRATION GRADIENTS).....	53
3.7 GENERATION OF A SEMAPHORIN HAPTOTAXIS ARRAY FOR OGPCs .....	54
3.8 CONCLUSION .....	59
<b>CHAPTER 4: POLYMERS FOR PLATELET ACTIVATION AND SORTING OF MEGAKARYOCYTIC CELL LINES.....</b>	<b>60</b>
4.1 PLATELETS - A SPECIAL TYPE OF CELL .....	61
4.2 PLATELET FORMATION.....	61
4.3 PLATELET ACTIVATION .....	62
4.4 CURRENT HAEMOSTATS .....	66
4.5 IDENTIFICATION OF PLATELET ACTIVATING POLYMERS APPLYING POLYMER MICROARRAY TECHNOLOGY.....	68
4.6 ANALYSIS OF ACTIVATION STATE IN STATIC AND FLOW EXPERIMENTS .....	74
4.7 ACTIVATION MECHANISM OF POLYMERS .....	80
4.8 CONCLUSIONS FOR PLATELET ACTIVATION .....	83
4.9 MEGAKARYOCYTIC CELL LINES.....	84
4.10 POLYMERS SORTING MEGAKARYOCYTIC CELL LINES .....	86
4.11 MORPHOLOGY AND PROTEIN BINDING STUDIES.....	89
4.12 INFLUENCE ON MATURATION AND GENE REGULATION.....	91

4.13 CONCLUSION FOR SORTING OF MEGAKARYOCYTIC CELLS.....	96
<b>CHAPTER 5: EXPERIMENTAL .....</b>	<b>97</b>
5.1 GENERAL INFORMATION .....	97
5.1.1 Equipment.....	97
5.1.2 Microscope Slides and Coverslips.....	98
5.1.3 Chemicals and Solvents .....	98
5.1.3 Polymer Libraries.....	98
5.2 EXPERIMENTAL FOR CHAPTER 2.....	100
5.2.1 Preparation of Acrylate Functionalised Masks .....	100
5.2.2 Inkjet Printing for In Situ Formation of Polymer Spots.....	100
5.2.3 Preparation of Polymer Coated Coverslips.....	101
5.2.4 Scanning Electron Microscopy (SEM) and energy dispersive X-ray spectroscopy (EDX) .....	101
5.2.5 Water Contact Angle Measurements .....	102
5.2.6 Atomic Force Microscopy.....	102
5.2.7 Cell Culture .....	103
5.2.8 Cell population Doubling Time .....	104
5.2.9 Immunocytochemistry of hESCs on Polymer Coverslips .....	104
5.2.10 Flow Cytometry Analysis.....	105
5.3 EXPERIMENTAL FOR CHAPTER 3.....	106
5.3.1 Preparation of Masked Glass Slides.....	106
5.3.2 Inkjet Printed Gradients .....	106
5.3.3 X-Ray Photoelectron Spectroscopy.....	107
5.3.4 Cell Culture .....	107
5.3.5 Image Acquisition and Analysis.....	108
5.3.6 Modification of Gradients with 6-Aminofluorescein.....	109
5.3.7 Modification of Gradients with Semaphorin 3F .....	109

5.3.8 Protein Gradient Verification: Fluorescence Intensity Measurement .....	110
5.4 EXPERIMENTAL FOR CHAPTER 4.....	111
5.4.1 Platelets and Red Blood Cells .....	111
5.4.2 Polymer Microarray Fabrication .....	111
5.4.3 Static Microarray PRP Studies and Fluorescence Microscopy.....	112
5.4.4 Upscale of Polymers on Coverslips .....	113
5.4.5 Scanning Electron Microscopy.....	113
5.4.6 Shear Studies on the Cone and Platelet Analyser.....	114
5.4.7 Statistics.....	114
5.4.8 Megakaryocytic Cell Culture.....	115
5.4.9 Polymer Microarray Studies.....	115
5.4.10 Proteinbinding on Polymer SDS-Page and MS analysis .....	116
5.4.11 Flow Cytometry .....	117
5.4.12 miRNA Array Profiling .....	117
<b>CHAPTER 6: REFERENCES .....</b>	<b>119</b>
<b>APPENDICES .....</b>	<b>I</b>
POLYACRYLATE LIBRARY .....	V
POLYURETHANE LIBRARY .....	XXVIII
PUBLISHED PAPERS .....	XLI

## ***Declaration of Authorship***

The research described in this thesis was carried out by the author under the supervision of Prof. Mark Bradley at the University of Edinburgh between January 2009 and June 2012. The presented work has been either carried out by the author herself or if the work has been part of any collaboration, the candidate has made a substantial contribution to the work and it is clearly indicated when another researcher has mainly contributed to the work.

The work has not been submitted for any other degree or professional qualification except for the work contributed by Jonathan Murnane (Chapter 3), which has been part of his final Master of Science dissertation in Neuroscience at the University of Edinburgh in 2011. The title of his thesis is: “Response of microglia to the guidance molecules Semaphorin 3A and 3F and the development of a novel migration assay”.

Parts of the presented work in this thesis have been published in the scientific literature or are currently prepared for submission:

- A. Hansen, L. McMillan, A. Morrison, J. Petrik, M. Bradley; Polymers for the rapid and effective activation and aggregation of platelets. *Biomaterials* **2011**, 32, 7034-7041.
- A. Hansen, R. Zhang, M. Bradley; Fabrication of arrays of polymer gradients using inkjet printing. *Macromol. Rapid Commun.* **2012**, DOI: 10.1002/marc.201200193.
- A. Hansen, H. Mjoseng, R. Zhang, M. Kalloudis, V. Koutsos, P. de Sousa, M. Bradley; High-density polymer microrrays - identifying synthetic substrates to control stem cell fate. *In preparation*.
- A. Hansen, S. Corless, J. Petrik, N. Gilbert, M. Bradley; Controlling morphology and immobilisation of megakaryocytic cell lines. *In preparation*.



## ***Acknowledgements***

First of all I would like to thank Professor Mark Bradley for giving me the opportunity to carry out my PhD in his laboratory and for his constant support and advise.

Moreover, I would like to thank all members of Ilika Ltd who sponsored my research and who gave me constantly more ideas when presenting my work.

My collaborators, without whom most of the cell work would have not been possible, should be also thanked at this place:

Dr. Paul de Sousa and his team, especially Heidi K. Mjoseng, who have allowed me to work at their facilities and who have helped me with the human embryonic stem cell work.

Dr. Vasilios Koutsos, Dr. Sefiane and Mike Kalloudis for providing me with lovely AFM pictures when the chemistry's own instrument was not working and who also allowed me to measure the water contact angle at their place.

Dr. Anna Williamson and MSc Jonathan Murnane who have been very enthusiastic about the polymer gradients and who have carried out the neuron cell work on the polymer gradient arrays.

Dr. Loraine McMillan, Dr. Alex Morrison and, in particular, Dr. Juraj Petrik and his team who were the best support I could have imagined for the platelet studies. Without their enthusiasm for this work and their questions and advice, I would have never come that far!

I would also like to thank all members of the Bradley group who have made me feel welcome. Especially, Dr. Rong Zhang who has been a great support when it came to the invention of new polymer microarray formats and all technical up and downs that are part of a PhD. I wish you all the best for your career in China!

Also, I would like to thank Salvatore, Mei, Albert and Graham who have introduced me to the work on polymermicroarrays and printer "Susie" at the beginning of my PhD. And I hope that "Superman" Christian and Alison will enjoy working on this topic in the future as well!

Thanks also to the “biolabgirls” Nana, Emma, Geraldine, Rosario and Nina who have been a great support with all kind of cell work. A special thanks goes here to our “muscle man” Juanma, who has been a gentleman and carried the nitrogen tanks back and forth....

I would also like to thank Jeff for taking care of me in times of needs and trouble.

My undergraduate students Johanna, Julia and Tom who have worked with me on diverse projects and gave me lessons in Spanish and karate should also be mentioned here. Even though their work is not part of this very thesis, I would like to thank them for all their effort and work - I wish you all the best for your future!

Moreover, I would like to thank all my friends in Edinburgh and all over the world who have always made me laugh when it was absolutely needed. Thanks to Matt and Martha; my dancing partners TJ (a natural talent!), funny Dan and Mr. Grumpy; my coffee Greeks, my cooking and hiking mates Emma, Nana, Martin and Cairnan, my home support Julia, Storki, Maike, Dirk, Cathy, Nora and Abue, my sis Shu and big bro Nick!

Last but not least, I would like to thank my family for all their love and support throughout the whole time. And, of course, Frank who has been the best support I could have ever wished for.

## **Abbreviations**

A.U.	Arbitrary units
ADP	Adenosine diphosphate
AFM	Atomic force microscopy
ANOVA	Analysis of variance
BA	<i>tert</i> -Butyl acrylate
BCA	<i>tert</i> -Butylcyclohexyl acrylate
bFGF	Basic fibroblast growth factor
BSA	Bovine serum albumin
cDNA	Complementary deoxyribonucleic acid
CNS	Central nervous system
d	Day
DAPI	4',6-Diamidino-2-phenylindole
DMEM	Dulbecco's modified eagle medium
DMF	<i>N,N</i> -Dimethylformamide
e.g.	For example
ECM	Extracellular Matrix
EDC	1-Ethyl-3-(3-dimethylaminopropyl) carbodiimide
EDX	Energy dispersive X-ray spectroscopy
EGF	Epidermal growth factor
FDS	Trideca-fluoro-1,1,2,2-tetrahydrooctyl-dimethylchlorosilane
FITC	Fluorescein isothiocyanate

g	Relative centrifugal force
GPIIb	Glyco protein II b
h	Hour
hESC	Human embryonic stem cell
mESC	Mouse embryonic stem cell
HMWK	High-molecular-weight kininogen
HTS	High-throughput screening
iPSC	Induced pluripotent stem cell
min	Minute
miRNA	Micro ribonucleic acid
Neu5Gc	<i>N</i> -Glycolylneuraminic acid
NHS	<i>N</i> -Hydroxysuccinimide
NMP	<i>N</i> -Methyl-2-pyrrolidone
Oct-4	Octamer binding transcription factor 4
OGPC	Oligodendrocyte precursor cell
PA	Polyacrylate
PBS	Phosphate buffered saline
PDMS	Polydimethylsiloxane
PE	Phycoerythrin
PEG	Polyethylene glycol
pH	Potential hydrogen
pHEMA	Poly(hydroxyethyl methacrylate)

PK	Prekallikrein
PMA	Phorbol 12-myristate 13-acetate
PMEDSAH	Poly(2-methacryloyloxy)ethyl dimethyl-(3-sulfopropyl)ammonium hydroxide
PPP	Platelet poor plasma
PRP	Platelet rich plasma
PU	Polyurethane
rpm	Revolutions per minute
s	second
SAM	Self-assembled monolayer
SDS	Sodium dodecyl sulfate
SEM	Scanning electron microscopy
Sema	Semaphorin
SSEA	Stage-specific embryonic antigen
SNBTS	Scottish National Blood Transfusion Service
TMSA	3-(trimethoxysilyl)propylmethacrylate
TPA	12-O-tetradecanoylphorbol-13-acetate
TPO	Thrombopoietin
UV	Ultra violet
vWF	von Willebrand's factor
vWFR	von Willebrand's factor receptor
XPS	X-ray photoelectron spectroscopy

# **Chapter 1: Introduction**

## **1.1 Biomaterials and Biocompatibility**

In general, biomaterials are characterised by their ability to coexist in close contact with body tissue without causing an unacceptable degree of harm.<sup>1</sup> The most recent definition by David F. Williams describes biocompatibility as the following:

*“Biocompatibility refers to the ability of a biomaterial to perform its desired function with respect to a medical therapy, without eliciting any undesirable local or systematic effects in the recipient or beneficiary of that therapy.”<sup>2</sup>*

Such materials are not a recent innovation as over 2000 years ago, biomaterials such as gold, silver and wood were used as substitutes for body parts.<sup>3</sup> Over the last century, new ceramics, metals and polymers have been designed which display well defined mechanical, chemical and biological properties such as mechanical strength, corrosion resistance and biodegradability. This large portfolio of properties of today’s biomaterials offer the chance to tailor them towards the application in unique biological environments and their application in complex, diverse areas such as tissue engineering, invasive sensing or in gene transfection systems.<sup>4-7</sup>

Normally, there are several characteristics that are combined by a perfect biomaterial when being implanted into the host:

- Lack of cytotoxicity towards the host (biosafety)
- Fulfillment of required material-tissue interactions (promotion or inhibition)
- Minimal immune response and inflammation
- Optimal chemical, physical and mechanical properties (such as strength, stress- and pressure endurance).<sup>4,8</sup>

Since biocompatibility is a complex mechanism which is still not predictable, the investigations of the processes after a biomaterial is placed into a host (foreign body responses) are very important.<sup>8,9</sup> In this context, blood-material interactions are the most prominent ones which lead to a complex series of events that are highly interlinked (Figure 1.1).

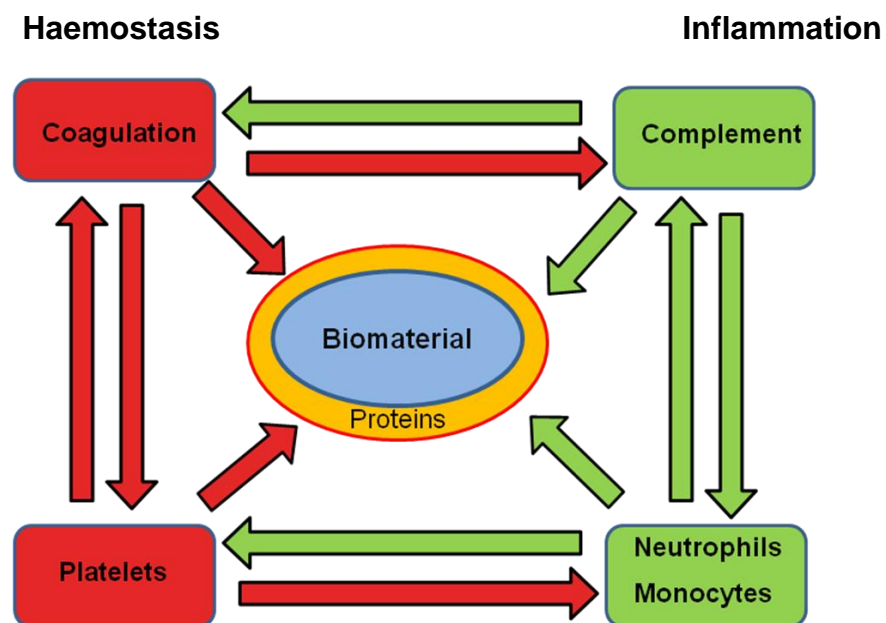


**Figure 1.1:** Blood-material interactions leading to thrombosis and inflammation reactions.<sup>6</sup>

In the first step after implantation, proteins and peptides adsorb onto the surface of the foreign biomaterial. These molecules mediate the binding and activation of cells such as monocytes, leukocytes and platelets. The coagulation cascade and the complement cascade are triggered, resulting in haemostasis and inflammation reactions.<sup>9</sup> The level of these responses depend strongly on the transplanted biomaterial and determine whether the material is tolerated or leads to complications and/or rejection.

Depending on the transplanted device, the risk of thrombotic complications varies between 2-10%.<sup>9</sup> However, it is still unknown how much of an inflammatory and thrombosis response is tolerable for a person. Furthermore, small diameter vascular grafts cannot be introduced to the human body as the resulting thrombogenicity is too high. Hence, surface modifications of already used devices or completely new biomaterials that reduce further host responses are desirable.<sup>9</sup>

## ***1.2 High-throughput Screening of Biomaterials***

High-throughput screening (HTS) of materials is defined as a methodology which identifies suitable materials for a certain purpose by screening a large compound library.<sup>10</sup> It is a powerful tool when the correlation of performance and the theoretical predictions of the performances from the structure and composition of a molecule, formulation or material is poor. This is the case for biomaterials, where the complex biological response to special surfaces has not been completely understood.<sup>10</sup>



### 1.2.1 Microarrays as Tool for HTS

Microarrays are high-throughput tools that consist of a flat material (e.g. glass or silicon) on which numerous probes are deposited in a defined and known 2D grid.<sup>11,12</sup> Each feature can be seen as a single independent assay, which can be replicated and which allows the whole assay to be carried out under identical conditions with minimal amounts of probe material.<sup>13,14</sup> Today, microarrays are widely used in biological areas and have given rise to commercially available DNA and protein arrays.<sup>14,15</sup> Depending on the intended application of the microarrays, the substrate on which the probes are deposited as well as the deposition technique have to be carefully chosen. In Table 1.1 a brief overview of the frequently used substrates, surface modifications and probe deposition mechanisms are given.

**Table 1.1:** Frequently used microarray features.

Feature	Option
Substrate	Glass <sup>16</sup> Silicon <sup>17</sup> Plastic <sup>18</sup>
Surface Modification	Aldehyde/ Amino-modifications <sup>19</sup> Natural and synthetic polymer coating <sup>20,21</sup> Gold-coating <sup>22,23</sup>
Deposition Technique	Contact Printing <sup>20,21</sup> Inkjet Printing <sup>24,25</sup> Photolithography <sup>26</sup>

### **1.3 Printing Techniques**

For the deposition of different probes on a substrate, a variety of printing techniques have been developed that can be divided into contact and non-contact printing methods.<sup>27</sup> In the first case material is deposited by direct physical contact of the substrate with an inked stamp of some type, while non-contact printing techniques avoid any type of contact with the substrate. Here, the ink is dropped onto the substrate in a very precise manner. In general, contact printing systems are simpler in design, faster and less expensive. Non-contact instruments allow printing on more fragile substrates and enable more flexible printing designs.

#### **1.3.1 Contact Printing Approach**

In the contact printing approach, features are generated by a high precision X-Y-Z robot holding pins that dip into the compound solution (ink) and dispose it at a specific site by physical contact.<sup>28</sup> The chemical and physical properties of the pin, solution and the substrate as well as the printing parameters of the robot (speed, number of depositions) affect the printing quality. In particular, the wettability of substrate and pin as well as the viscosity and surface tension of the liquids have an influence on the uniformity and amount of deposition. External factors like humidity and temperature have additional influences and have to be regulated for a good printing result.<sup>28</sup>

There have been a range of different pins developed to optimise the printing of specific inks. The most common ones are solid and split and stealth pins (Figure 1.2).

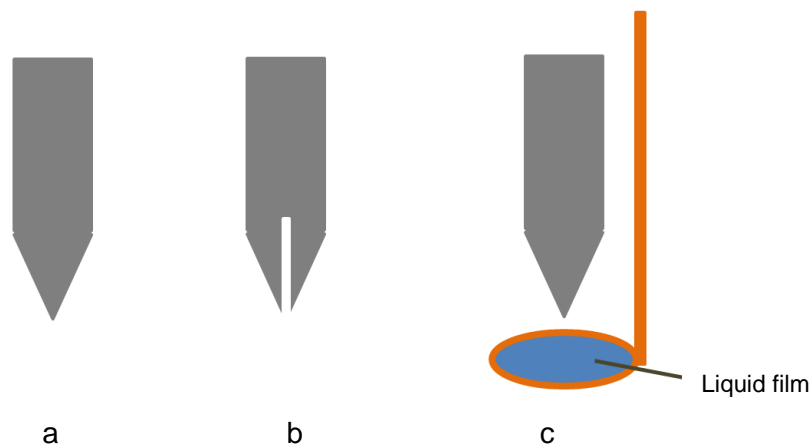


**Figure 1.2:** *Different types of pins used in the contact-printing approach. a) Solid pin; b) split pin; c) ring and pin system.*

### **Solid pins**

Solid pins are plain needles (Figure 1.2a), which are robust and give an excellent spot-size reproducibility. The size of the created spot can be varied by changing the pin diameter and with it the amount of liquid which is transferred. The disadvantage of solid pins is that the ink only lasts for one print - they have to be washed and reloaded after each deposition.<sup>29</sup>

### **Split and Stealth pins**

The pins are characterised by having a narrow slit and cavity in the centre of the needle which enables the print of several hundred spots after a single load (Figure 1.2b).<sup>30,31</sup> These pins are the most widely used in the biological section. A pre-blotting step is required to guarantee a uniform spot deposition, which is also depending on the slit width and slit inclination. The printing environment has to be adjusted to keep sample evaporation at a minimum by e.g. controlling the humidity in the printer casket.<sup>31</sup> Split and stealth pins are not suitable for the deposition of viscous material such as polymer solutions that might block the split pin.

### **Ring and pin system**

In this system a liquid film is generated by dipping a ring into the ink-well and removing it. A liquid film is captured in the ring, through which the solid metal pin is moved. The ink is deposited onto the substrate without disrupting the liquid film (Figure 1.2c).<sup>32</sup> The film serves as reservoir, allowing multiple prints of the same solution. During these prints, temperature and humidity have to be controlled to ensure the stability of the film over the printing period.<sup>33</sup>

### **Microcontact Printing**

The combination of traditional photolithography to form a very precise stamp and the contact-printing technique to transfer the ink in a fast and effective manner gave rise to microcontact printing. This technique allows patterning of large surface areas with resolution down to the submicrometer range.<sup>34,35</sup> The stamp is often generated as shown in Figure 1.3.<sup>36</sup> In the first step a template (master) is created on silicon. After applying a light-sensitive material (photoresist), UV irradiation through a photomask generates local reactions on the photo-sensitive material. After baking, developing and removing the non-irradiated areas of the substrate, the master can be used to generate a polydimethylsiloxane (PDMS) stamp, whose elevated areas correspond to indented regions of the master.<sup>36</sup>

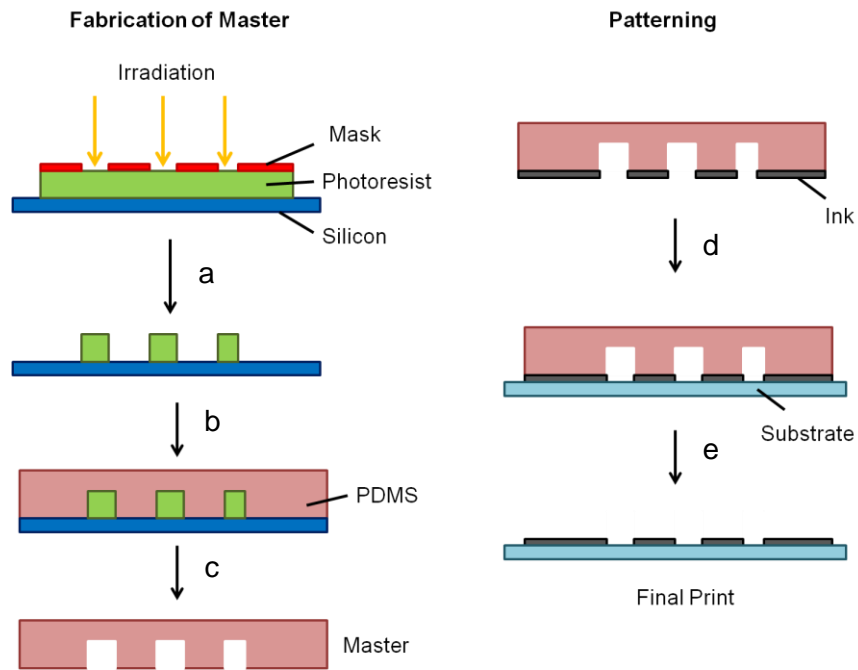


**Figure 1.3:** Microcontact printing. *a) The master is fabricated by irradiation of the photoresist through a mask, generating a precise mould. b) The mould is used as template for polydimethylsiloxane (PDMS). c) The photoresist is peeled off to obtain the master. d) After inking and applying the stamp onto a substrate via physical contact, e) the ink is transferred onto the substrate.*<sup>36</sup>

After the stamp is peeled off, it can be used for inking (Figure 1.3). The ink can thereby diffuse into the bulk of the stamp material, allowing the creation of a ink reservoir for multiple prints. By direct physical contact of the stamp and the substrate, the ink is transferred to the substrate. As the stamp can be easily deformed, the pressure has to be controlled to ensure that the correct features are obtained.<sup>37,38</sup>

### 1.3.2 Inkjet Printing Approach

The main advantages of inkjet printing approaches over contact printing are the gentle deposition (allowing the printing on fragile substrates), better control of deposition (enabling the printing of a wider range of spot sizes), while the accurate movement of the nozzle makes it possible to print complex patterns and grids.<sup>39</sup>

There are three different technologies used in the inkjet printing approach: thermal, piezo and solenoid methods (Figure 1.4).

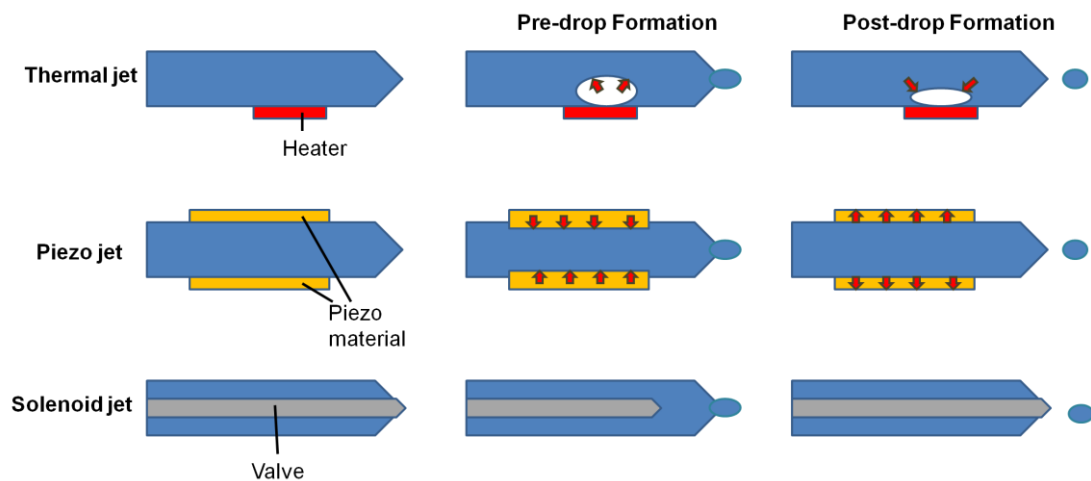


**Figure 1.4:** Inkjet printing techniques. Thermal, piezo and solenoid jets and the cross sectional view of the nozzles pre- and post-drop formation.<sup>40</sup>

#### Thermal jet

In the thermal or bubble jet a resistive element in a small chamber containing the ink is rapidly heated. The high temperature (350-400 °C) vaporises a thin film of ink above the heater and the resulting bubble forces the ink out of the nozzle. The void in the chamber after the ejection of the drop, is filled by replacement fluid afterwards.<sup>40</sup>

The advantages of this technology are the generation of very small drop sizes and

low printhead costs. However, thermal jet printers are limited to the inks which can be used. Normally these systems are optimised for certain ink compositions that are aqueous or part-aqueous as they allow an easy vaporisation.<sup>40</sup> While the printing principle is used in desktop printers, there is no commercial available industrial microarrays based on this method. However, scientific research groups have modified normal desktop printers for the delivery and patterning of (bio)molecules.<sup>41</sup> Despite the heating process, cellular materials could be successfully printed.<sup>42</sup>

### **Piezo jet**

In the piezo inkjet printer a pressure wave is used to eject droplets from the nozzle. The pressure is generated by a rapid dimensional change of the piezoelectric material (usually lead zirconium titanate). The amount of deposited ink is controlled by the duration and amplitude of the applied voltage to the piezo material.<sup>40</sup> Hydrophobic and hydrophilic coatings of the nozzle can also improve the printing results depending on the characteristics of the ink.<sup>43</sup> In contrast to thermo jets, the piezo inkjet technology is not limited to certain inks and is equipped with printheads that have a long life (if no mechanical damages occur). However, since the printheads are relatively expensive, the piezo jet is classified as high cost technique.<sup>40,42</sup> A combination of the piezo technology with heated nozzles can also be applied for the printing of highly viscous liquids such as waxes.<sup>44</sup>

### **Solenoid jet**

In this printing method, a pressurized liquid in a nozzle is dispensed by the quick opening and closing of high speed valves, which are electrically controlled. The

volume of the deposited material depends on the applied pressure within the nozzle, the viscosity of the fluid, the nozzle dimensions and the pulse width controlling the valve opening. The printed volume can vary between nanoliters to several microliters.<sup>45</sup>

## **1.4 Types of Microarrays**

### **1.4.1 DNA Microarrays**

Microarrays of known oligonucleotides or DNA sequences are used to measure the expression levels of genes, to detect single nucleotide polymorphisms and mutations or to genotype regions of a genome amongst multiple others.<sup>46-50</sup> The principle of DNA microarrays is based on the specific pairing of complementary nucleic acid sequences through the formation of hydrogen bonds. A higher percentage of complementary nucleic acids results in a stronger binding of DNA strands for the correct sequence rather than a mismatch. After hybridization of the genetic material onto the arrays, non-specific binding sequences are washed off, leaving the fluorescently labelled complementary DNA (cDNA) strands behind. The fluorescent intensities from each spot give the identity and the relative amount of the immobilised probes. DNA arrays have been used to examine changes in gene expression in case of diseases such as cancer and are useful tools for the identification of targets for drugs and biomarkers of complex diseases.<sup>12,51,52</sup>



### **1.4.2 Protein Microarrays**

Protein microarrays can be classified into two different types: analytical microarrays and functional microarrays.<sup>53</sup>

Analytical microarrays consist of an immobilised library of antibodies or aptamer and are used to profile protein mixtures. They allow the investigation of the binding affinities and protein expression levels of the different proteins.<sup>53,54</sup> Hence, they can be used as diagnostic tools by profiling the different expression patterns of proteins and comparing the results between healthy and disease tissues.<sup>55</sup>

Functional protein microarrays consist of full-length proteins/ protein domains that are deposited. They are applied for the investigation of protein-protein, protein-DNA, protein-RNA or protein-small molecule interactions.<sup>56,57</sup>

### **1.4.3 Polymer Microarrays**

To identify suitable polymers for certain applications in a rapid and effective manner, polymer microarrays were independently invented by the research groups Langer, Voelcker and Bradley.<sup>20,21,58-60</sup>

#### **Langer Approach**

The research group of Langer focuses on the generation of polymer microarrays for cellular applications using poly(hydroxyethyl methacrylate) (pHEMA) dip-coated microscope slides as a cytophobic basis for the polymer probes. The coating prevents any cell attachment while being non-toxic and allowing printed material “*to penetrate in the matrix where the material can physically entangle*”.<sup>21,61</sup> The polymer

features are either pre-synthesised or are *in situ* synthesised on the slide by using a contact printing or inkjet printing approaches.<sup>61</sup> For the *in situ* polymerisation non-volatile monomer, crosslinker and photoinitiator solutions are printed on top of each other. UV irradiation activates the initiator and after the polymerisation reaction, the rest solvent is removed *via* vacuum extraction.<sup>10,21</sup>

### **Voelcker Approach**

The polymer microarrays generated by Voelcker *et al.* use plasma polymerisation to create star polyethylene glycol (PEG) or glucoside coatings which prevent cellular adherence.<sup>62</sup> Similar to the Langer approach, the polymer features on the coated slides are *in situ* synthesised by step-wise contact printing of monomers, crosslinker and photoinitiator with solid pins followed by UV irradiation and water wash.<sup>58,62</sup> By incorporating epoxy-groups in the cytophobic layer, the plasma polymerisation technique enables the covalent immobilisation of polymers and biomolecules.<sup>58</sup>

### **Bradley Approach**

The Bradley group has developed three types of polymer microarray approaches using contact and non-contact printing techniques.

The first developed polymer microarray consisted of microscope slides that were dip-coated in agarose solution.<sup>60,20,29</sup> Preformed polymer solutions (1 % (w/v) in *N*-methyl-2-pyrrolidone (NMP)) of polyacrylates and polyurethanes are deposited on the slides in a fast and efficient manner by contact-printing using solid pins.<sup>29,63</sup>

A second type of polymer microarray has been invented to maximise the amount of polymer features on one slide.<sup>24</sup> For this purpose, a hydrofluoro mask was generated

on the microscope slide which defines the polymer position and size. To enable the anchoring of the acrylate monomers, an acrylate silane is coated on the empty features. Monomer, crosslinker and photo- or redox initiator are printed on top of each other and form *in situ* polymers after irradiation and/or heating.

For the generation of complex microarrays which take several hours, it was shown that a paraffin oil layer can be applied on top of the microscope slide. This prevents the evaporation of printed features for more than four hours and with it the uneven distribution of printed molecules within the spot.<sup>25,64</sup> The polymer spots generated *via* this method are relatively large (600  $\mu\text{m}$ ) and extensive washing is required to remove the oil film.<sup>25</sup>

The third approach towards generating polymer microarrays is presented in this thesis and deals with the fabrication of gradient polymer microarrays. In this case, gradient lines instead of single polymer spots are generated *via* inkjet printing whose polymer composition changes along the length of the line. Hydrofluoro masks define the length and width of the final gradient lines. In contrast to the previous polymer microarrays, the gradient array can be used for the investigations of cellular migration and is the first tool which combines a high-throughput approach with true combinatorial approaches (gradients).

## ***Aim of the Thesis***

The aim of this thesis was to develop new types of polymer microarrays for cellular based applications. Diverse polymer microarrays have been fabricated which were used to identify polyacrylates which

- control human embryonic stem cell fate and have the potential to be future synthetic cultivation substitutes in place of current biological substrates.
- support adherence of suspension and adherent cell lines.
- activate platelets more rapidly and efficiently than the natural agonist collagen in static and flow experiments. Subsequently the mechanism of this activation process was further investigated with protein binding studies.
- sort megakaryocytic cell lineages according to their maturation status.

Moreover, the first gradient polymer microarray was developed which also enabled the fabrication of protein gradients. These were used to develop a haptotaxis assay to control and investigate the cellular migration of oligodendrocyte precursor cells.

## **Chapter 2: High-Density Polymer Microarrays: Identifying Synthetic Substrates to Control Stem Cell Fate**

As described in Chapter 1, polymer microarrays are a high-throughput tool for the fast and effective screening of thousands of different substrates simultaneously. The number of deposited materials on an array (normally a microscope slide) depends on the feature sizes, the distances between them and the fabrication method used in their construction, be it *via* printing needles or ink-jet nozzles.

### **2.1 Types of Polymer Microarrays**

Polymer microarrays are traditionally generated by contact-printing of preformed polymers or monomer solutions onto cytophobic materials such as agarose or poly(2-hydroxyethyl methacrylate) using flat tipped needles. Due to the spreading of printed solutions when printed onto cytophobic substrates, the polymer spots generated are typically about 300-350  $\mu\text{m}$  in size.<sup>20,65</sup> Hence, the largest arrays that can be prepared on a coated microscope glass slide consists of 1728 features with 576 polymers in triplicates.<sup>24</sup>

The application of ink-jet printing for the fabrication of polymer microarrays enables a reduction in spot size to 200  $\mu\text{m}$ , which is attributed to the use of a hydrofluorous mask which defines the spot size, their exact location and prevents unwanted spreading of the deposited solutions on the slides.<sup>24</sup> The size of the deposited polymer spots depends on the nozzle of the printer (defining the drop size) and the

number of drops per printed feature. The largest arrays printed in this manner consists of 2436 polymer features and have been successfully applied for the identification of suitable binding materials for mouse embryonic stem cells. The development of a larger polymer microarray was, however, desirable for the investigation of polymers with a large variability in their monomer composition in regard to stem cell binding and growth.

## **2.2 Stem Cells**

Stem cells possess the unique ability to undergo cell division while maintaining an undifferentiated state (self-renewal) and having the capacity to differentiate into other cell types (potency).<sup>66-68</sup> The potential of stem cells to differentiate into diverse cell types (plasticity), migrate to the site of damaged tissue (homing) and to unite with other types of tissue (engraftment) gives hope that damaged or diseased tissue can be replaced or reconstructed in the future.<sup>69-72</sup>

Generally, it can be distinguished between embryonic, adult and induced pluripotent stem cells. While embryonic stem cells can differentiate into any mature cell of the three primary germ layers (pluripotency), adult stem cells can only undergo lineage restricted differentiation (multipotency) and are located in all types of tissue acting as a repair/replacement system for the body.<sup>67,68,73-76</sup> Another type of pluripotent cells are engineered induced pluripotent stem cells (iPSCs) which are derived by transfection of specific genes that are associated with stem cellness into non-pluripotent cells (adult somatic cells).<sup>77-80</sup> Despite being similar to natural pluripotent stem cells in morphology, expression of proteins, potency and self-renewal, it is still

being investigated to what extent iPSCs simulate embryo-derived pluripotent stem cells.<sup>79,80</sup> For all stem cells it is essential to control culture conditions in order to prevent unwanted/uncontrolled differentiation. Transcription factors such as Oct-4, Nanog and Sox2 are typically used as markers to access the level of pluripotency.<sup>81-86</sup>

### 2.3 Embryonic Stem Cells

Embryonic stem cells (ESCs) are isolated from cells located in a region of an early embryo (5 d, blastocyst) known as the inner mass (Figure 2.1).<sup>67,68,87-89</sup>

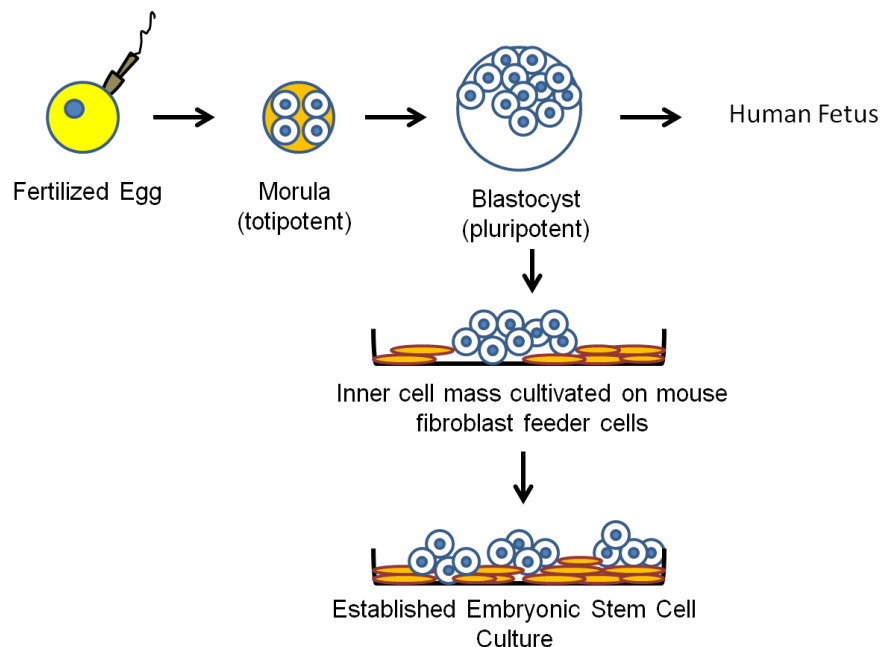


**Figure 2.1:** *Human embryonic stem cell generation. After in vitro fertilisation, the early stage embryo (morula) becomes a blastocyst with pluripotent inner mass cells. Cultivation of these cells on mouse fibroblast feeder cells generates embryonic stem cells that can be used in the laboratory.*<sup>90</sup>

Cell line derivation is a complex process which is not completely understood - hence, the derivation of hESC lines is mostly carried out on human or mouse feeder cells and not on proteins or peptides of the extracellular matrix (ECM) (unlike the actual

cultivation). Feeder cells are thought to imitate better the conditions in the body and are hence beneficial for the creation of stem cell lines with true stem cell characteristics. Mouse feeder cells have several disadvantages over human fibroblasts as they increase the risk of transmission of infectious diseases from animal to humans (zoonosis). Moreover, it has been observed that a non-human sialic acid (Neu5Gc) from mouse feeder cells can be incorporated into hESCs.<sup>91</sup> As specific antibodies against this sialic acid are present in the human body, transplanted hESCs would be killed by the body's own immune system, leading to rejection of the transplanted cells.<sup>91</sup>

For the hESC derivation *in vitro* fertilised embryos that are classified as “not suitable” for embryo transfer - either because of poor morphology or because of the law-enforced cryo-storage limitation time (UK: 55 years since 2009 - present a good source for hESC lines.<sup>92</sup> The embryos would be normally discarded and offer therefore a more ethical acceptable source for stem cell lines than fully intact embryos.<sup>93,94</sup> The success rate for hESC line formation depends on the quality of the used embryo. The probability to generate hESC lines is about 15% for embryos that are suitable for a transplantation, while this probability shrinks to 1-3% for embryos with a poor morphology.<sup>95-101</sup>

Once the hESC lines are established, the cells are normally grown on human feeder cells or, alternatively, in fully synthetic, serum-free medium such as mTESR or StemPro on animal- or human-derived ECM protein substrates.<sup>95,96</sup> While the risk of pathogen transmission in the feeder-free cultivation system is low and scaling-up can be easily achieved, the ECM proteins are expensive and the extraction and/or



production in large quantities for clinical therapies is difficult to realize. In addition, the self-renewal ability of some hESC lines is not supported.<sup>92,93</sup>

#### **2.4 Current Substrates for Stem Cell Cultivation without Feeder Layer Cells**

The self-renewal and controlled differentiation of hESC on a complete synthetic substrate in fully-defined and serum-free medium is a necessary step to allow stem cell therapy to become a reality. However, as the identification of substitutes for complex ECM proteins has proven to be challenging, the most widely applied hESC substrate is Matrigel<sup>TM</sup>; an ECM analogue, which is extracted from Engelbreth-Holm-Swarm mouse sarcoma cells.<sup>102-105</sup> The main components of Matrigel<sup>TM</sup> are basement membrane components such as collagen, laminin and entactin, but also a variety of growth factors such as basic fibroblast growth factor (bFGF) or epidermal growth factor (EGF).<sup>103</sup> Batch-to-batch variability and the potential exposure of non-human sialic acid (an immunogenic molecule) to stem cells prevent its use as a substrate for clinical-grade hESCs.<sup>106</sup>

The search for defined protein and peptide substitutes has shown that in long term studies (> 10 passages) immobilised human plasma vitronectin and human recombinant laminin-511 can be used as a stem cell substrate.<sup>106-108</sup> In both cases these proteins are present in the ECM and are crucial for cell-adhesion and cell-migration.<sup>106,108,109</sup> In addition, a variety of synthetic heparin-binding peptides (singly or in combination) and a short peptide version of vitronectin also facilitated the long-term culture of hESC in defined, serum-free medium.<sup>110,111</sup>

In contrast to proteins and peptides, synthetic polymer coatings that can control stem cell fate would offer a cheap, scalable alternative that would survive long-term storage conditions and allow facile sterilisation. Moreover, polymers could be easily modified to control differentiation of stem cells into defined lineages by attaching certain peptides or small molecules.<sup>87,112</sup>

So far there have been several synthetic polymer matrices identified which support hESC propagation.<sup>113-115</sup> However, only one polymer - poly(2-methacryloyloxy)ethyl dimethyl-(3-sulfopropyl)ammonium hydroxide (PMEDSAH) - has been shown to support hESC growth of the H9 cell line during long-term studies in undefined and defined, serum-free medium.<sup>112</sup> While the cell line H9 could be passaged for more than 10 passages on the polymer substrate maintaining pluripotency, the hESC line BG01 could only be cultivated for 3 passages under the same conditions. It was also shown that the defined medium StemPro had to be used for successful cultivation (differentiation was observed with mTESR). While StemPro is a defined medium, the concrete composition of the medium is not published, making it difficult to identify the protein binding characteristics for the substrate.<sup>112</sup>

Further investigations are needed to identify synthetic, polymeric hESC substrates that support the propagation of a variety of hESC lines under defined conditions and open the door for the production of clinical-grade stem cells on a large scale. As some surfaces support maintenance of cells but not their propagation or control of differentiation and are only selective for certain hESC lines, it is essential to screen a large variety of polymer substrates to identify optimal matrices.<sup>87</sup> Polymer-microarrays are a promising tool for this search as multiple polymers can be screened in a time-effective manner under identical conditions.

## 2.5 Fabrication of High-Density Polymer Microarrays

Polymer microarrays with more than 7000 features were generated in a two-step fabrication process (Figure 2.2a,b). In the first step, an aqueous sucrose solution was printed to generate a mask. The uncoated areas of the slide were treated with a hydrophobic fluoro-silane, which defined the subsequent spot size and prevented or reduced unwanted cellular attachment. The spot sizes and with it the general array size could be easily varied by changing the number of sugar drops per feature (Table 2.1).

**Table 2.1:** Variation of spot size and subsequent array size. The features were ink-jet printed with a microdrop printer (microdrop GmbH, Germany)

<b>Sugar drops per spot</b>	<b>Distance between Spots (X and Y direction) [<math>\mu\text{m}</math>]</b>	<b>Total number of spots (X direction x Y direction)</b>
15	800	29 x 62
12	700	33 x 70
6	500	47 x 99
3	450	53 x 110
2	400	59 x 124
1	300	79 x 165

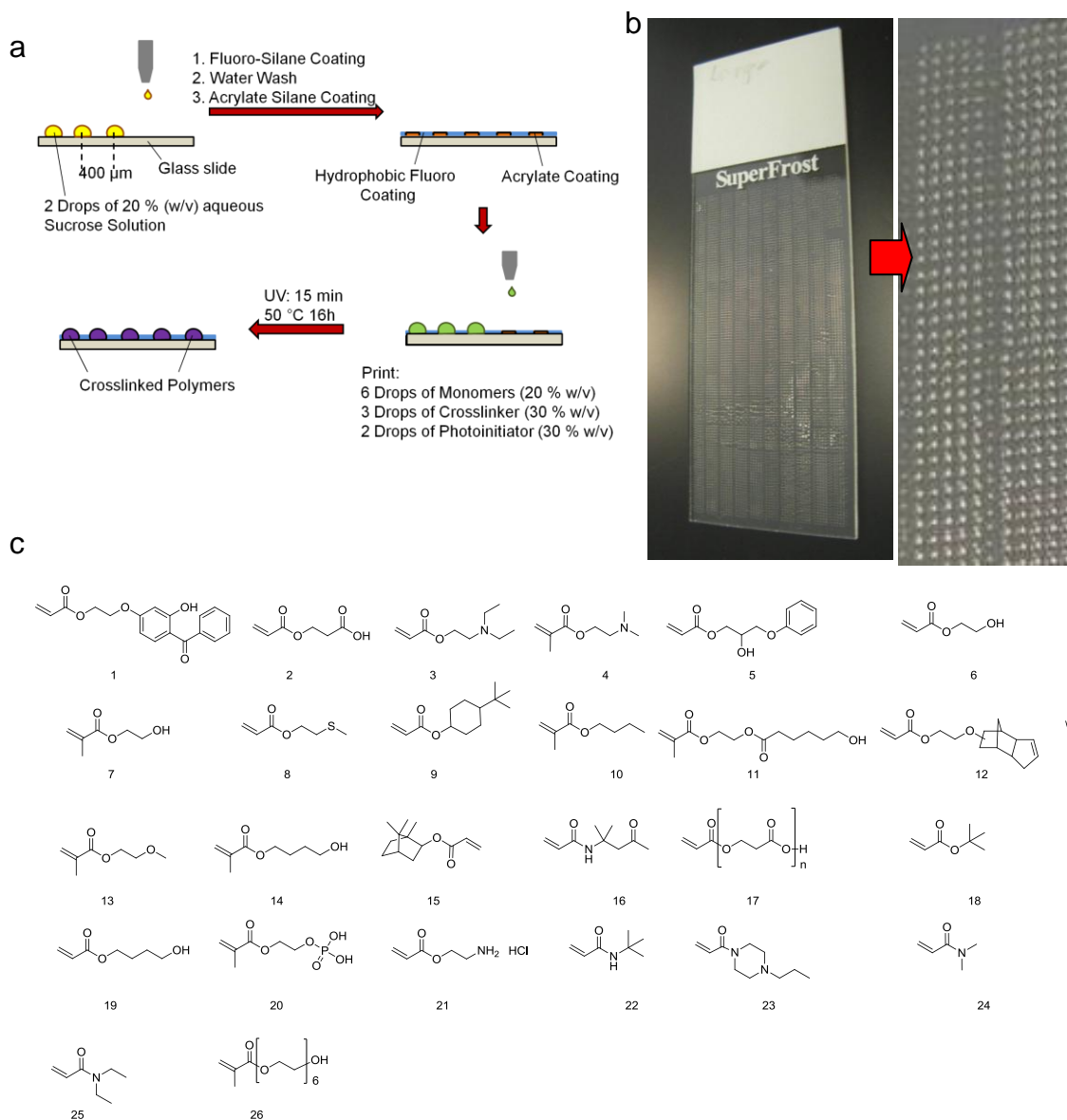


**Figure 2.2:** The fabrication of a high-density polymer microarray. **a)** The fabrication process. In the first step a fluoro-mask is prepared to define spot sizes and to prevent/reduce background cellular attachment. In the second step the monomers, crosslinker and photoinitiator are printed on the acrylate functionalised areas forming crosslinked polymers after UV irradiation.<sup>24</sup> **b)** Image of the final high-density array with 7316 polymer features, 50 columns (with 124 spots in the y direction); Insert shows magnification of ten columns. **c)** Acrylate and acrylamide monomers used for the fabrication of the polymer spots.

In the second step, the sucrose spots were removed, revealing glass features that were subsequently coated with an acrylate silane. For the fabrication of a high-density array, two monomers (out of 26 different acrylates and acrylamides) were printed in different ratios (20% steps) along with a crosslinker and a photoinitiator, allowing the efficient generation of a large number of compositions with a range of characteristics (Figure 2.2c).

This method allowed the fabrication of a polymer microarray consisting of 7316 features (with diameters of  $200 \pm 20 \mu\text{m}$ ) and displayed a smooth, uniform morphology (scanning electron microscopy, Figure 2.3a). The uniformity of the monomers mixed within the spots was investigated using energy dispersive X-ray spectroscopy (EDX) for polymers containing the monomers 2-hydroxyethyl methacrylate and ethylene glycol methacrylate phosphate (Figure 2.3).

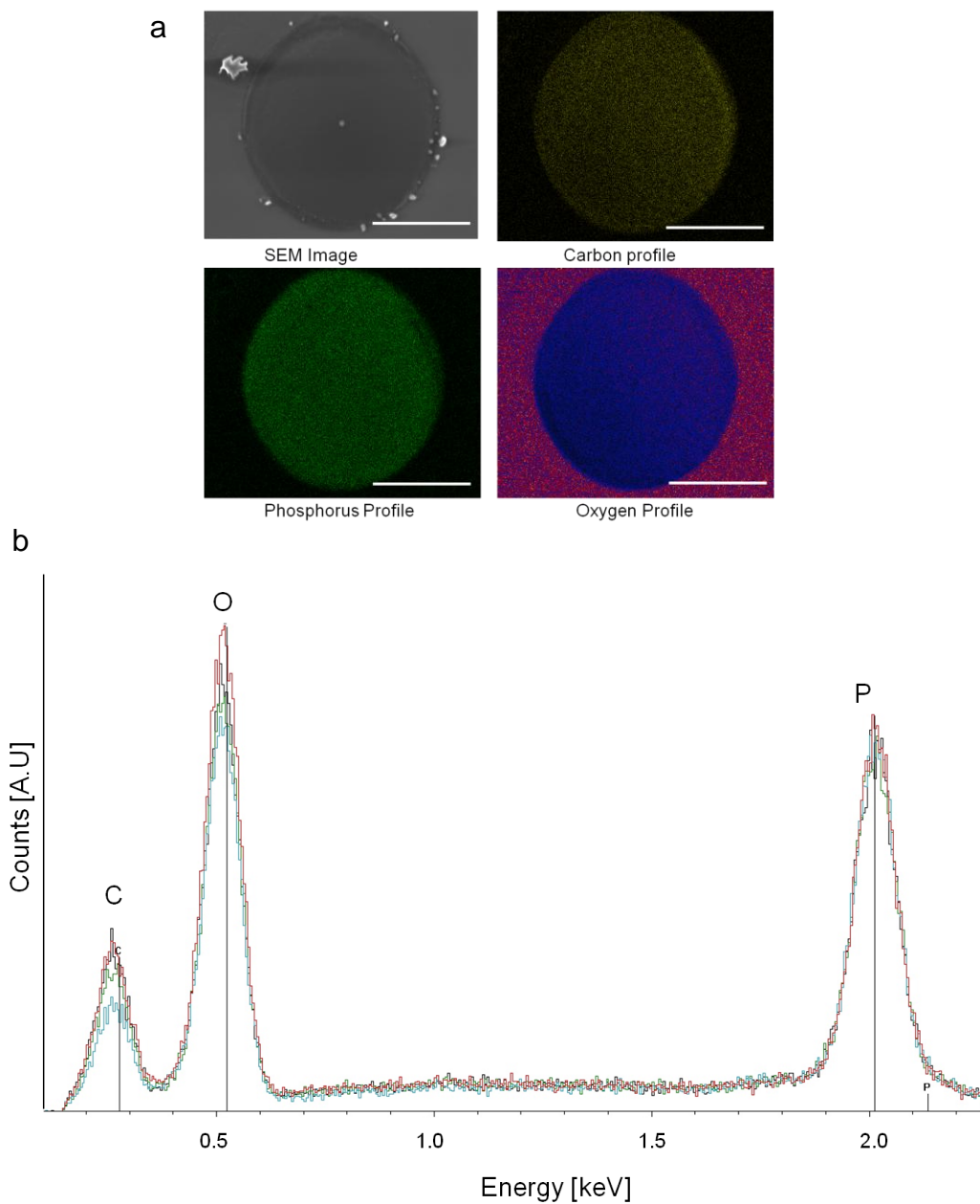


**Figure 2.3:** SEM and EDX-profile of polymer spots containing the monomers 2-hydroxyethyl methacrylate and ethylene glycol methacrylate phosphate. **a)** Colour intensity profile for a whole polymer feature. Bars = 100 $\mu$ m. **b)** Carbon, oxygen, phosphorus signal intensities for central and side regions of a representative polymer spot ( $n=3$ ): black, red - centre of spot, blue, green - edge of spot.

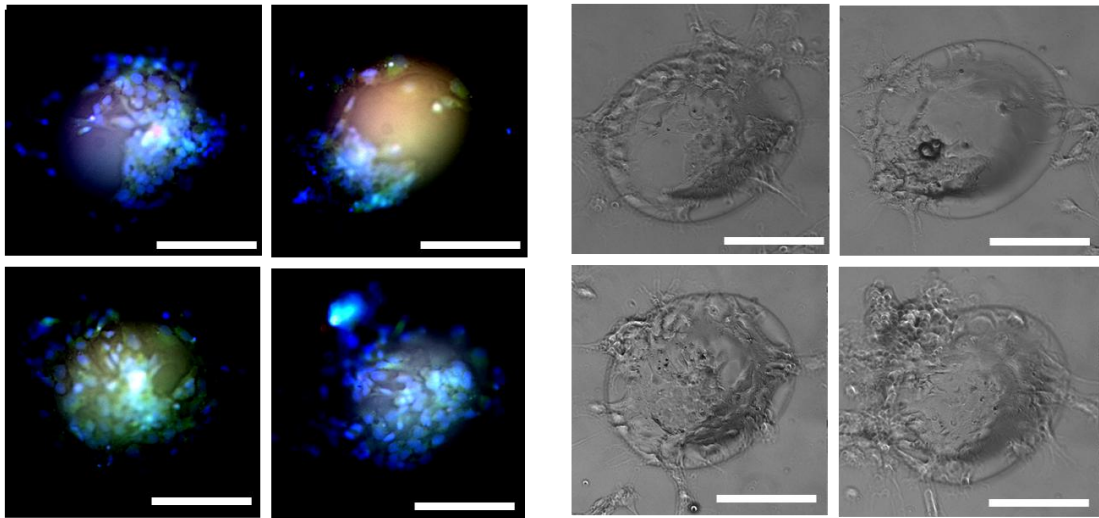
This analysis demonstrated uniform carbon, oxygen and phosphorus intensity profiles across the features, showing that the element content was equally distributed (Figure 2.3b).

The variety of acrylates/acrylamides and group diversity make the array an ideal platform for the identification of appropriate matrix polymers for the stable, robust phenotypic control of *in vitro* stem cell cultivation. The hESC line RH1 was incubated for 4 d on the high-density arrays, and the cells were subsequently fixed, stained with 4',6-diamidino-2-phenylindole (DAPI, blue nucleus stain) and a FITC-labelled antibody to the Octamer binding transcription factor 4 (Oct-4, stem cell marker) (Figure 2.4).<sup>95‡</sup> All hESCs that had been captured by the polymers showed Oct-4 expression, demonstrating pluripotency of the cells. The number of cells bound on the 26 polymers is shown in Figure 2.4b.

---

<sup>‡</sup> All hESC work was jointly carried out with Heidi K. Mjoseng in the Centre for Regenerative Medicine, Edinburgh (research group of Dr. De Sousa).

a



b

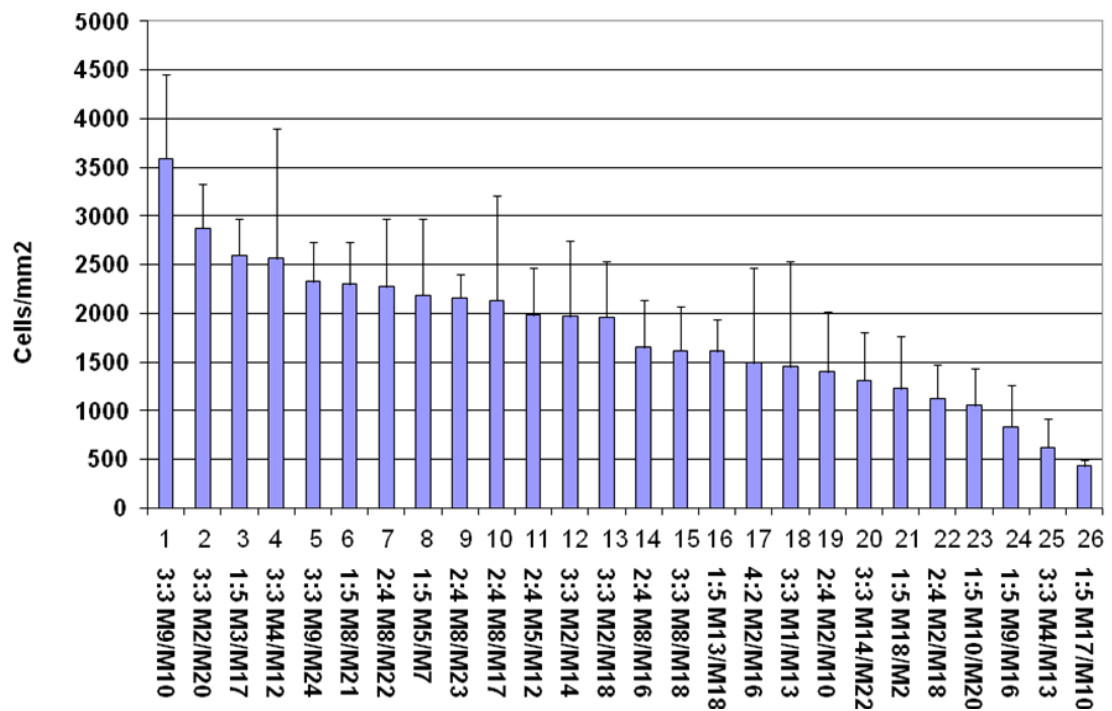


**Figure 2.4:** Analysis of polymer microarrays after hESC incubation. **a)** Typical images of features from a strong-binding polymer on the high-density array after 4 d of incubation. Cells are stained with DAPI (blue) and an antibody against Oct-4 (green). Bars = 100  $\mu$ m. **b)** Polymer array analysis after 4 d incubation with hESCs. Graph shows number of cells binding (with standard deviation of 10 replicates ( $n=2$ )).



The top cell binding polymer in the microarray studies consisted of the hydrophobic 4-*tert*-butylcyclohexyl acrylate (monomer 9) and *n*-butyl methacrylate (monomer 10) in equal ratios. This is in contrast to many previous studies where charged surfaces were successfully used for hESC cultivation.<sup>116,117</sup>

The most prominent monomers appearing in seven of the 26 identified hESC binding polymers were 2-carboxyethyl acrylate (monomer 2) and 2-(methylthio)ethyl methacrylate (monomer 8). Most monomer combinations with these monomers bound cells, but only at one specific ratio. This suggests that the specific ratios display very different characteristics and that only minor ratio changes are tolerated by the hESCs. This finding is in accord with previous studies where hESC binding strongly depended on the acid content of the surface and the medium.<sup>75</sup> To gain an understanding of the interaction between the identified polymer substrates and hESC growth, surface wettability and surface roughness of the polymers were determined. While the surface wettability (measured as water contact angle) has been correlated to protein adsorption and cellular binding, it has been suggested that surface roughness has an influence on cellular adherence and proliferation.<sup>116,118-120</sup> For the characterisation of the surface properties, the five best binding polymers of the microarray (Figure 2.4b) were coated onto coverslips and analysed.<sup>74,121</sup> The water contact angles for the identified polymers 1, 2, 4 and 5 varied between 46 – 59 ° (Table 2.2), values that are in a range normally supporting cellular attachment.<sup>116</sup> Polyacrylate 3 had a water contact angle of 37 ° which was expected since the 2-carboxyethyl acrylate (monomer 17) contains carboxylic acid groups and was in fivefold excess to the second monomer 2-(diethylamino)-ethyl acrylate (monomer 3). Atomic force microscopy (AFM) showed that the surfaces of the polymers was

generally smooth.<sup>‡</sup> While the polymers 1 and 3 gave values of about 0.14 - 0.15  $\mu\text{m}$ , the surface roughness of the polymers 2, 4 and 5 varied between 0.01 – 0.04  $\mu\text{m}$  (Table 2.1, Figure 2.5).

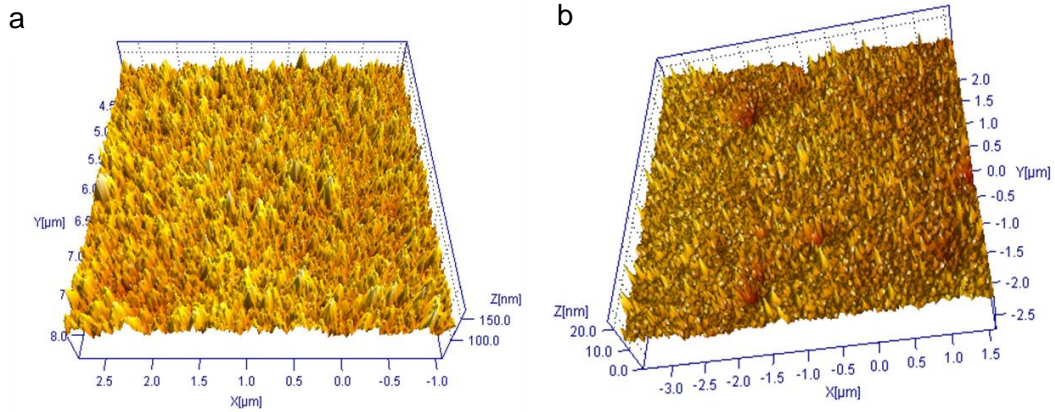


**Figure 2.5:** Representative roughness profiles for the polymers supporting hESC proliferation recorded by AFM: **a)** polymer 1 and **b)** polymer 4.

However, the roughness did not have any influence on the cell proliferation as the overall cellular expansion time on the hit polyacrylates were comparable to Matrigel<sup>TM</sup> (41.3 – 53.1 h, Table 2.2).

---

<sup>‡</sup> The AFM images and corresponding measurements were kindly provided by Michail Kalloudis (research group of Dr. Koutsos).

**Table 2.2:** Characterisation of the five best polymers identified from the high-density array that supported hESC proliferation and self-renewal. Presented data for water contact angle and cell doubling time (standard deviation (n=5)).

Polymer	Composition	Water Contact Angle	Root Mean Square Roughness	Overall Cellular Expansion Time*
		[°]	[ $\mu\text{m}$ ]	[h]
1	3:3 M9/M10	55.7 $\pm$ 2.6	0.138 $\pm$ 0.015	48.5 $\pm$ 7.3
2	3:3 M2/M15	56.0 $\pm$ 3.3	0.038 $\pm$ 0.005	53.1 $\pm$ 7.5
3	1:5 M3/M17	37.3 $\pm$ 1.9	0.148 $\pm$ 0.030	51.6 $\pm$ 4.8
4	3:3 M4/M12	45.7 $\pm$ 1.0	0.017 $\pm$ 0.010	43.8 $\pm$ 1.9
5	3:3 M9/M24	58.7 $\pm$ 3.2	0.014 $\pm$ 0.005	43.2 $\pm$ 12.2

\* Matrigel<sup>TM</sup> gave a cell doubling time of 41.3  $\pm$  7.4 h.

To determine the ability of the polymers to maintain the characteristics of hESCs over several passages, cells were seeded on the five best polyacrylates and the positive control Matrigel<sup>TM</sup> and incubated for 35 days (being passaged approximately every 7 days). As expected, the cells adhered easily to the different polymers, showing a similar morphology to the Matrigel<sup>TM</sup> control.

After five passages, cells were fixed and stained with fluorescent labelled Nanog and Oct-4 antibodies as these transcription factors are critically involved in the self-renewal of hESCs.<sup>122,123</sup> As shown in Figure 2.6a, the fluorescence intensity for both markers on the positive control Matrigel<sup>TM</sup> as well as the polyacrylates 1, 2, 4 and 5 were comparable, showing that the polymers maintained stem cell pluripotency. Cells on polymer 3 were positive for Nanog staining but failed to show strong

expression of Oct-4, showing progressed differentiation. hESCs were harvested and analysed by flow cytometry for quantitative analysis of markers of hESC differentiation: SSEA-1 and SSEA-4 (Figure 2.6b).<sup>123,124</sup> While SSEA-4 is expressed by hESCs it becomes down regulated upon loss of pluripotency, while SSEA-1 is up-regulated in the case of differentiation. About 90% of the hESCs maintained their pluripotency after 35 days of culture (SSEA-4 positive, SSEA-1 negative) on the control Matrigel<sup>TM</sup> and polymer 1. The identified polyacrylates 2, 4 and 5 had a slightly lower population (~80%) of undifferentiated cells that were SSEA-4 positive. Polymer 3 had a high differentiation rate, only maintaining 29% of the cells in their pluripotent state. This might be due to the lower water contact angle which was shown to be less ideal for stem cell cultivation.<sup>116</sup> While short term cultivation on this polymer might be possible (as shown on the high-density array results), long-term cultivation is not supported.

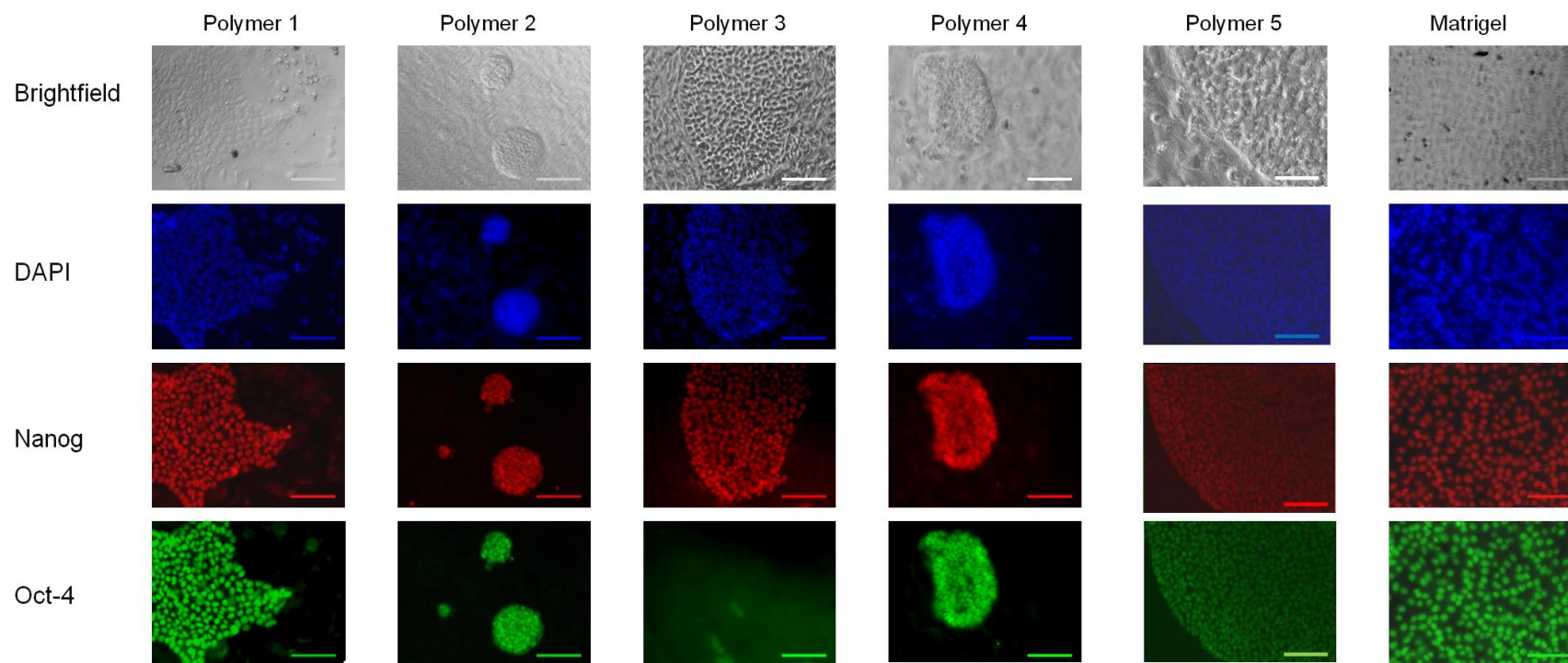


**Figure 2.6a:** Representative images of immunostained hESCs cultivated on Matrigel<sup>TM</sup> and polyacrylates 1-5 for 5 passages: DAPI (blue), stem-cell marker Nanog (red) and Oct-4 (green). Scale bars = 100 μm.

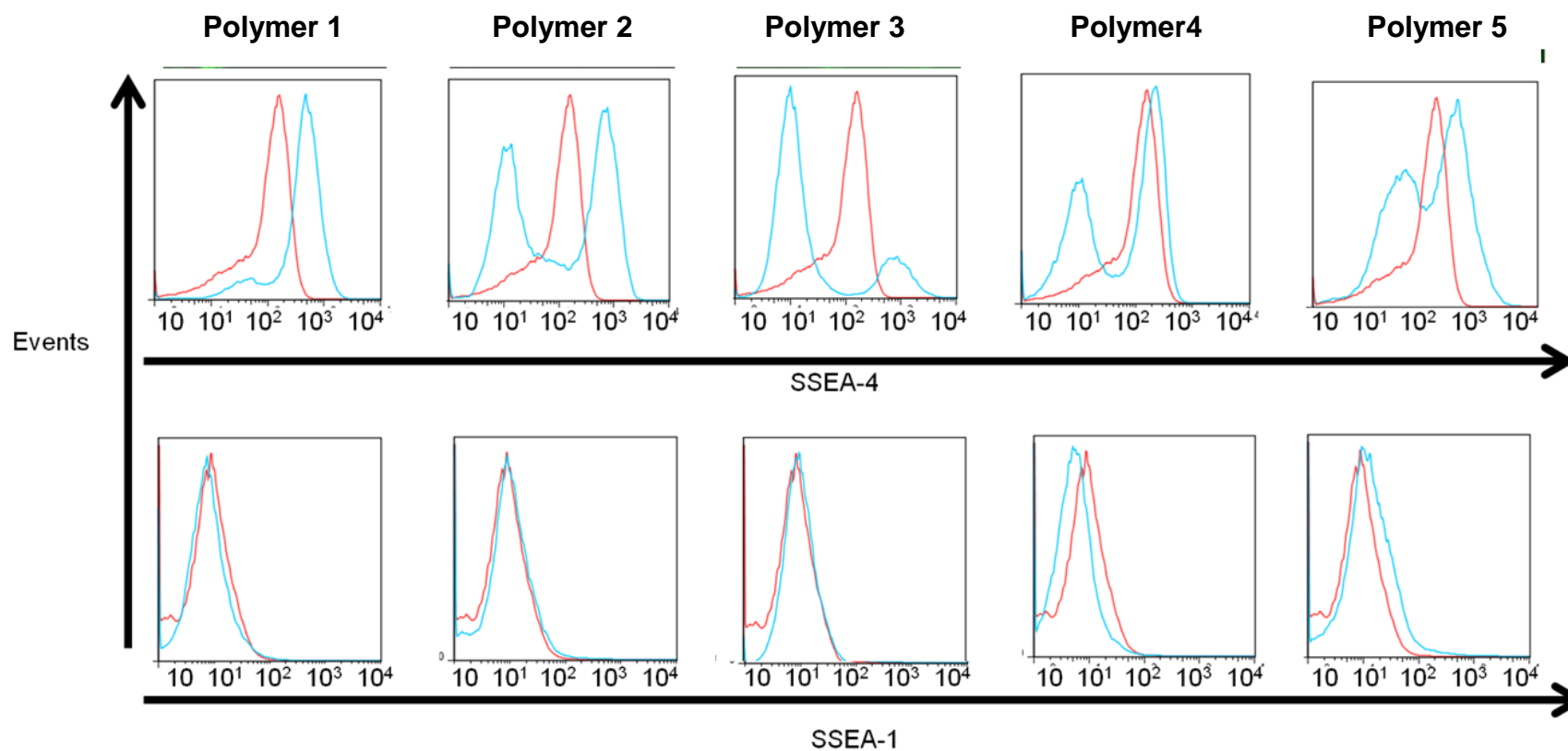


**Figure 2.6b:** Representative flow cytometry analysis of hESCs cultivated on Matrigel<sup>TM</sup> and polyacrylates 1-5 for 5 passages. hESC were stained for stem cell marker SSEA-1 and SSEA-4. Red population: Matrigel<sup>TM</sup>, blue population: cells on polymers.

## **2.6 Conclusion**

In summary, it has been shown that the high-density polymer approach takes polymer screening to a new level by allowing up to 7000 different polymeric materials to be simultaneously evaluated. The high-density array is suitable for cellular adherence studies and allows a more rapid and more uniform analysis of a larger number of polymers than previous high-throughput techniques and polymer microarrays. Up-scaling of the identified hit polymers confirmed the successful application of the high-density array approach. Immunocytochemistry and flow cytometry showed in a qualitative and a quantitative way the successful stem-cell maintenance on synthetic substrates. It has been shown in long-term studies that the best binding polyacrylates 1 (poly(4-*tert*-butylcyclohexyl acrylate-co-*n*-butyl methacrylate) (50:50)), 2 (poly(2-carboxyethyl acrylate-co-ethylene glycol methacrylate phosphate) (50:50)), 4 (poly(2-(diethylamino)ethyl methacrylate-co-ethylene glycol dicyclopentenyl ether acrylate) (50:50)) and 5 (poly(4-*tert*-butylcyclohexyl acrylate-co-*N,N*-dimethylacrylamide) (50:50)) allowed for fully xeno-free and feeder-free hESC cultivation which is desirable for clinical applications in the future.

## ***Chapter 3: Fabrication of Arrays of Polymer Gradients using Inkjet Printing***

*Parts of the presented work have been previously published as:*

A. Hansen, R. Zhang, M. Bradley; Fabrication of arrays of polymer gradients using inkjet printing. *Macromol. Rapid Commun.* doi:10.1002/marc.201200193.

The large variety of readily-available monomers and their possible combinations can give rise to a wide variety of polymeric materials with diverse physical and chemical characteristics and numerous applications.<sup>127-129</sup> By applying combinatorial or high-throughput chemistry techniques, polymeric materials and optimised formulations can be identified for specific applications in a rapid and effective manner.<sup>130-132</sup> For example, a true combinatorial approach using material gradients was applied in the discovery of polymer combinations with optimised dewetting and cellular interaction properties.<sup>133-135</sup> In contrast, non-combinatorial polymer microarray approaches offer discrete materials and not a combinatorial continuum (gradient) allowing thousands of defined, individual polymers to be investigated for the exploration of the link between polymer composition and cellular/protein adherence.<sup>24,136-138</sup> The generation of polymer microarrays with multiple polymer gradients, combining both high-throughput and combinatorial methods, is therefore of high interest.



### 3.1 Current Gradient Fabrications via Printing Techniques

Two types of gradients can be generated: concentration and composition gradients (Figure 3.1). Concentration gradients are easy to fabricate by changing the total quantity of deposited material along the gradient length. The composition of the material remains constant, subsequently, the properties of the deposited material do not change. In contrast, in composition gradients the quantity of deposited material remains constant but the mixture of which the material is composed of changes along the gradient length. This gives materials with distinct properties in different segments.

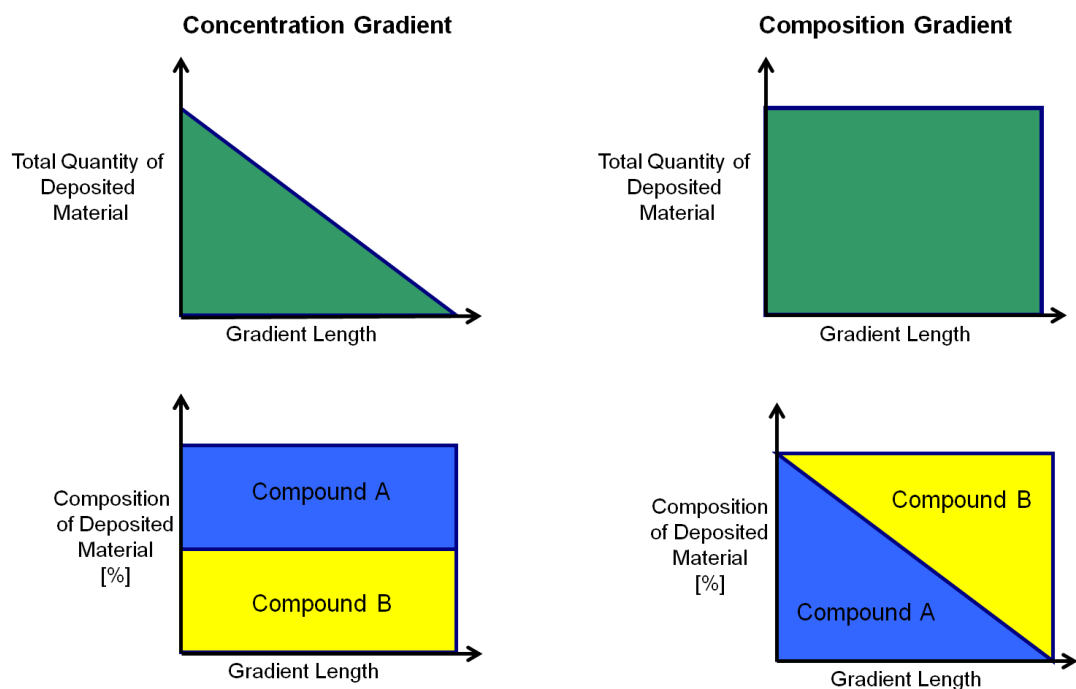


**Figure 3.1:** Types of Gradients. The concentration gradient is characterised by a “quantity change” of deposited material, the composition gradient leads to a controlled variation in the composition of the final compound. Here, the quantity of the material along the gradient length remains constant.

A number of methods have been developed to generate polymer gradients including plasma and electropolymerisation as well as photopolymerisation or controlled diffusion.<sup>140-146</sup> Moreover, microfluidic devices have been used to control the infusion rates of two monomer solutions to give polymer gradients while biomolecules can be attached upon such gradients by controlled physical adsorption or covalent immobilisation.<sup>142,147-154</sup> Microcontact and ink-jet printing techniques have been used to generate concentration gradients of proteins and small molecules or self-assembled monolayers (SAMs).<sup>155-157</sup> While biomolecule gradients have been used for the control of cellular alignment, stem cell differentiation or the determination of minimal inhibition concentrations of antibiotics, the functionalisation of surfaces with SAMs in a gradient manner have been applied for controlled droplet movement or the adsorption of proteins and cellular adhesion.<sup>133-161</sup> The generation of concentration gradients *via* printing techniques can be easily achieved as it requires the direct deposition of materials. In the case of microcontact printing, the type of gradient (radial or lateral) is controlled by the type of stamp used, whereas the steepness of the gradient can be varied by changing the contact time and the ink concentration (Figure 3.2).<sup>157,158</sup>

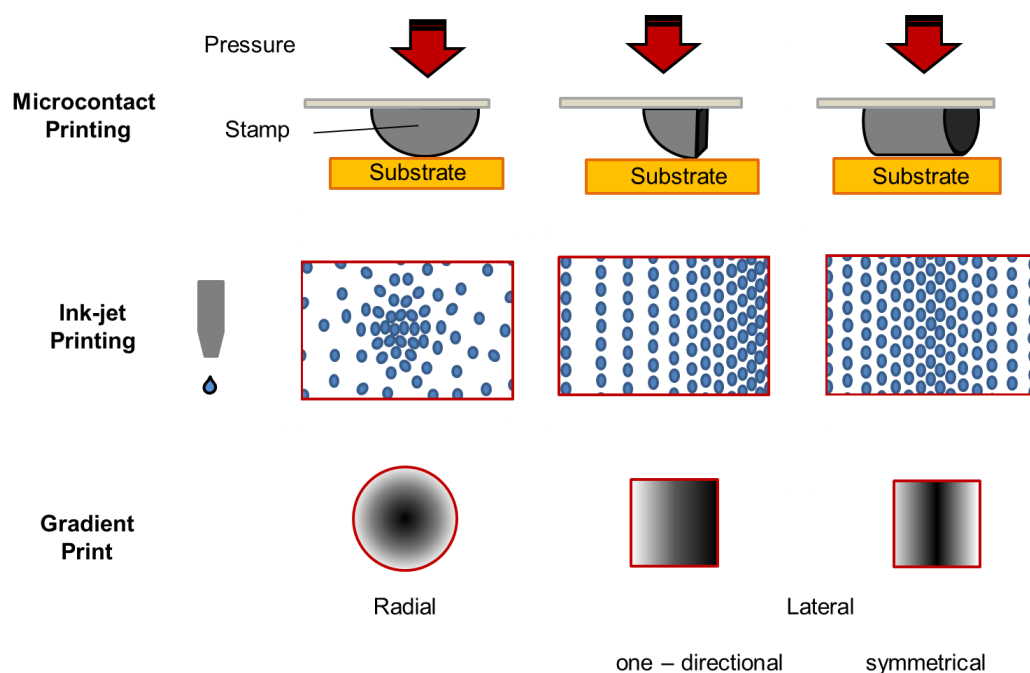


**Figure 3.2:** The generation of different concentration gradients using microcontact printing of elastomeric stamps or ink-jet printing. While for the contact printing approach different stamps are used to fabricate radial, one-directional or symmetrical lateral gradients, the ink jet printing approach makes use of the flexible deposition of single droplets via the nozzle.<sup>158,162</sup>

The fabrication of concentration gradients *via* ink-jet printing is carried out by printing features in close or far-proximity from each other (Figure 3.2). As the nozzle can be flexibly moved, the gradient fabrication is only limited by the drop sizes of the ink (resolution can be up to 1  $\mu\text{m}$ ).<sup>163</sup> The concentration gradient steepness and form can be easily modified by changing the printing pattern (Figure 3.2).<sup>158,162</sup>

In contrast, the generation of composition gradients *via* printing techniques is challenging as it requires not only a pure deposition but also a controlled mixing process that varies the content of the deposited material. As the generation of composition gradients on a microarray platform was required for the simultaneous evaluation of different polymer compositions for biological studies, a new technique had to be developed.

### **3.2 Cellular Migration**

In organisms, cells have to migrate in specific directions to certain locations in order to ensure proper organism development, growth and repair at site of injuries. Problems in cellular migration during development can lead to congenital abnormalities, and in adult life can cause vascular disease, tumour formation and metastasis.<sup>164-174</sup> For organised cellular movements to occur, external signalling molecules are important that direct specific cells to the different locations. While chemoattractants lead to a movement of the cells towards the higher concentration of the molecule, chemorepellents have the opposite effect. The term cellular migration can be divided into different forms, depending on how the cells are receiving the signals and how the cells move/ respond. The most studied type of cellular migration is chemotaxis, which describes a directed cellular movement along a soluble signal gradient. Diverse assays have been developed to measure chemotaxis in a qualitative and quantitative manner. The most applied method is the Boyden chamber assay, which was originally introduced for the analysis of leucocyte chemotaxis.<sup>172</sup> In this assay, two compartments of a chamber are separated by a microporous membrane (Figure 3.3). Cells are placed in the upper part and migrate through the membrane due to the chemotactic agents in the lower compartment, which diffuses into the upper part and creates a chemotactic gradient. After an appropriate incubation time, the cell amount in the lower part of the separating membrane can be analysed.

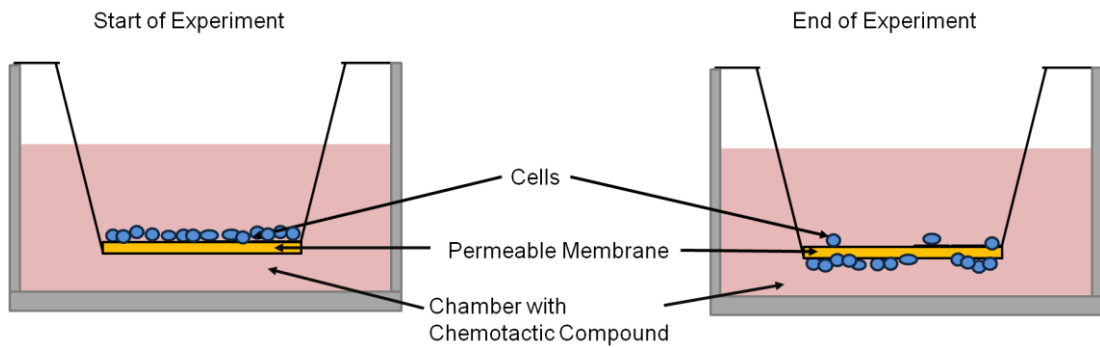


**Figure 3.3:** *Principle of Boyden Chamber. At the beginning of the experiment, the cells are in the upper chamber. The chemotactic compound in the lower compartment induces chemotaxis through the permeable membrane into the lower compartment. At the end of experiment, the membrane is fixed and the cell amount analysed.*<sup>172</sup>

Similar techniques include devices with chambers arranged side-by-side, connected via a narrow channel which allows the cellular migration from one chamber into the other (Dunn and Zigmond Chamber) or flow-based microdevices which create stable concentration gradients and investigate the cellular movements by live microscopy.<sup>173-176</sup> Other types of cellular migrations in the liquid phase are necrotaxis (necrotic or apoptotic cells release the chemoattractant molecules) and chemokinesis (random cellular movement without directional component) which can be investigated with the same types of apparatuses as described for chemotaxis.<sup>164-169</sup> As these assays are simple and commercially available, the investigation of cellular movement in liquid phases is well understood.

A different form of cellular movement is haptotaxis which describes the directed cellular movement on a surface with bound or expressed gradients of signal molecules. The most common haptotactic surface is the extracellular matrix (ECM) which can control the cellular movement of certain cell types by expressing or binding specific ligands. The formation of new blood vessels (angiogenesis) or the directed movement of neuron cells are examples for haptotaxis in biological

systems.<sup>170,171</sup> For the investigation of haptotaxis, Boyden chambers are commercially available which have permeable membranes that are coated on one side with widely studied ECM proteins such as fibrinogen or collagen.<sup>177-179</sup> However, the generation of a tailored high-throughput chemoattractant/repellant microarray is of interest for the investigation of biological events that depend on proteins bound to the ECM, which are not constantly present and/or are not widely studied, such as semaphorins.

### ***3.3 Semaphorins as Chemoattractants/Chemorepellents in Cellular Migration***

Semaphorins are a family of signaling proteins which are important in the axon guidance of neuron cells, immune response, vascular growth and tumor progression.<sup>180</sup> The protein family consists of secreted and transmembrane proteins that are present in invertebrates, vertebrates and viruses. The molecular size of the semaphorins varies between 400 and 1000 amino acids.<sup>181,182</sup> All semaphorins are characterised by a highly conserved domain at the *N*-terminus (sema-domain) which is about 500 amino acids long and contains 14 to 16 conserved cysteine residues and a *N*-glycosylation site.<sup>183-185</sup> Semaphorin 3F (Sema3F) and semaphorin 3A (Sema3A) are chemoattractants or repellents (respectively) for oligodendrocytes in the central nervous system (CNS).<sup>186</sup> This type of cell is responsible for the formation of the insulating myelin sheaths on axonal segments that are essential for fast and effective nerve conduction (Figure 3.4).

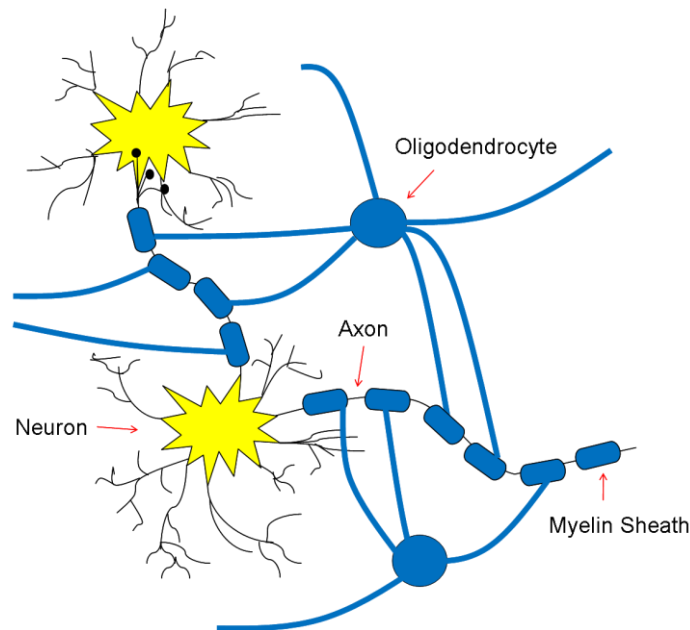


**Figure 3.4:** *The interaction between neuron cells and oligodendrocytes in the central nervous system. Depending on the area of the CNS and the species, the amount and thickness of myelin sheaths formed by the oligodendrocytes varies.*<sup>181</sup>

In case of demyelination, e.g. by the autoimmune disease multiple sclerosis, the axons can no longer effectively conduct nerve signals, which leads to physical and cognitive disabilities.<sup>186-188</sup> So far, there is no cure for such demyelinating diseases but it is hoped that further investigations of the migration of oligodendrocytes and their precursor cells (OGPCs) by Sema3A and Sema3F will provide a better understanding of the biochemical processes.

While Sema3A inhibits migration of oligodendrocytes and their precursor cells during development, Sema3F is a chemoattractant for these cells. After pathology, there is a recapitulation of these pathways, and Sema3A production by cells in demyelinated lesions inhibits OGPC migration into lesions and their maturation into myelinating oligodendrocytes.<sup>189-191</sup> The comprehension of the concrete interplay of both semaphorins is the key for understanding how myelin repair in multiple sclerosis works and might lead to a therapy to improve remyelination in the disease.

To investigate the effect of the semaphorins in more detail, a haptotaxis assay based on a polymer gradient microarray with Sema3A and Sema3F attached was explored. The ideal polymer would support large numbers of OGPCs while not exerting a migration effect on the cells.

### ***3.4 Generation of Microarrays with Polymer Gradient Lines (Composition Gradients)***

To generate multiple gradient lines on a single microscope glass, ink-jet printing was chosen as the fabrication method of choice as it offers rapid and precise deposition of material in a very flexible manner. To obtain lines with a gradient of monomer compositions, a similar technique to that used for the spotted microarrays was applied (see Chapter 2, Figure 3.5) where a “masked” fluoruous coating was used to determine the specific shape of the deposited polymers as well as reducing or limiting cellular attachment. The first step in the process consisted of masking the glass slide by printing lines (5 mm x 0.5 mm) of 20% aqueous sucrose (w/v) (Table 3.1, Figure 3.5).



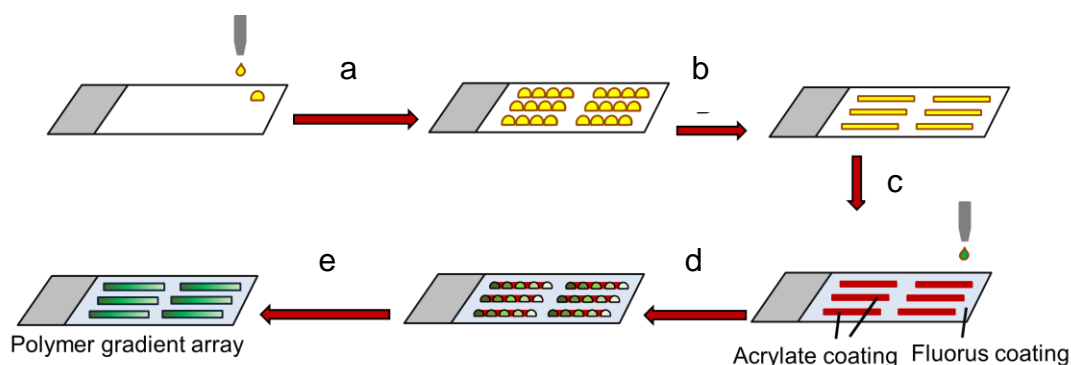


**Figure 3.5:** The fabrication of polymer gradient arrays. **a)** Sugar mask printing (20 % w/v) defines the polymer gradient length and width. **b)** Sugar spots in close proximity (200  $\mu\text{m}$ ) merge to form lines. **c)** The microscope slide is made hydrofluorous by treating with (tridecafluoro-1,1,2,2-tetrahydrooctyl) dimethylchlorosilane. After removal of the mask (water wash), the lines are derivatized with 3-(trimethoxysilyl)propyl methacrylate. **d)** The acrylate monomers are printed in a gradient manner on the functionalised lines. **e)** After compression, irradiation and incubation the polymer gradient array is generated.

The glass slide was coated with (tridecafluoro-1,1,2,2-tetrahydrooctyl) dimethylchlorosilane and the sucrose masking removed. The exposed glass surfaces were functionalised with 3-(trimethoxysilyl)propyl methacrylate, enabling the anchoring of the *in situ* synthesised polymers. Polymer gradients were generated by printing monomers together with a crosslinker and a photoinitiator across the acrylate functionalised surface. After compression of the printed features with a second hydrofluorous slide, the slides were UV irradiated for 20 min and incubated at 50 °C for 16 h to ensure complete polymerisation. To identify the optimal compression technique and printing scheme for the generation of linear gradients, different combinations of initiator and monomer ratios of 2-hydroxyethyl methacrylate and ethylene glycol methacrylate phosphate were printed and evaluated (see Table 3.1). The phosphate monomer allowed phosphorus (2p) analysis *via* X-Ray photoelectron spectroscopy (XPS). As shown in Figure 3.6, the compression and printing scheme is crucial for the successful generation of linear gradients.

**Table 3.1:** Printing Schemes

Line	Masking Procedure	Polymer Gradient Generation							
		Print	Compounds	Deposited Drops on Position along Gradient Length [ $\mu\text{m}$ ]					
				417	1250	2083	2916	3750	4583
Length: 5 mm Width: 0.5 mm	25 spots (each 3 drops of 20 % (w/v) sucrose) printed 0.2 mm apart in 3 lines (each line 0.2 mm apart)	1	Monomer A	36	30	0	0	0	0
			Monomer B	0	0	0	0	30	36
			Crosslinker	18	15	0	0	15	18
			Photoinitiator	9	9	0	0	9	9
			Redoxinitiator <sup>i</sup>	0	0	8	8	0	0
		2	Monomer A	16	8	4	2	1	0
			Monomer B	0	1	2	4	8	16
			Crosslinker	5	5	5	5	5	5
			Photoinitiator	3	3	3	3	3	3
			Redoxinitiator <sup>i</sup>	8	8	8	8	8	8
		3	Monomer A	19	15	12	8	3	0
			Monomer B	0	3	8	12	15	19
			Crosslinker	5	5	5	5	5	5
			Photoinitiator	2	2	2	2	2	2
			Redoxinitiator <sup>i</sup>	0	0	0	0	0	0

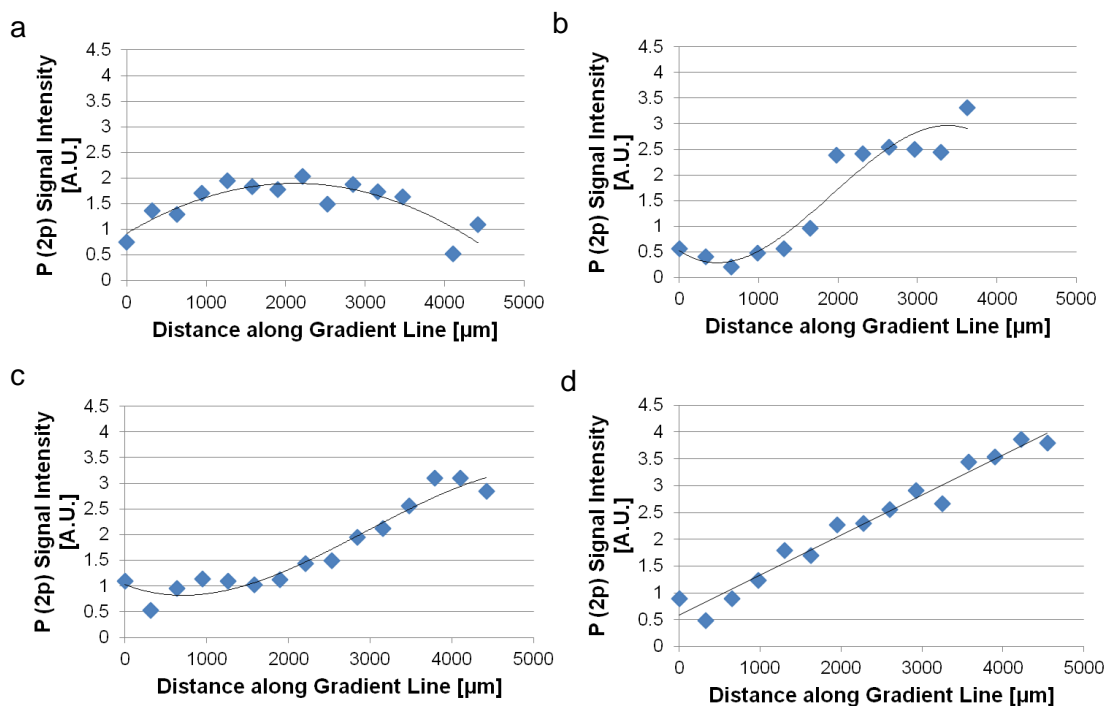


**Figure 3.6:** XPS analysis of polymer lines generated with 2-hydroxyethyl methacrylate and ethylene glycol methacrylate phosphate. **a)** Printing scheme "1" with fixation by paper clamps; **b)** printing scheme "1", **c)** printing scheme "2" using redox-and photoinitiator, **d)** printing scheme "3" using only photoinitiator.

The first printing schemes consisted of monomers being deposited at either end of the lines separated by a space of 2500 μm apart within which initiator drops were placed. It was expected that compression of the printed features would result in blending of the monomer solutions in the centre, giving a linear polymer gradient. For compression, a second fluorinated slide was placed on top of the printed array. To ensure further fixation, paper clamps were used after the first printing attempt of printing pattern 1 (Figure 3.6a). However, this fixation resulted in a high pressure applied and led to uncontrolled blending of the monomers and, subsequently, no gradient formation. Compression without further fixation gave phosphorus-profiles with plateaus but virtually no central mixing and hence no linear gradient formation

(Figure 3.6b). Printing schemes with a continuous increase of the deposited monomers along the lines gave linear gradient profiles (Figure 3.6c and d). Gradients generated with a smaller amount of initiator gave a slightly more linear profile which might be due to less diffusion effects (Figure 3.6d). To ensure that the gradients generated *via* printing scheme “3” were independent of the location on the microscope slide, gradient lines on the centre and on edges of the microscope slide were generated and analysed *via* XPS (n=7, Figure 3.7a). Visualisation of the gradient was also accomplished by adding 5(6)-carboxyfluorescein to one of the monomer solutions prior to printing and polymerisation (Figure 3.7b) allowing the composition of the polymer to be known simply by determining its location along the gradient (Figure 3.7, Appendix Figure1).

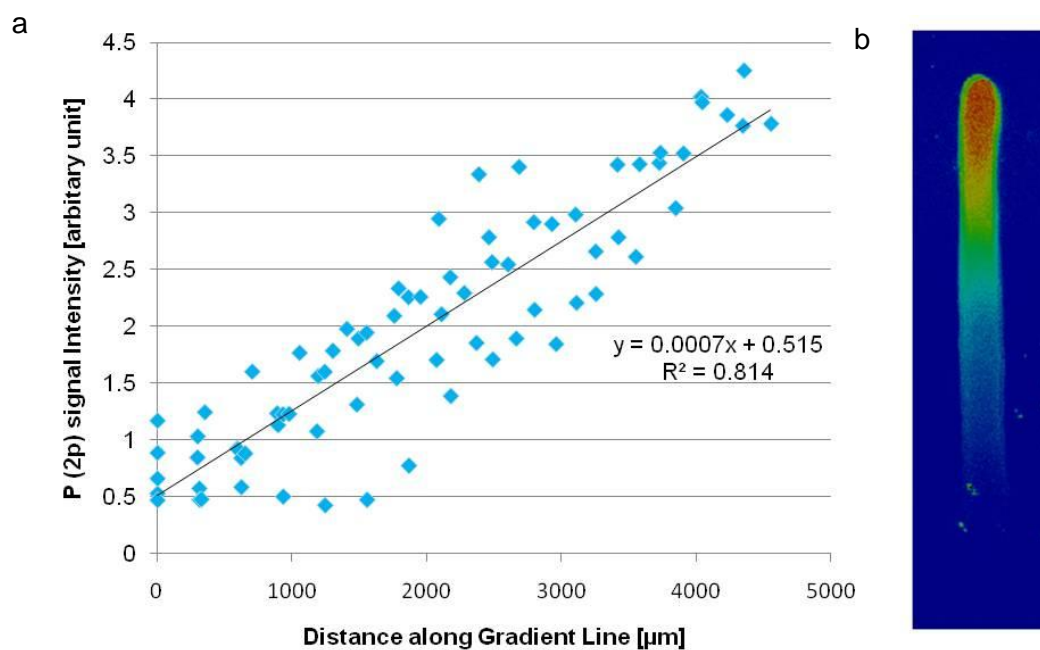


**Figure 3.7:** **a)** The average XPS data measurements of the P (2p) signal intensity along the gradient array consisting of ethylene glycol methacrylate phosphate and 2-hydroxyethyl methacrylate (B6 and B22) (n=7). **b)** Visualisation of the gradient prepared with (2-diethylamino)ethyl acrylate and 2-hydroxyethyl methacrylate mixed with 1 % (w/v) 5(6)-carboxyfluorescein.

An array with 84 polymer gradients each consisting of two monomer combinations with (2-diethylamino)ethyl acrylate (monomer A) and a variety of second acrylate and acrylamide monomers (B1-23 with different functional groups) was fabricated (Figure 3.8).

Monomer print and Image of Array

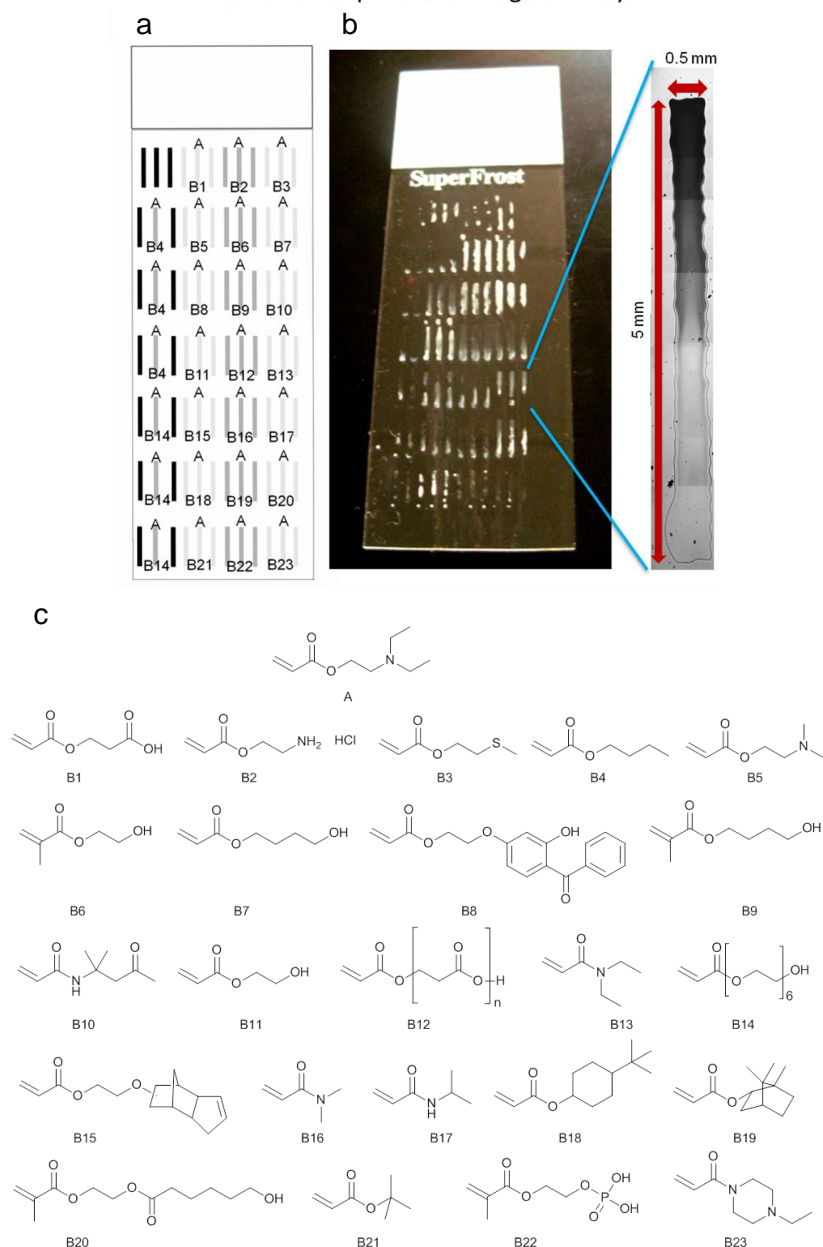


**Figure 3.8:** *a) Polymer gradient array: Grey lines represent triplicates of two-component gradients of monomer A and monomers B1-23. The black lines represent XPS-control gradients consisting of monomers B22 and B6 (ethylene glycol methacrylate phosphate and 2-hydroxy-ethyl methacrylate). b) Image of polymer gradient array with a mosaic of a polymer gradient line (5 mm x 0.5 mm). c) Monomers used for the preparation of the gradient arrays.*

### 3.5 Cellular Binding Studies on Polymer Gradient Arrays

The adhesion and growth of the suspension cell line K562 on the polymer gradients was explored. After 3 d incubation, the K562 cells were fixed and counted along the gradients (Figure 3.9a) giving a clear understanding of how the different types of monomer affect cellular adhesion and growth. An overview of the cellular adherence on all different gradient line compositions is given in Appendix Figure 3.1. In accordance with previous studies, monomers A and B5 ((2-dimethylamino)ethyl acrylate) demonstrated high cellular adhesion (up to 10000 cells/mm<sup>2</sup>, Figure 3.9b) in all ratios.<sup>134</sup> According to the previous studies, the best binding co-polymers consisted of a hydroxyl monomer and an amine-monomer in a ratio of 70:30 (4000 cells/mm<sup>2</sup>, Figure 3.9c). The gradient arrays showed that the best binding material for K562 was a composition of monomer A and monomer B12 (2-carboxyethyl acrylate oligomer) in a ratio of 40:60, with over 15000 cells/mm<sup>2</sup> bound (Figure 3.9d), while the related monomer B1 (2-carboxyethyl acrylate) did not demonstrate any increasing cell binding effect (Figure 3.9e).<sup>134</sup> Adherence studies carried out with the adherent cell line (HeLa) showed that a high content of alcohol containing monomers e.g. (2-hydroxyethyl methacrylate (> 90%) and 4-hydroxybutyl acrylate (> 50%) and certain amides (*N*-isopropylacrylamide (> 60%) and 2-diethylacrylamide (> 75%) were found to improve HeLa cell binding (Figure 3.10).<sup>24§</sup> These results demonstrate the successful application of the polymer gradient arrays and give detailed information about how far the variation in monomer content is tolerated by cells.

---

<sup>§</sup> The analysis of the adherent cell line HeLa was jointly carried out with Dr. Rong Zhang.

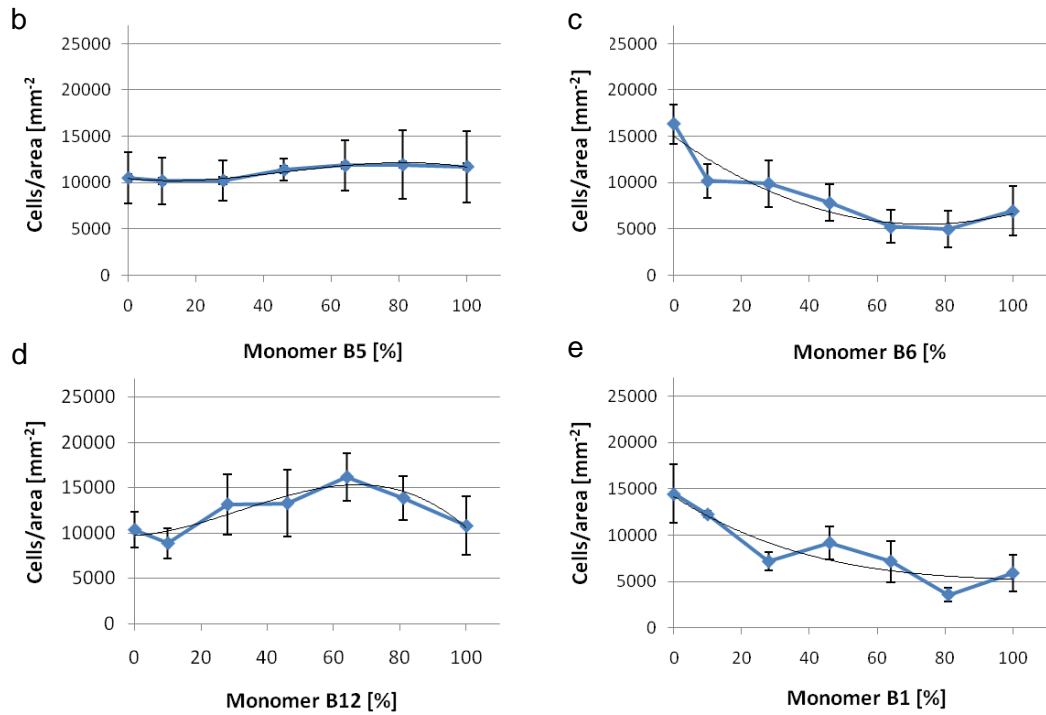
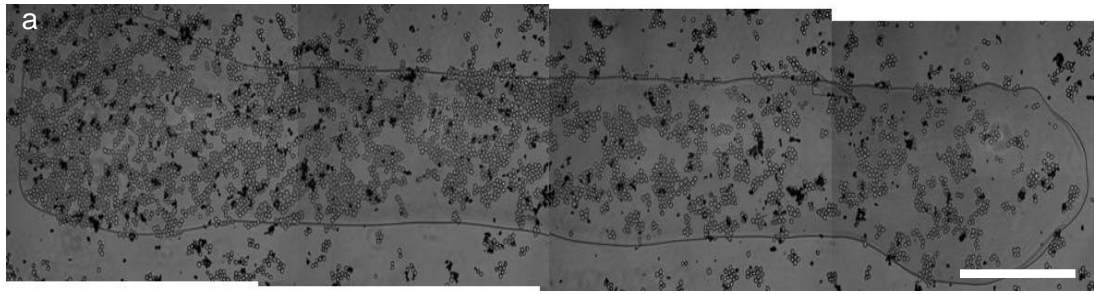


**Figure 3.9:** *a*) Mosaic of a typical polymer gradient with K562 cells attached (high-content imaging of four segments 5 mm x 0.5 mm, scale bar = 0.5 mm). *b-e*) Representative gradient profiles of the number of bound cells as a function of monomer composition. Monomer A is (2-diethylamino)ethyl acrylate, monomer B is (2-dimethylamino)ethyl acrylate (*b*); 2-hydroxyethyl methacrylate (*c*); 2-carboxyethyl acrylate oligomer (*d*); 2-carboxyethyl acrylate (*e*)(standard deviation,  $n=6$ ).



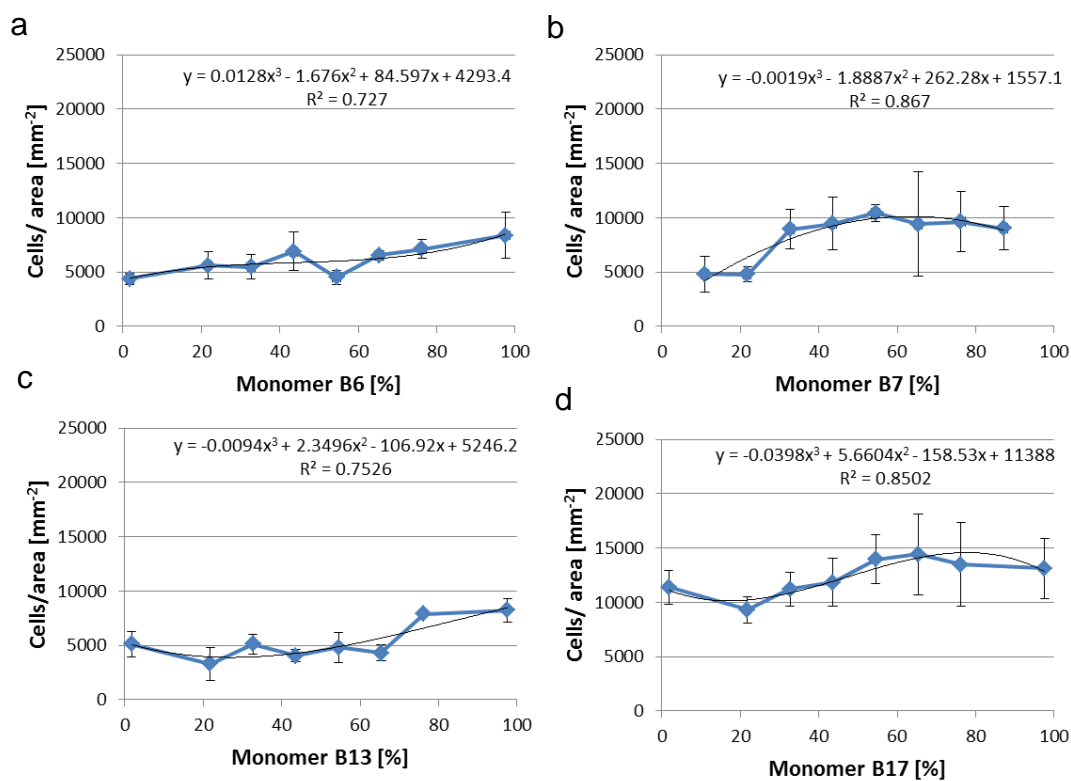


**Figure 3.10:** Cell binding profiles of HeLa cells across polymer gradients. Monomer A is (2-diethylamino)ethyl acrylate, monomer B is **a)** 2-hydroxy ethyl methacrylate; **b)** 4-hydroxybutyl acrylate; **c)** N,N-diethyl acrylamide; **d)** N-isopropylacrylamide (standard deviation,  $n=3$ ).

### 3.6 Generation of Molecule Gradients (Concentration Gradients)

The polymer gradient arrays allow the further modification and generation of small molecule, peptide or protein concentration gradients. By applying common activation strategies, polymer gradients with 2-carboxyethyl methacrylate or the active ester *N*-acryloxysuccinimide can be used to generate concentration gradients (Figure 3.11).

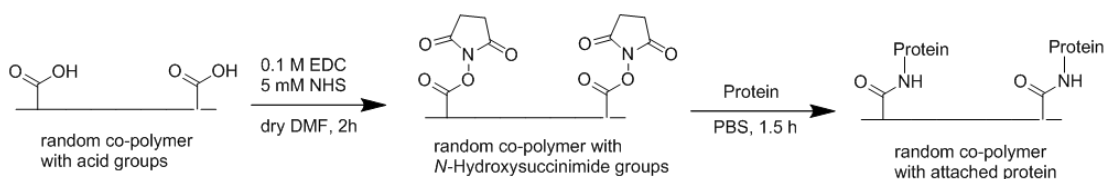


**Figure 3.11:** Coupling-scheme for attaching proteins to an acid functionalised polymer substrate. This strategy can be used for any molecule containing an amine-group.

To generate a gradient of a readily visualised dye, polymer gradients composed of *N*-acryloxysuccinimide and 2-hydroxyethyl methacrylate were fabricated and derivatisation with 6-aminofluorescein to give fluorescent gradient lines (Figure 3.12).

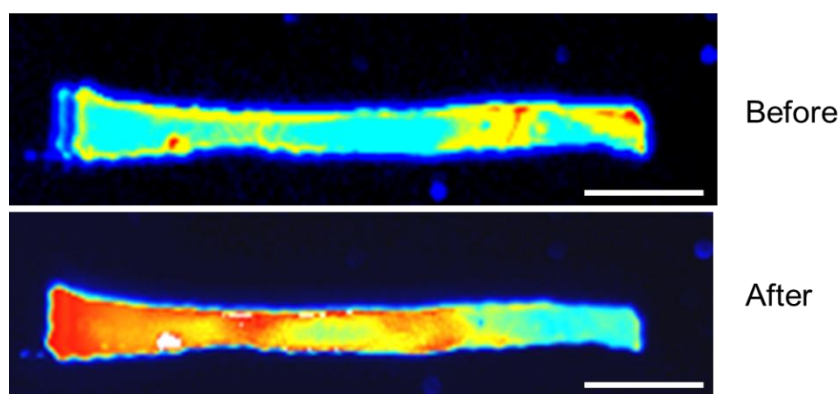


**Figure 3.12:** Visualisation of the polymer gradients prepared from *N*-acryloxysuccinimide and 2-hydroxyethyl methacrylate shown before and after the coupling with 6-aminofluorescein. Scale bars = 1mm.

### **3.7 Generation of a Semaphorin Haptotaxis Array for OGPCs\*\***

Polymer gradients with 2-carboxyethyl methacrylate were the basis for the protein gradients as they enable the immobilisation of proteins in a gradient manner by applying common peptide coupling strategies. To ensure that the migration behaviour of OGPCs is independent from the polymer and only controlled by the protein, preliminary studies with polymer gradient lines containing 2-carboxyethyl methacrylate as a monomer were carried out. It was determined that gradient lines composed of *tert*-butyl acrylate or *tert*-butylcyclohexyl acrylate with 2-carboxyethyl methacrylate were the best substrate for cell binding showing constant numbers of bound cells along the whole gradient length. For the generation of a protein gradient arrays with Sema3F, the polymer gradients were generated as described before (Chapter 3.4.) and the acid groups were activated by incubating the arrays with a mixture of 1-ethyl-3-(3-dimethylaminopropyl) carbodiimide, 0.1 M and *N*-hydroxysuccinimide (5mM) in dry dimethylformamide (DMF) for 2 h. This was followed by the coupling of Sema3F (100 µg/mL) in PBS for 1.5 h (Figure 3.11). The successful coupling was verified by fluorescence imaging before and after the coupling and the subsequently binding to a specific, Cy5 tagged Sema3F antibody (Abcam, UK) (Figure 3.13).

---

\*\* The cellular binding studies of OGPCs in this chapter were carried out by Jonathan Murnane and Dr. Anna Williams. They are also part of the Master Thesis of Jonathan Murnane.

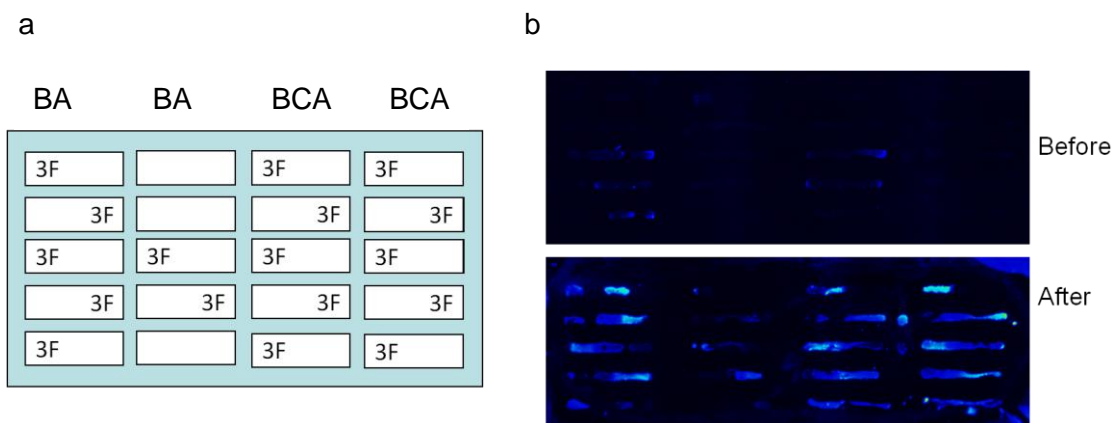


**Figure 3.13:** *Sema3F* gradient microarray **a)** Layout scheme, 3F = high concentration of *Sema3F* on that particular end of the gradient, Gradient monomers: 2-carboxyethyl methacrylate with BA=tert-butyl acrylate or BCA=tert-butylcyclohexyl acrylate. Lines without *Sema3F* served as negative controls. **b)** Protein microarray lines before and after incubation with a Cy5-labelled *Sema3F* antibody.

The fluorescence distribution of each gradient line was calculated by measuring the fluorescence intensity at 15 adjacent areas along each line. As it can be seen in Figure 3.14, the resulting graphs give a linear relation between fluorescence intensity and calculated *Sema3F* content bound to the polymer gradient. As negative controls served polymer gradients without *Sema3F* (Figure 3.14c). All fluorescent studies were independent of the monomer composition of the polymer gradients.

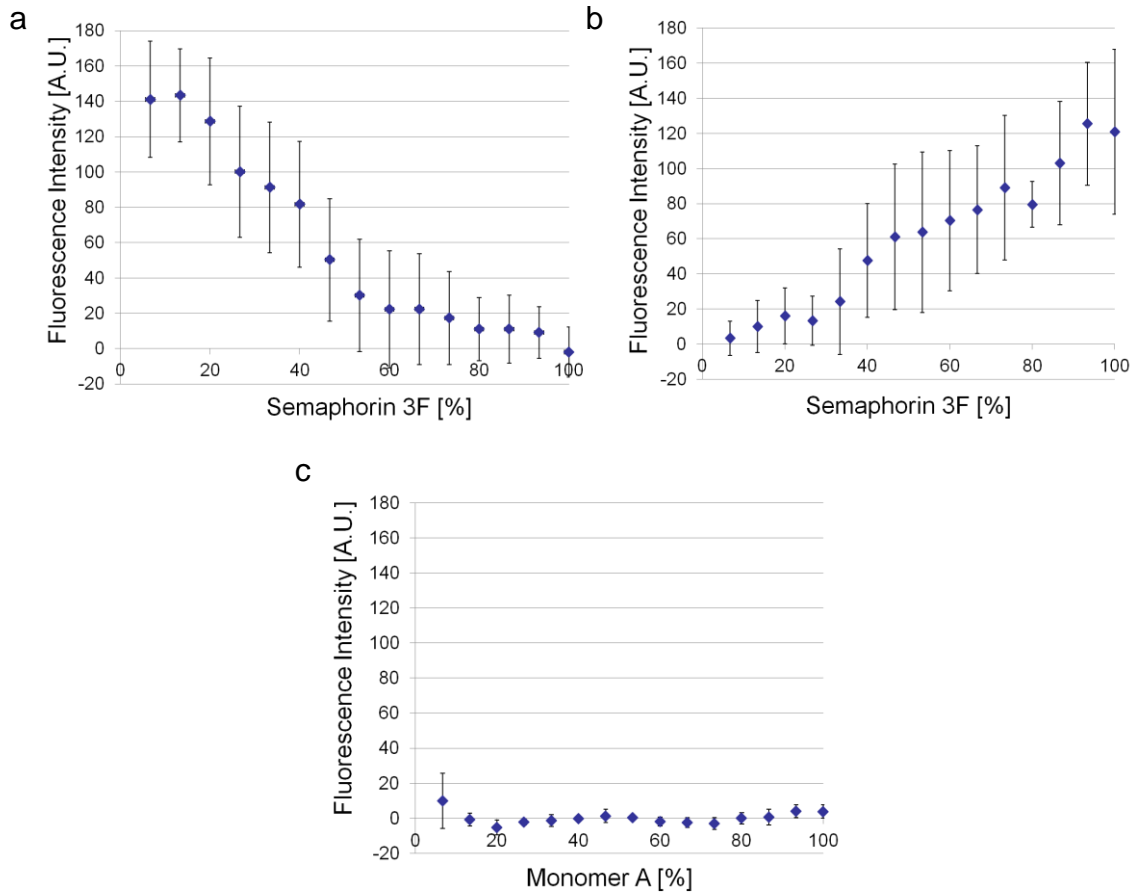


**Figure 3.14:** *Fluorescence Intensity profiles for the gradient lines after semaphorin 3F antibody staining. a). Gradient lines with increasing Sema3F content (n=10), b) gradient lines with decreasing Sema3F content (n=7), c) negative control - gradient without Sema3F coupled to the polymers (n=3).*

After establishing the successful coupling of Sema3F onto the polymer gradients, rat OGPCs were incubated onto the protein gradient arrays for 18 h. After washing and fixing, the cells were counted at each end of the gradient lines. On the control gradients and at the end of the gradient line without Sema3F approximately 400 cells/ mm<sup>2</sup> adhered. In contrast, those gradient line ends with the protein attached to it, gave binding of about 600 cells/mm<sup>2</sup> (Figure 3.15).

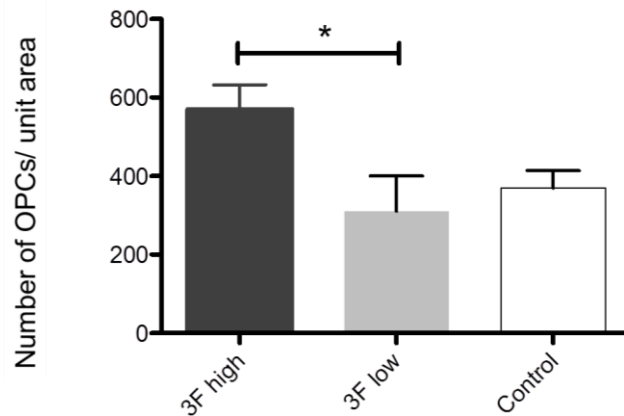


**Figure 3.15:** Cell binding of OGPCs on the Sema3F gradients. Gradient ends with a high concentration of Sema3F bound significantly more cells than those ends with a low protein concentration.  $P < 0.01$  by one-way ANOVA.

Since the difference between the cellular binding on high and low protein concentrations is statistically significant ( $P < 0.01$  by one-way ANOVA), the result underlines the chemoattractant effect of Sema3F on OGPCs in *in vitro* studies. To monitor the migration of the cells on the protein gradients, images of the end of the gradients were taken every 10 min after the cells were plated. As shown in Figure 3.16, cells could be seen migrating towards the higher protein concentrations.

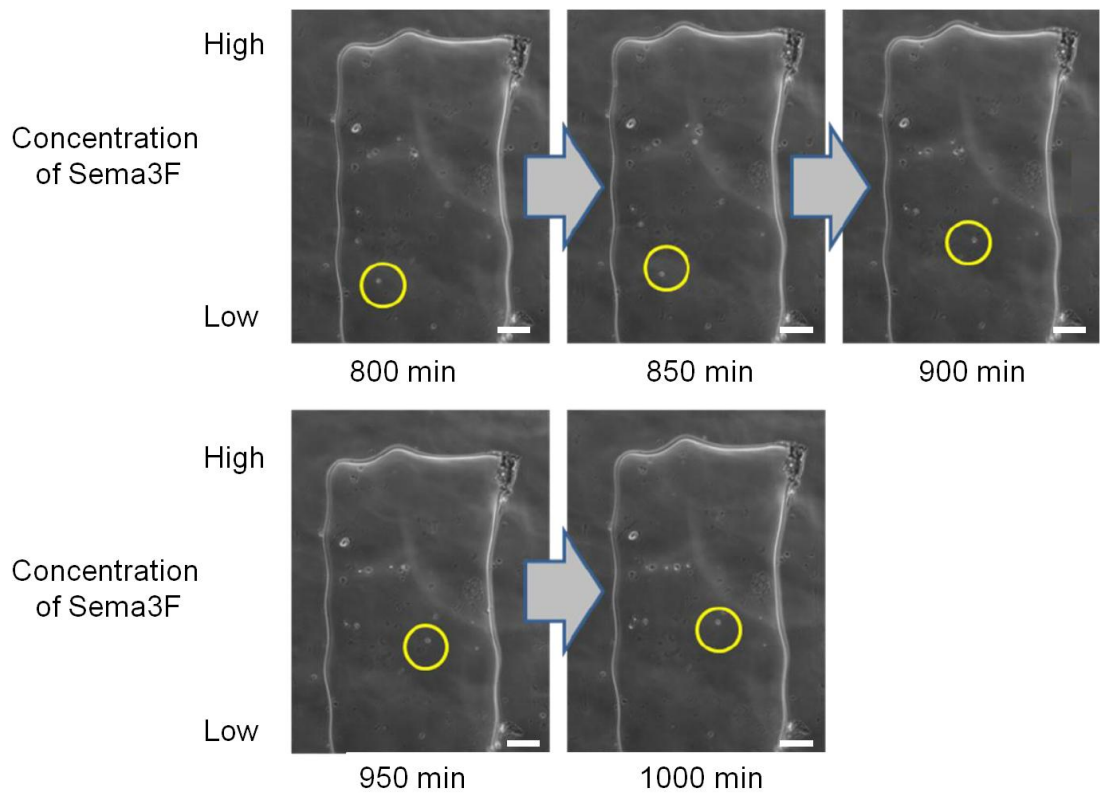


**Figure 3.16:** Time-lapse recording of OGPCs at one end of a Sema3F gradient. Highlighted in a yellow circle is a cell migrating towards the higher protein concentration. Scale bars = 100  $\mu\text{m}$ .

To date, studies testing the chemotactic effect of Sema3F on oligodendrocytes or axon growth cones have been carried out in solution only. Thus, this is the first haptotaxis investigation for this system. In the brain, the protein Sema3F is bound to the ECM, in the presented system, a polyacrylate mimics the ECM to which the Sema3F is bound, thus offering a synthetic mimic of Sema3F binding to concentration dependency.

### **3.8 Conclusion**

This study served to illustrate the ability of polymer gradient arrays to determine the optimal combination of two acrylate monomers in cellular adherence studies. Cellular binding results corroborate previous polymer microarray investigations with the gradient array identifying the best binding combinations but, due to the continuum approach, explored in detail the precise composition of monomers which leads to the highest cell binding. Furthermore, it has been shown that the arrays can be readily modified to allow the fabrication of gradients with controlled characteristics. Thus, coupling with proteins could be achieved and used for an investigation of processes such as controlled cellular migration. For the generation of a haptotaxis assay, two polymers from a carboxy-gradient line array were identified which adhered OGPCs but did not exert migration preferences themselves. By coupling the chemoattractant Sema3F onto the polymers, protein concentration gradients were generated that successfully lead to the migration of OGPCs. This presents the first haptotaxis assay for this protein system and might be useful for further *in vitro* studies to fully understand multiple sclerosis.



## ***Chapter 4: Polymers for Platelet Activation and Sorting of Megakaryocytic Cell Lines***

*Parts of the presented work have been previously published as:*

A. Hansen, L. McMillan, A. Morrison, J. Petrik, M. Bradley; Polymers for the rapid and effective activation and aggregation of platelets. *Biomaterials* **2011**, 32, 7034-7041.

Platelets play a central role in mediating haemostasis and thrombosis by reacting rapidly to vascular injuries with platelet adherence and activation leading, finally, to the formation of a “haemostatic plug”.<sup>192</sup>

While most biocompatibility studies on platelets have focussed on materials which avoid platelet activation for potential use in transplantation, fast and effective platelet aggregation is desired and even essential for haemostasis of (severe) injuries. For centuries, cauterisation has been the prime method for haemostasis.<sup>193</sup> The first material specially tailored for bleeding control was oxycellulose, developed in 1942 and is still in use today.<sup>194</sup> Since the first haemostatic agent, new materials such as fibrin sealants or surgical stapling have been developed.<sup>195,196</sup> While naturally derived products based on fibrin, chitosan, collagen or plant extracts offer effective haemostasis with mostly degradable end-products, the extraction and purification steps are time- and cost-intensive.<sup>197-199</sup> An alternative to these products could be a synthetic polymer, which would offer advantages such as tuneable structure and shape, ease of functionalisation, synthesis and purification, prolonged long-life times

and consistency of generation while leading to rapid, controllable and efficient platelet activation.

#### 4.1 Platelets - a Special Type of Cell

The usual platelet level in the peripheral blood of humans is about  $150\text{--}400 \times 10^9$  cells/L.<sup>200</sup> For up to ten days, platelets circulate in the blood system until they are destroyed and replaced by new “cells”. Platelets are anucleated and vary in size (2-4  $\mu\text{m}$ ) and density. These characteristics are independent of platelet age and can be explained by a closer look at their formation process.<sup>201</sup>

#### 4.2 Platelet Formation

The mechanism by which platelets are produced has been studied since 1906 when Wright discovered that megakaryocytes are the giant precursor cells of the anuclear platelets.<sup>202</sup> As platelet formation and release cannot be investigated in detail *in vivo*, cultivated megakaryocytes from bone marrow and permanent cell lines of megakaryocytic lineage such as MEG-01 have been used to study the exact process *in vitro* (Figure 4.1).<sup>203</sup>

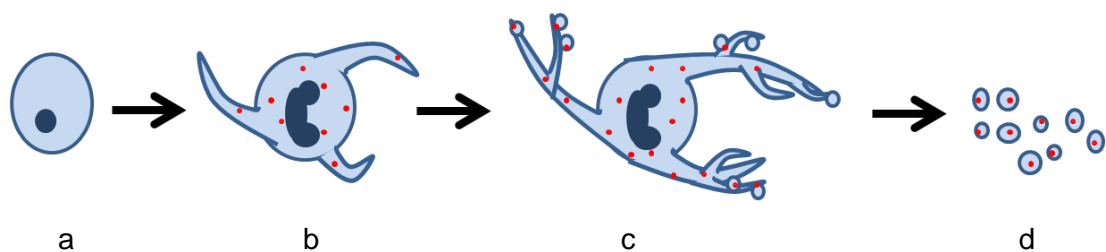


**Figure 4.1:** The maturation process of megakaryocytes. **a)** Premature cell; **b)** polyploid cell producing platelet specific compounds; **c)** mature megakaryocyte with proplatelets; **d)** release of platelets.<sup>203</sup>

While megakaryocytes mature, they undergo endomitosis – a process of repeated cycles of DNA replication without cell division. As a result the cells become polyploid and increase in size until they are approximately 100-150  $\mu\text{m}$  in diameter.<sup>204-206</sup> In addition, the cells build and store platelet specific components such as von Willebrand's factor receptor (vWFR) and the fibrinogen receptor complex gpIIb/IIIa.<sup>16</sup> After achieving a “yet-to-be-ascertained state of preparedness”<sup>16</sup>, the megakaryocytic cytoplasm begins to generate long pseudopodia whose ends get decorated with platelet-sized swellings (proplatelets).<sup>207</sup> The final platelets are released from the ends of the pseudopodia due to shear forces in the bone marrow or the pulmonary circulation (Figure 2).<sup>208,209</sup> During this process, each megakaryocyte releases hundreds to thousands of platelets into the pulmonary circulation. All platelets vary in shape and in density of the different storage components depending on the distribution of these within the mother megakaryocyte.<sup>201</sup> In cultivated megakaryocytic cell lines, incubation with thrombopoietin or phorbol myristate acetate resulted in a proportion of cells becoming polyploid and releasing platelet like particles.<sup>203-207</sup>

### **4.3 Platelet Activation**

After injury to blood vessels, a haemostatic plug is formed consisting predominately of platelets that undergo a process called activation. Generally, there are three phases of platelet activation (primary haemostasis) that stop bleeding within seconds to minutes (see Figure 4.2).<sup>207</sup>

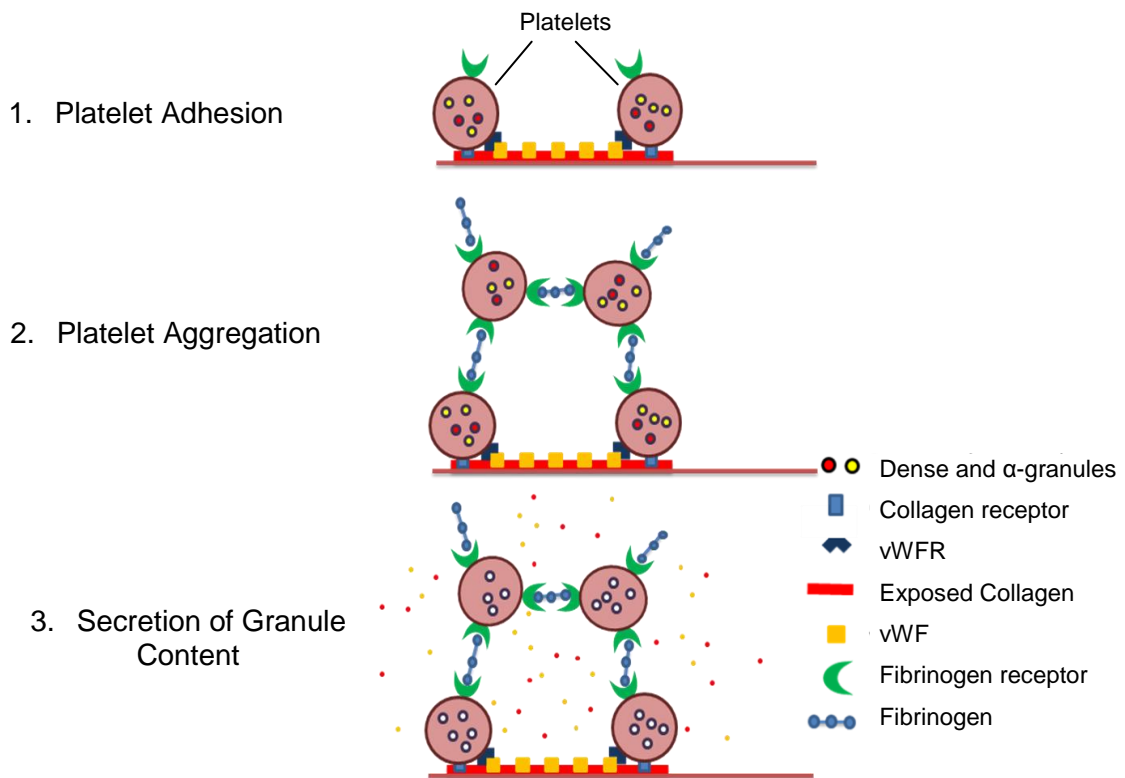


**Figure 4.2:** Primary haemostasis and its three phases of platelet activation (adhesion, aggregation and granule content secretion) leading to a platelet plug.<sup>207</sup>

The initial phase of platelet activation is platelet adhesion in which platelets bind to sub-endothelial matrix proteins like collagen, von Willebrand's factor (vWF) or fibrinectin which are exposed after injury.<sup>210,211</sup> Artificial surfaces such as vascular grafts that can bind protein stimuli for platelets (e.g. collagen or vWF) can also initiate adherence. In this case, the amount and distribution of adsorbed proteins depends on the artificial surface and has an impact on platelet adhesion.<sup>212,213</sup>

In the second step of platelet activation, self-association of platelets into a plug can be observed - the so called platelet aggregation step. Thereby, fibrinogen interacts with the fibrinogen receptor complex gpIIb/IIIa on the platelet surface. This is

enabled by high calcium concentration, which holds the glycoprotein complex together and enables the binding to fibrinogen.<sup>210,214</sup>

In the last step of primary haemostasis, the platelets' granule contents are released into the extracellular space. The two major granules in platelets are the dense and  $\alpha$ -granules which contain specific mediators (e.g. adenosine diphosphate (ADP)) and proteins (like vWF or fibrinogen) that contribute to stable platelet plug formation.<sup>215-</sup>

<sup>217</sup> For further stabilisation of the platelet plug, proteins in the blood plasma (coagulation factors), respond in a complex cascade to form fibrin strands, which strengthen the platelet plug. This process is called secondary haemostasis and takes place over minutes to hours (Figure 4.3).<sup>218-220</sup>

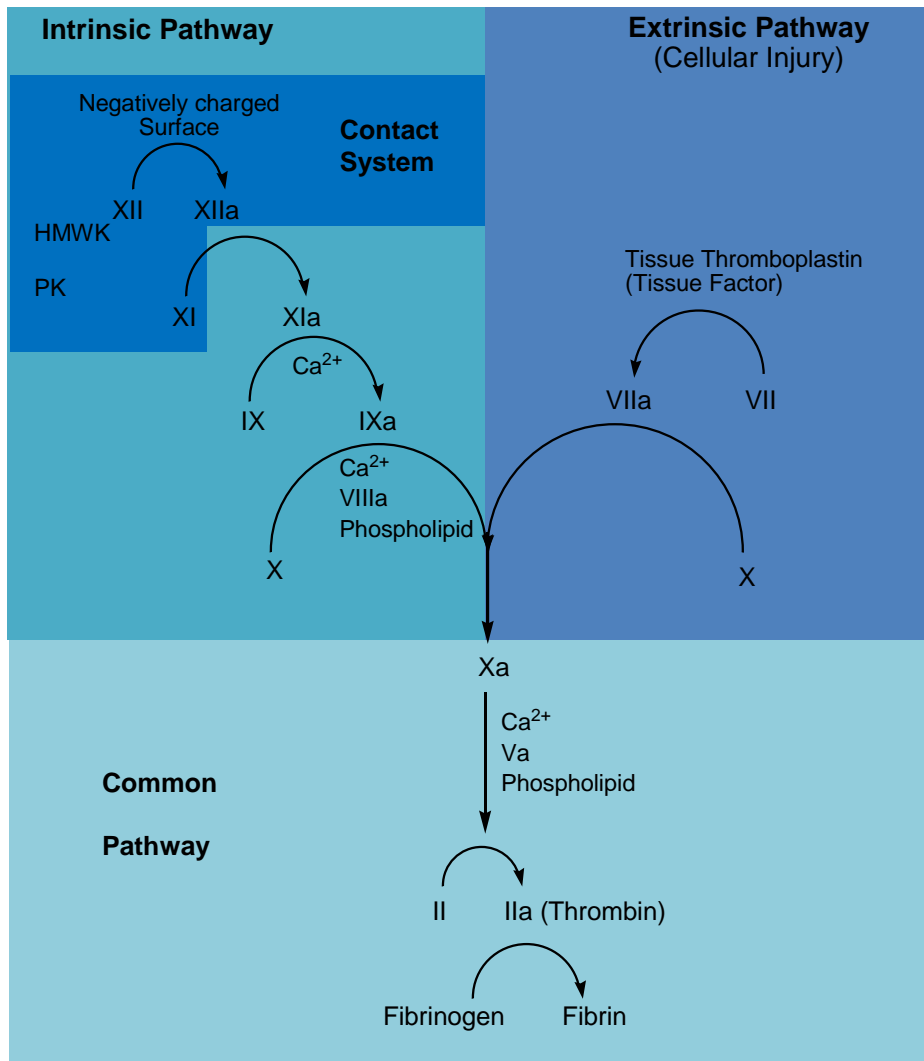


**Figure 4.3:** Secondary haemostasis and its three different pathways. HMWK=high-molecular-weight kininogen, PK=prekallikrein.<sup>218-220</sup>

In this cascade thrombin is the central enzyme which is responsible for the conversion of fibrinogen into fibrin. It can be generated in two ways: the intrinsic and the extrinsic pathway. While the extrinsic pathway is initiated by tissue thromboplastin - exposed after tissue injuries - the intrinsic pathway is set off when foreign surfaces cause complex interactions with the four proteins known as the “contact system”: factor XII, XI, high-molecular-weight kininogen (HMWK) and prekallikrein (PK). In the end, factor XII is processed into XIIa and starts the

coagulation cascade. Since the contact system proteins are always present in blood, this pathway is called intrinsic.<sup>207,220</sup> To ensure that fibrin and thrombin are generated only at the site of injury, antiproteases circulate throughout the system or are bound to endothelial cells and neutralise activated coagulation proteases.<sup>207</sup> In the last phase of stable clot formation (tertiary haemostasis), the fibrin monomers are associated into protofibrils and finally into long fibrils. Factor XIIIa cross-links the fine fibrils *via* covalent bonds into thick fibrin bundles which lead to the formation of so-called coarse clots.<sup>207</sup>

#### **4.4 Current Haemostats**

Several techniques have been developed to support natural haemostasis in case of severe injuries where it is crucial to minimise blood loss efficiently. Conventional techniques such as ligatures and tourniquets can be labour intensive and are not very effective in controlling bleeding in case of complex injuries or where the access of the area of bleeding is difficult.<sup>221</sup> Topical haemostatic agents are useful in these situations. They can be classified according to their basic component causing coagulation.

##### **Collagen-based Agents**

Since the 1970s bovine collagen-based agents have been used to seal wounds.<sup>222</sup> As described in Chapter 4.2.1 platelets recognise collagen fibrils, adhere to them and get aggregated.<sup>223,224</sup> To enhance to the coagulation result, these agents are commonly combined with a procoagulant substances such as thrombin. As the used collagen is

derived from bovine, foreign body responses can be caused and the use of thrombin in combination increases the rate of intravascular thrombosis.<sup>225</sup>

### **Fibrin-based Agents**

Fibrin-based agents consist of human fibrinogen combined with thrombin plus further coagulation factors and/ or compounds that stabilize clots.<sup>226</sup> By mixing the different components, an insoluble fibrin matrix is formed *via* the final common pathway (Chapter 4.1.2).<sup>227,228</sup> The characterisation of the fibrin sealants depend on the fibrinogen concentration: higher concentration give stronger sealants which form slower clots. As fibrin-based agents use pooled human plasma products, there is always a risk of blood borne pathogen transmissions. Despite screening of blood donors and various purifications and viral inactivation processes, paravirus B19 transmissions *via* fibrin based agents have been reported.<sup>229</sup> Moreover, the use of thrombin in the sealants increases the rate of intravascular thrombosis.<sup>225</sup>

### **Cellulose-based Agents**

The first material specially tailored for bleeding control was oxidized cellulose. The haemostatic effect is caused by blood absorption, surface interactions with proteins and platelets and activation of both the intrinsic and extrinsic pathways.<sup>230</sup> In addition, it has bacteriostatic properties due to the acid groups (low pH).<sup>231</sup> Despite having been used for decades, it is known to cause immune responses and can also cause postoperative neurological complications such as impairment in motor or sensory function of the lower extremities (paraplegia).<sup>232-234</sup>



## **Inorganic Agents**

The best investigated inorganic haemostat is QuikClot (Z-Medica, USA), which is based on zeolite.<sup>235</sup> The mechanism of action is related to the absorption of water from the bleeding site. Thereby the concentration of platelets and clotting factors is increased, leading to an immediate stop of bleeding. As this process is exothermic, cauterization- effects might take place as well, sealing local blood vessels but also damaging the tissue surrounding it.<sup>236</sup>

## **Polymer Agents**

So far there have been polymer dressings on the market, which consist of liquid absorbing hydrogels which expand to occlude the wound and create backpressure to stop bleeding.<sup>237</sup> Polyethylene glycol (PEG)-based agents are currently under investigation which cross-link with inherent proteins or under exposure of light.<sup>221</sup>

### ***4.5 Identification of Platelet Activating Polymers Applying Polymer Microarray Technology***

For the identification of polymers that activate platelets in a rapid and effective manner, polymer microarray studies were carried out. To ensure that the investigations would be reliable and accurate and that the platelets would not be activated by the agarose background of the arrays, preliminary studies were carried out in which the platelet rich plasma (PRP) was incubated on dip coated agarose or

collagen I slides.<sup>○</sup> As shown in Figure 4.4a, adhesion of platelets on the agarose slide was very poor in comparison to those coated with collagen I (positive control, Figure 4.4b).

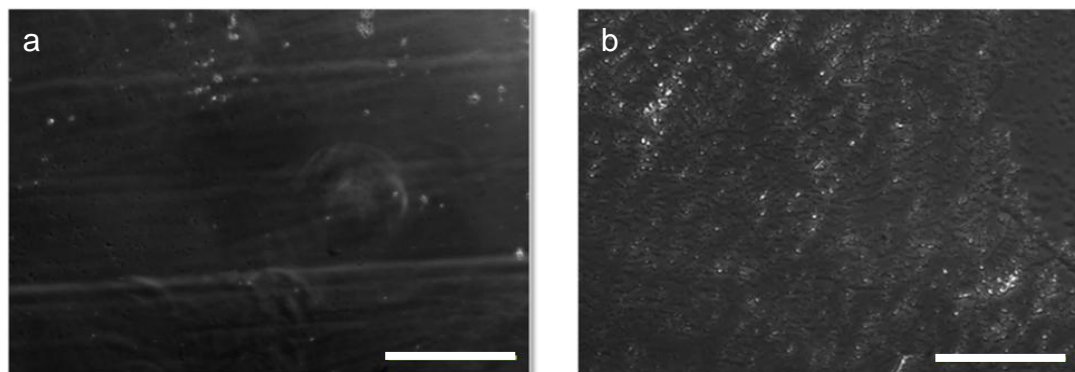


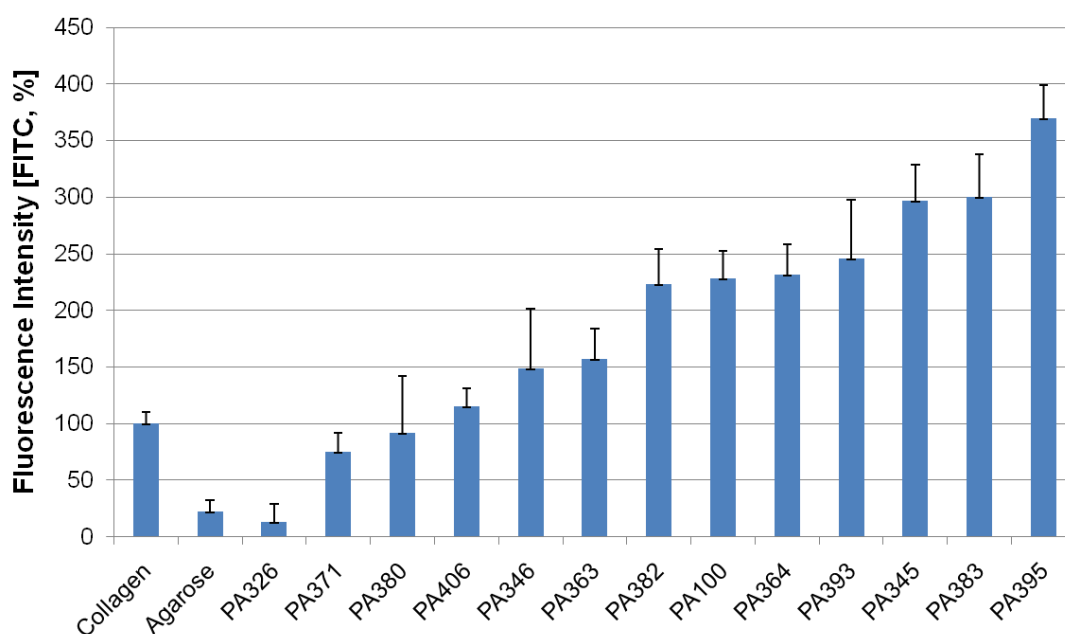
**Figure 4.4:** Phase contrast images of PRP incubated on dip coated slides for 30 min. *a) Agarose, b) Collagen type I. On agarose slides few platelets adhered, while on collagen many platelets adhered and became aggregated. Bar scale =100  $\mu$ m.*

Thus, analysis of polymer microarrays would be possible with only a negligible background of platelet activation and with only the polymer samples themselves being the source for any adhesion/ activation. The positive control (collagen I) was placed on the slides by dip coating the end of the polymer microarray into the protein solution. Interestingly, studies showed that collagen contact printed onto the agarose did not lead to platelet binding. This was rationalised by the fact that the collagen was buried in the agarose coating or due to the inability to form the triple helical structure necessary for recognition by platelets.<sup>220,238</sup> Employing the polymer microarray approach, 291 polyacrylates (with sixteen replicates) were simultaneously tested for platelet adhesion (cell-surface interaction) and aggregation (cell-cell interaction). For this purpose the microarrays were incubated with PRP for 30 min,

---

<sup>○</sup> All work with blood components were carried out by the author in the laboratory facilities of Dr. Petrik Juraj and Dr. Alex Morrison at the SNBTS.

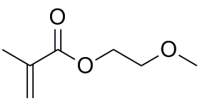
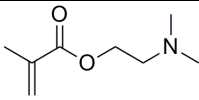
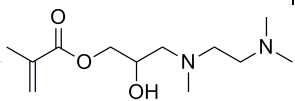
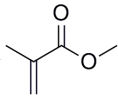
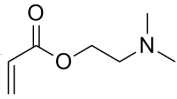
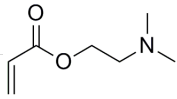
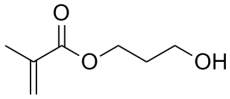
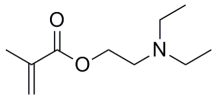
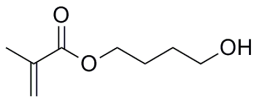
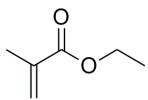
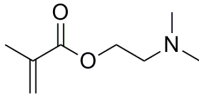
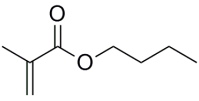
washed in PBS and the bound platelets were stained with the antibodies CD41-FITC and CD62P-PE. The antibody CD41 was used as a marker for a general identification and quantification of the platelets on the polymer spots as it recognises gpIIb which is present on all platelet membranes.<sup>239</sup> In contrast, CD62P (P-selectin) is only present on the outside of the platelet membrane after activation and was used to check if the platelet binding polyacrylates activated the platelets.<sup>240</sup> In Figure 4.5 the fluorescence intensity of platelet binding on polymer spots is depicted in relative comparison to the positive control collagen (the numeric data for the positive (collagen) and negative (agarose) control were obtained by measuring 64 randomly selected sites of the same size as the polymer spots).



**Figure 4.5:** Relative fluorescence intensity measured on the polymer spots after incubation with PRP for 30 minutes and staining with CD41-FITC. The positive control collagen I was set to 100%. The depicted results were obtained from three independent polymer microarrays each with 16 polymer replicates incubated on different dates with platelets from different blood donors. The error bars give the standard deviation. Reproducibility of all data was confirmed via one-way ANOVA ( $p < 0.05$ ).

The best polymer PA395 showed a fourfold increase in platelet binding in comparison to collagen. Closer examination of the composition of the polymers revealed that all platelet binding polymers contained a monomer with a sterically non-hindered tertiary amine (which will be protonated at physiological pH) (Table 4.1). Increases in the level of the tertiary amine monomer (within the same polyacrylate combination) led to a significantly higher platelet binding, underlining its crucial part in the activation process. For instance, PA393 containing 10% of the tertiary amine monomer and 90% ethylmethacrylate gave rise to a 2.5 fold increase in platelet binding in comparison to collagen. In contrast, PA395 consisting of the same monomers as PA393 but with 50% ethylmethacrylate and 50% of the tertiary amine was 3.5 times better than collagen. In the case of PA345 and PA346, the opposite effect was observed - the lower amine containing polyacrylate led to higher platelet binding. The potential reason for this phenomenon might be twofold. Firstly, the polymers containing two tertiary amines per monomer, give a very high charge density at lower compositions and ratios (Table 4.1). Moreover, the alcohol group in the tertiary amine monomer might also be influencing platelet binding.

**Table 4.1:** Composition of platelet binding polyacrylates.

Polymer	Monomer 1	Monomer 2	Ratio
PA100			70:30
PA345			90:10
PA346			70:30
PA363			90:10
PA364			70:30
PA371			50:50
PA380			50:50
PA382			70:30
PA383			50:50
PA393			90:10
PA395			50:50
PA406			70:30

The different platelet binding capabilities between collagen and the identified polymers could be easily observed *via* fluorescence microscopy (Figure 4.6).

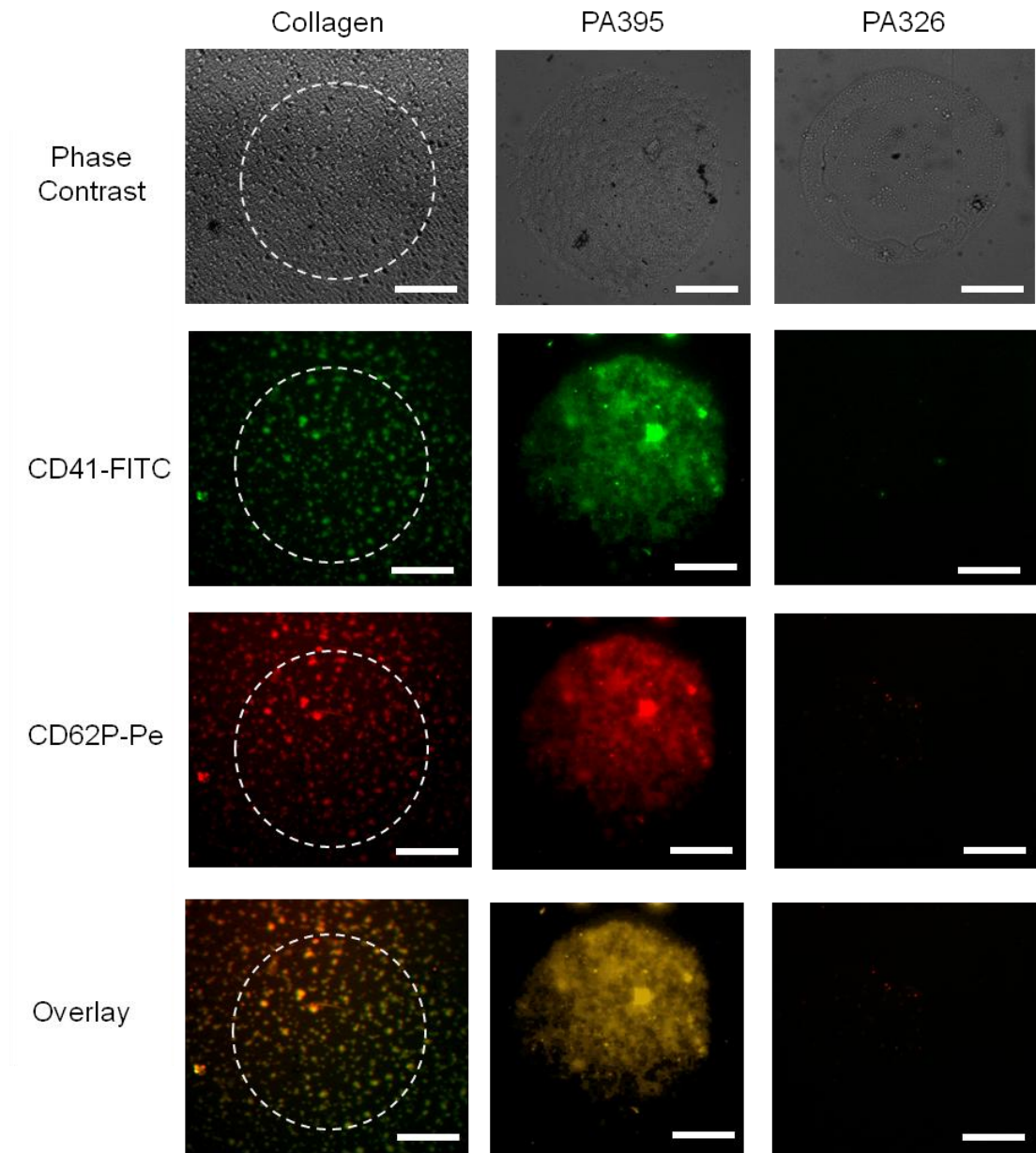


**Figure 4.6:** Fluorescence images of collagen and polymers after being incubated for 30 min with PRP and stained with CD41-FITC and CD62P-Pe. Collagen and PA395 bind platelets successfully; PA326 does not show any platelet adhesion. The dashed, circled area on the collagen represents an area equivalent to a polymer spot.

In all cases where platelet adhesion was observed, both antibodies, CD41-FITC and CD62P-Pe, bound, indicating that all platelet binding polymers give rise to activation, as does collagen. These images also underline the varying amounts of platelets that are bound to collagen and the identified polyacrylates. In the case of collagen, the platelets were observed to bind in small patches, while the polyacrylate PA395, which showed a fourfold increase of platelet binding, gave a dense platelet network with less space between the single particles (Figure 4.6). In the case of the platelet non-binding polymers such as PA326, platelet adhesion was comparable to the agarose background.

#### **4.6 Analysis of Activation State in Static and Flow Experiments**

The different activation states of the platelets indicate how effective the materials are in inducing adhesion and aggregation. Under static conditions, a “single-stage aggregation” can be assumed where stable aggregations occur between shape-changed platelets.<sup>241,242</sup> This means that the materials causing the highest activation response leads over time to secondary activation and recruitment of platelets and thus to an enhanced haemostatic effect. In static experiments, PRP was incubated on polymer coated coverslips for 30 min and the concrete state of activation was investigated *via* scanning electron microscopy. The description of the activation status was carried out according to the investigations by Goodman.<sup>241</sup> In Figure 4.7a, the platelet response to collagen (positive control) is shown. The platelets have mostly a dendritic shape with some flattened pseudopodia. In contrast, the negative control bovine serum albumin (BSA) does not show any obvious platelet binding

which underlines that the samples were not activated beforehand (Figure 4.7b). Some polymers, such as PA395, showed results similar to collagen I (Figure 4.7c). The platelets were mostly dendritic or pseudopodial, forming a lot of aggregates. However, they seemed to be significantly larger and complex on the polymer. Other polyacrylates such as PA406 (Figure 4.7d) gave fully spread-out platelets where the fluid portion of the cytoplasm (hyaloplasm) was spread between the pseudopodia in a way that the pseudopodia could not be defined any more. Fibrin clots, being part of the second step of haemostasis, could also be seen for PA383 (Figure 4.7e). Here, the material leads to uniform, high activation of the cells and it can be assumed that in accordance with the “single-stage aggregation” theory, more platelets bound over time to the fully activated platelets.<sup>241,242</sup> (Representative images for all other polymers and platelet activations can be seen in Appendix Figure 2).

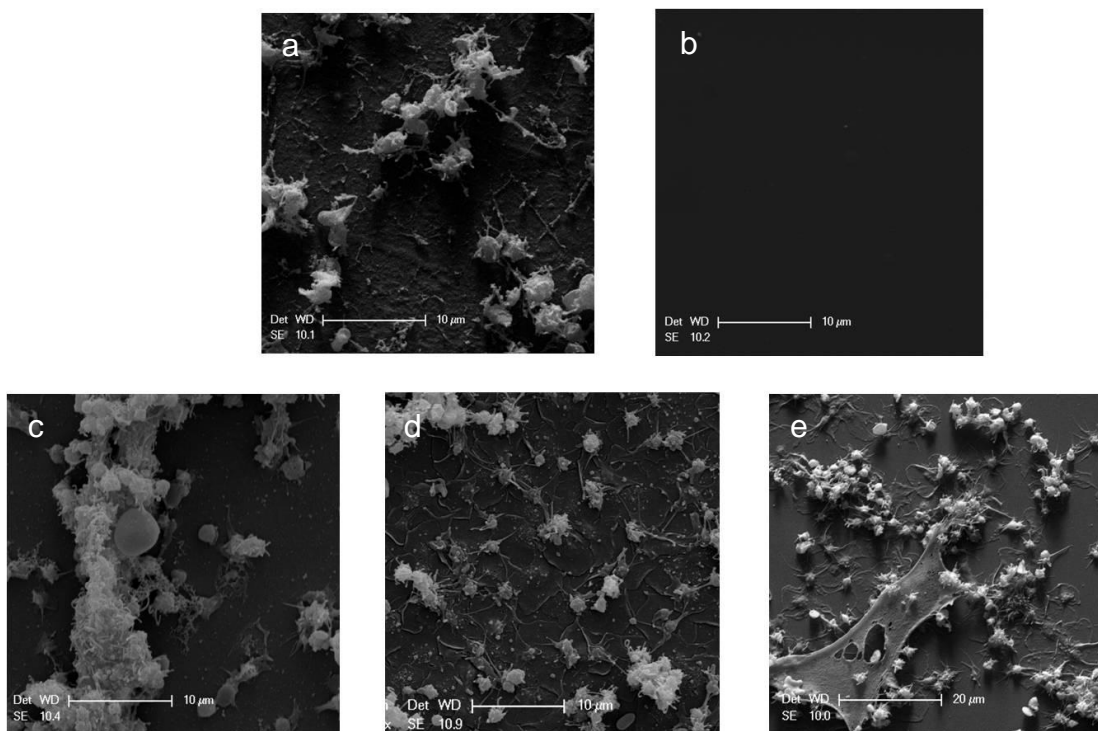


**Figure 4.7:** Scanning electron microscope images of platelets incubated for 30 min



on different substrates. **a) Collagen Type I, b) BSA, c) PA395, d) PA406, e) PA383.** The activation state of the platelets varies between collagen (dendritic cells), polymer PA395 (dendritic clusters) and the polyacrylates PA406 and PA383 (fully spread cells). In case of PA383 (e) fibrin clot formation as part of the second haemostasis step is visible.

In Table 4.2 an overview of the different platelet activation states on the different polyacrylates is given. It is worth noting that the number of platelets that bound to the different polymers does not indicate the activation state of the platelets. As can be seen (Figure 4.7, Table 4.2) collagen and the highest platelet binding polymer PA395 gave rise to a so-called “dendritic platelet” morphology.<sup>49</sup> In contrast, polyacrylate PA406 which showed comparable binding capability to collagen, gave “fully spread out platelets”.

To simulate the physiological milieu of platelets in a better manner, cone and plate(let) studies were carried out, in which PRP and whole blood samples or red blood cells are exposed to a shear rate of  $1800\text{ s}^{-1}$  for 4 min which simulates pseudo physiological flow (Figure 4.8).<sup>243,244</sup>

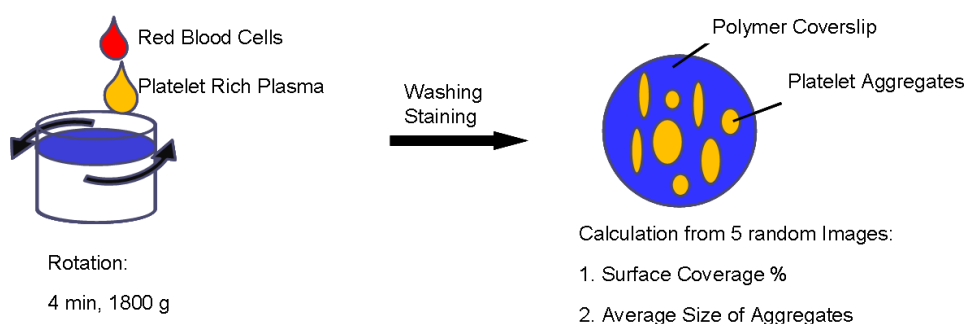


**Figure 4.8:** Principle of cone and plate(let) studies. A mixture of red blood cells and PRP is rotated on top of the polymer or collagen coated coverslips. After washing and staining, the surface coverage and average aggregate sizes are determined.

To test the effect of the identified polymers on the platelets under these conditions, polymer or collagen coated coverslips were placed in the analysis well of the cone and platelet instrument and the surface coverage and aggregate size of the platelets were determined following the rotation (Table 4.2, Appendix Figure 3).

**Table 4.2:** Platelet activation states in static experiments (by scanning electron microscopy) and surface coverage, aggregate size under physiologic flow (n=10). Values marked with an asterisk (\*) are statistically significant different to collagen (p<0.05).

<b>Substrate</b>	<b>Activation State<sup>⊙</sup></b>	<b>Surface Coverage [%]</b>	<b>Aggregate Size [μm<sup>2</sup>]</b>
<b>Collagen</b>	D, SD	11.1 ± 1.5	64.2 ± 15.5
<b>PA100</b>	D, SD	14.1 ± 2.3*	73.4 ± 9.4
<b>PA345</b>	SD	12.4 ± 1.5	83.8 ± 19.1*
<b>PA346</b>	SD	12.6 ± 0.7*	75.7 ± 11.1
<b>PA363</b>	S	13.8 ± 2.0*	90.3 ± 18.8*
<b>PA364</b>	D, SD	14.6 ± 3.3*	74.8 ± 10.7
<b>PA371</b>	D, SD	10.1 ± 1.6	74.0 ± 18.6
<b>PA380</b>	D, SD	14.0 ± 1.5*	80.4 ± 14.4*
<b>PA382</b>	D, SD	12.4 ± 3.1	82.4 ± 16.0*
<b>PA383</b>	S, FS	13.4 ± 1.8*	83.3 ± 18.9*
<b>PA393</b>	S, FS	13.6 ± 1.5*	78.8 ± 14.4*
<b>PA395</b>	D, SD	14.1 ± 0.9*	82.5 ± 17.9*
<b>PA406</b>	S, FS	15.0 ± 1.3*	91.9 ± 16.1*

<sup>⊙</sup> According to Goodman, D-dendritic, SD-spread dendritic, S-spread, FS-fully spread.<sup>241</sup>

The collagen coated coverslips, representing the natural agonist, resulted in a surface coverage of 11.1% and a platelet aggregate size of about  $64.2 \mu\text{m}^2$  (Figure 4.9a).

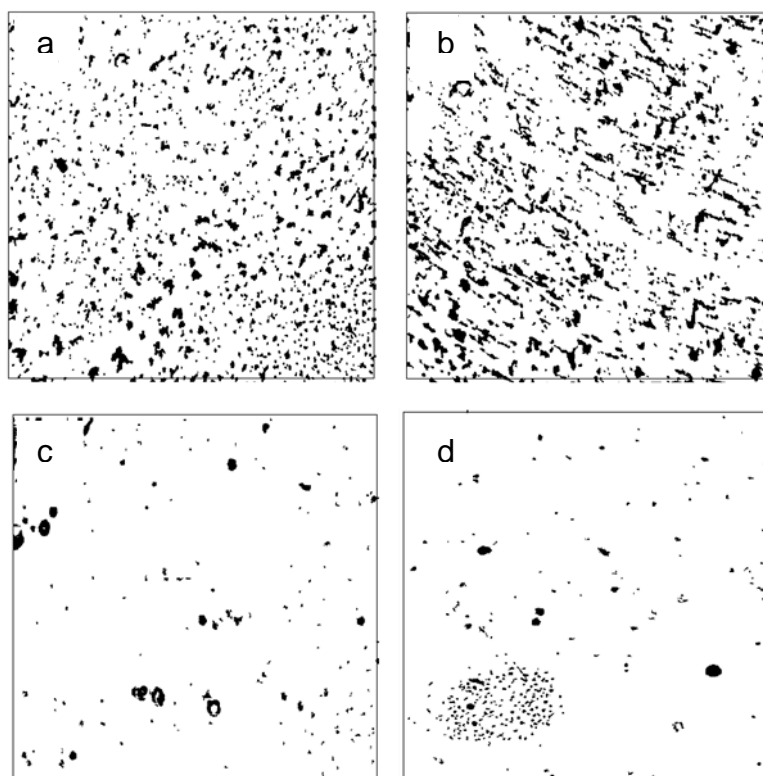


**Figure 4.9:** *Impact R test images showing the different surface coverage and aggregation sizes depending on the substrates. a) Collagen (surface coverage: 11%, aggregate size:  $57 \mu\text{m}^2$ ); b) Polyacrylate PA406 (surface coverage: 15%, aggregate size:  $102 \mu\text{m}^2$ ), c) PA406 incubated with red blood cells, without platelet rich plasma (surface coverage: 2.3%, aggregate Size:  $76 \mu\text{m}^2$ ), d) PA406 incubated with plasma without red blood cells and platelet rich plasma (surface coverage: 1.7%, aggregate size:  $42 \mu\text{m}^2$ )*

Most of the high-lighted polyacrylates resulted in a higher surface coverage than collagen with up to 15% coverage (PA406, Figure 4.9b). The lowest value of surface coverage was observed for PA371 (10.1%), which was in accord with the static microarray tests where it also showed a slightly lower binding than collagen (Figure 4.5). Polyacrylates PA345 and PA382 gave comparable platelet binding values to collagen on the cone and plate analyzer (surface coverage of 12.4%). In general, the aggregate sizes on the identified polymers varied between  $79$  and  $91 \mu\text{m}^2$  and were

significantly larger than on collagen ( $64 \mu\text{m}^2$ ) implying enhanced platelet activation and recruitment. PA363, PA380, PA383, PA393, PA395 and PA406 displayed high values for surface coverage and aggregation size under conditions of physiological flow and thus might well be suited for the rapid and complete activation of platelets. This outcome was expected from the static microarray studies for the polyacrylates PA383, PA393 and PA395 where they showed between 1.5 - 3.5 fold higher platelet binding. In contrast, the polymers PA380 and PA406 gave comparable results to collagen in the static studies. The reason for the improved binding capability might of PA380 and PA406 under flow conditions might be due to a slightly different aggregation process at shear rates between 1000 and 10000  $\text{s}^{-1}$  which involves additional receptors and ligands for platelet aggregation and adhesion.<sup>242</sup> Also, the interaction of platelets with the red blood cells might play an important role which was not considered in the static experiments. This might be especially the case for PA406 which gave even better results than PA395 - the best polymer in the microarray studies - for surface coverage as well as aggregation size. Shear rate studies without PRP that were carried out with red blood cells or plasma showed only few and small aggregates. This proved that the determined aggregates resulted from platelet adhesion and aggregation and not from the binding of other blood components or red blood cells (Figure 4.9c, 4.9d).

#### **4.7 Activation Mechanism of Polymers**

The mechanism involved in platelet activation and binding on biomaterials is still contentious.<sup>242,245</sup> The prevalent theory is that under static conditions platelet aggregations are predominantly mediated by the interaction of fibrinogen with the activated platelet integrin receptor gpIIb/IIIa. For this, fibrinogen has to bind to the artificial biomaterial, undergo a conformation change which leads to the final recognition by platelets and the initiation of the coagulation cascade.<sup>246</sup> Further proteins such as vWF also support binding of platelets and lead to activation. In contrast, serum albumin is a protein which should not affect platelet binding and activation, indeed it was less likely to be predominantly adsorbed on the platelet-activating polymers as this would hinder further recruitment of platelet-activating proteins. On the basis of this theory, the polymers, which showed successful platelet binding, were incubated with platelet poor plasma samples for 30 min. Thereafter, they were washed and stained with antibodies against fibrinogen, vWF and serum albumin. In Figure 4.10, the corresponding images after incubation with conjugated secondary antibodies are shown.

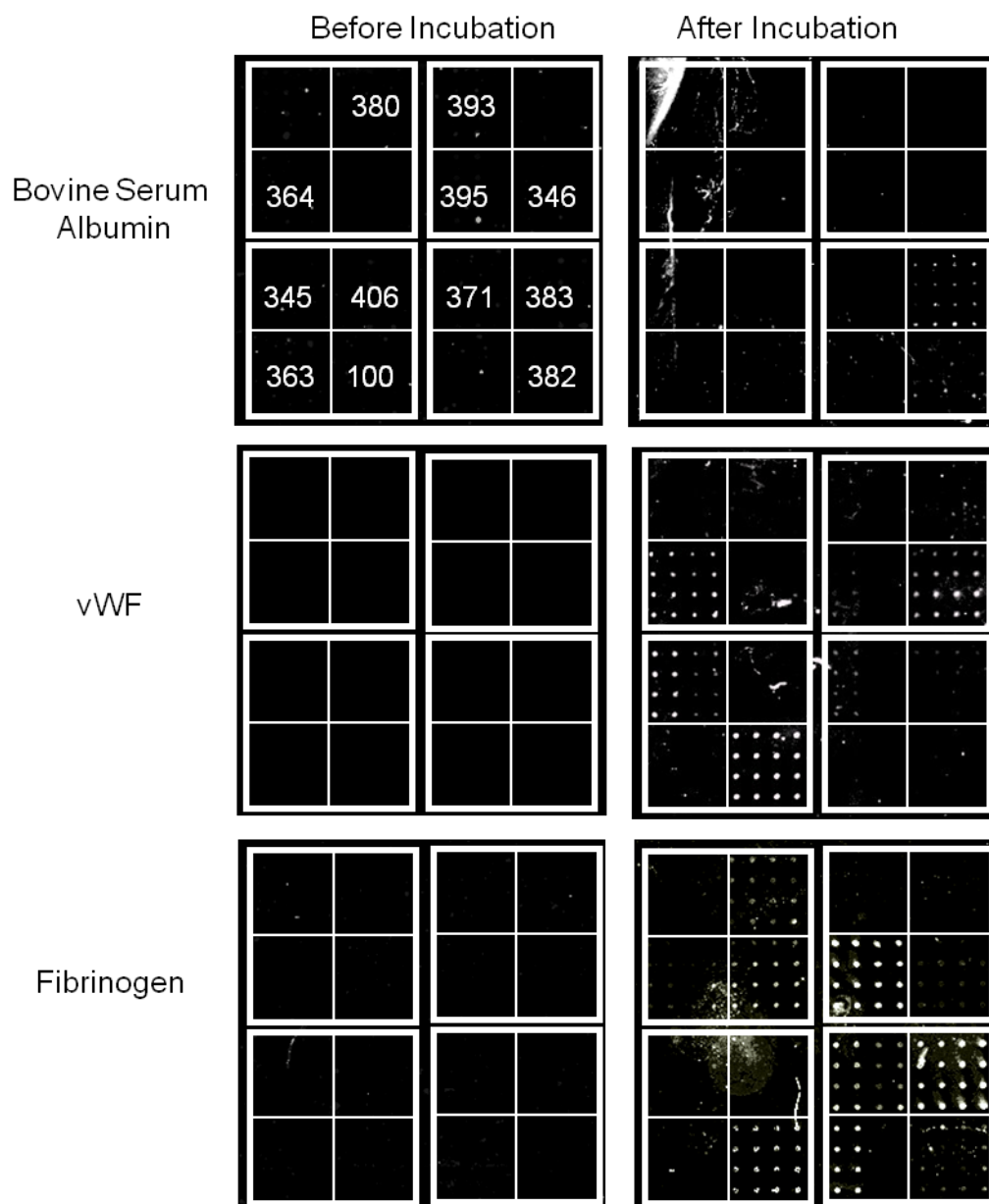


**Figure 4.10:** Protein adhesion of studies of bovine serum albumin, vWF and fibrinogen on “hit” polyacrylates visualised via antibody staining.

All polymers, except for PA383, did not bind serum albumin, which suggests that the polyacrylates are relatively selective in their protein binding affinities.<sup>247</sup> Adsorption of vWF and fibrinogen was observed on most polyacrylates, while some polymers such as PA100 and PA346 showed simultaneously binding of fibrinogen and vWF. Interestingly, the polymers PA363, PA393 and PA406 did not show any binding for

the tested proteins, although the polymeric structure of PA363 and PA393 are strongly related to the fibrinogen binding polymers PA364 and PA395, respectively (Table 4.2). Since these polyacrylates also lead to platelet aggregation and activation (Figure 4.6 and 4.7), the mechanism for this might be either *via* direct recognition by the platelets' receptors for collagen, fibrinogen or vWF e.g. or by recruitment of other proteins that can lead to platelet activation (such as fibrinectin which promotes/ supports platelet adhesion).<sup>248</sup> Since the coagulation and the complement system are highly interlinked, material-induced complement activation might also lead to platelet activation with possible recruitment of complement proteins onto the identified polyacrylates.<sup>249,250</sup>

#### ***4.8 Conclusions for Platelet Activation***

A high-throughput microarray procedure has been developed which allowed an investigation of platelet binding to potential biomaterials in a qualitative and quantitative manner. This method enabled the simultaneous screening of 291 different polyacrylates under the identical conditions, using minimum amounts of PRP. Out of this screen, twelve polyacrylates could be identified that showed comparative or higher platelet binding than the natural agonist collagen. Scanning electron microscopy studies gave further insights into the activation state of the platelets upon binding with polymers showing pronounced binding and a large spread out morphology, and shear rate studies allowed verification of the haemostatic value of the different polyacrylates. The basis for the haemostatic effect of most polymers could be found in the adsorption of proteins such as fibrinogen and vWF which leads to the recognition and adherence and aggregation of the platelets. The best polyacrylate in this study was PA406 (poly(n-butyl methacrylate-co-(dimethylamino)ethyl methacrylate (70:30)) as it lead to fully activated and spread platelets in the static experiments and outperformed collagen in the shear studies by giving significant higher surface coverage (15% vs. 11%) and aggregates about a third larger in size ( $92 \mu\text{m}^2$  vs.  $64 \mu\text{m}^2$ ). Due to the rapid and complete activation of platelets polymer PA406 is a promising candidate for the further development of wound dressings.



#### **4.9 Megakaryocytic Cell Lines**

As described in Chapter 4.7, human megakaryocytes are the giant precursor cells for platelets. As they present less than 0.1% of bone marrow cells and are therefore hard to collect and cultivate in large numbers, a variety of megakaryocytic cell lines have been established.<sup>251,252</sup> One of the most widely studied is the megakaryoblastic leukaemia cell line MEG-01, which has been extensively used as model for megakaryocytic maturation and platelet formation.<sup>253-256</sup> Upon incubation with megakaryocytic stimuli such as thrombopoietin (TPO), phorbol 12-myristate 13-acetate (PMA), 12-O-tetradecanoylphorbol-13-acetate (TPA) or Interleucin-6 the maturation process of the MEG-01 cell line can be increased. During this maturation process, the MEG-01 cells become multi-nucleated and they adhere and extend pseudopodia.<sup>255,257-259</sup> The differentiation pathway for megakaryocytes and erythrocytes are strongly related to each other as both cell lineages share a common precursor cell as shown in Figure 4.11.<sup>260,261</sup>

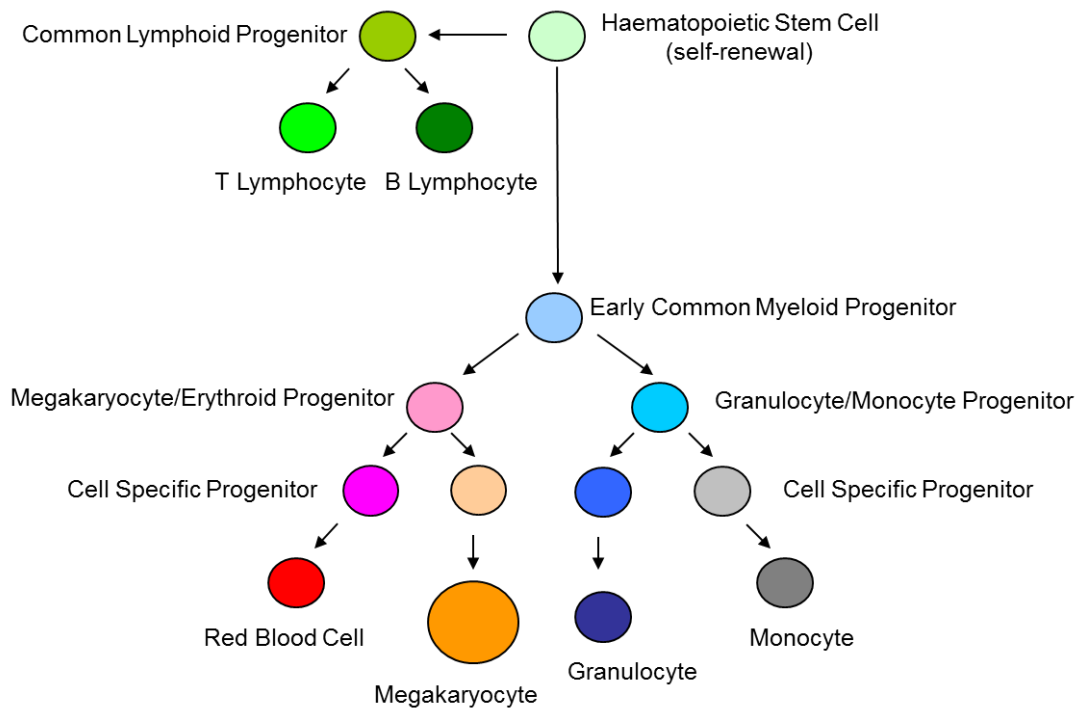


**Figure 4.11:** *The developmental pathway for blood cells. The haematopoietic stem cell generates common progenitor cells for lymphoid and for myeloid cells. Upon further maturation, progenitor cells for megakaryocytes and erythrocytes as well as progenitor cells for granulocytes and monocytes are formed.*

The bivalent maturity state of the common progenitor cell of megakaryocytes and erythrocytes can be compared to the erythroleukemic cell line K562 which expresses cell-specific markers of both cell types and which can undergo further differentiation into the specific lineage depending on the applied stimuli.<sup>262-267</sup> Similar to the cell line MEG-01, cellular changes in morphology and adherence properties can be observed after differentiation towards the megakaryocytic lineage is initiated.<sup>264</sup>

To facilitate the collection and cultivation process of human megakaryocytes, substrates would be of interest that could capture cells specifically out of complex samples (bone marrow or blood) without having a major impact on cellular differentiation. By using the cell lines MEG-01 and K562, the biomaterial could also be tested for megakaryocyte specificity.

#### **4.10 Polymers Sorting Megakaryocytic Cell Lines**

For the identification of polymers that could lead to the adhesion of the cell line MEG-01, polymer microarrays with 813 polymers - polyurethanes and polyacrylates - were fabricated by contact printing of preformed polymer solutions. The natural protein collagen served as a positive control. Polystyrene was used as a negative binding control since normally only a few suspension cells adhere to this material.<sup>253</sup> Polymer microarray studies were also carried out with the erythroid cell line K562 to identify polymers that specifically bind cells of the megakaryocytic lineage. For quantification of cellular binding, the cells were fixed, the nuclei stained with the fluorescent dye Hoechst 33342 and counted after fixation (Figure 4.12a, b). Polymers which only bound MEG-01 cells and not K562 cells were classified as specific for the megakaryocytic lineage.

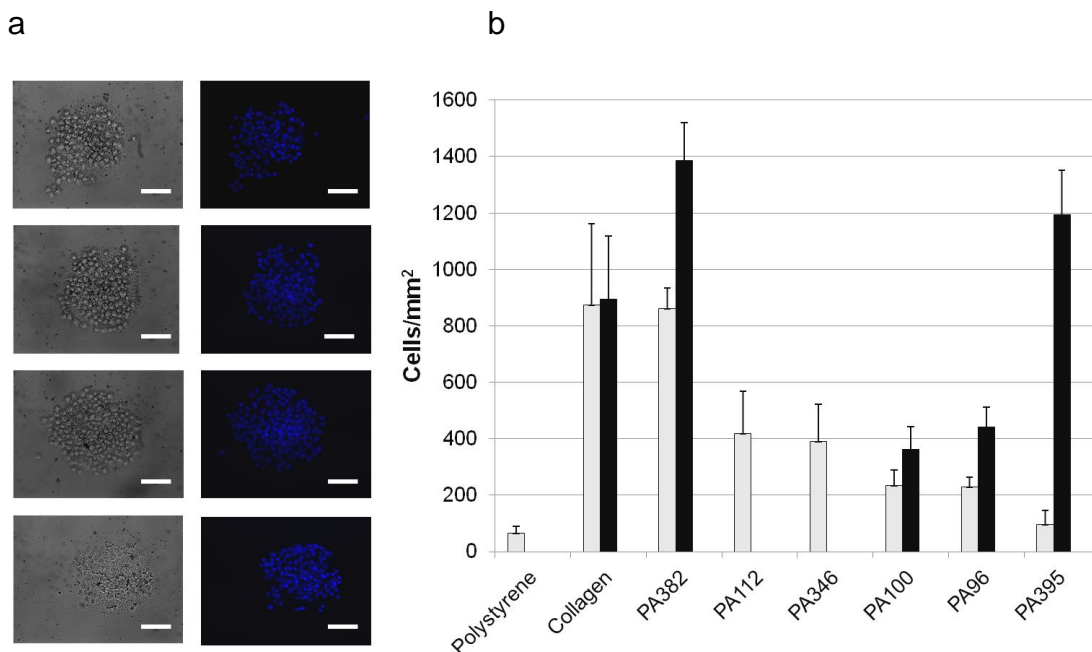


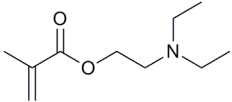
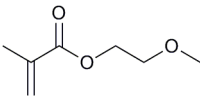
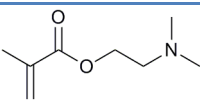
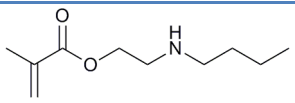
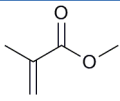
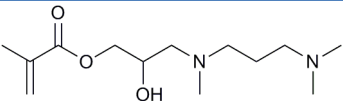
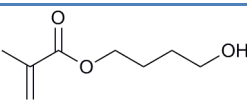
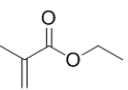
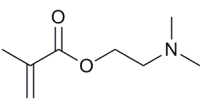
**Figure 4.12:** Microarray binding studies. **a)** Brightfield and fluorescence microscopy images of quadruplicate PA382 polymer spots showing binding of MEG-01 cells stained with Hoechst 33342. Scale Bar = 100  $\mu\text{m}$ ; **b)** Comparison of MEG-01 and K562 binding on polystyrene, collagen and the hit polymers for MEG-01 cells after 4 days of incubation ( $n = 2$  with 8 replicates). Grey-MEG-01, black-K562.

While cellular binding for MEG-01 cells on polystyrene was low (100 cells/mm<sup>2</sup>), the positive control collagen showed an attachment of approximately 900 cells/mm<sup>2</sup> for both cell lines, K562 and MEG-01. Five synthetic polymers (PA382, PA112, PA346, PA00 and PA96) were identified that showed enhanced cell binding of MEG-01 cells in comparison to polystyrene (Figure 4.12b). Polymer PA395 is shown as a representative for polymers that did not increase MEG-01 cell binding in comparison to polystyrene (100 cells/mm<sup>2</sup>). The best polymer for binding MEG-01 cells was PA382 with 900 cells/mm<sup>2</sup>, comparable to collagen. However, like the natural protein, the polymer also bound K562 cells, showing that it was non-specific for the megakaryocytic lineage. The polymers PA112 and PA346 lead to a 4-fold

increase in MEG-01 cell binding in comparison to polystyrene with both polymers being specific for the megakaryocytic lineage.

As shown in Table 4.3, all identified polymers that bound MEG-01 cells contained monomers with secondary amino groups. However, as PA395 gave strong adherence of K562 cells in contrast to MEG-01 cells, the secondary amine content must not be the only criteria for binding MEG-01 cells.

**Table 4.3:** Chemical compositions of the identified polyacrylates. Polymers listed showed enhanced MEG-01 cell binding in comparison to polystyrene except for PA395, which represents a structure of a non-binding polyacrylate for megakaryocytic cells.

Polymer	Monomer 1	Monomer 2	Ratio
PA96			90:10
PA100			70:30
PA112			70:30
PA346			70:30
PA382			70:30
PA395			50:50

#### **4.11 Morphology and Protein Binding Studies**

The top polymers were explored for their effect on cellular morphology and cellular proliferation of MEG-01 cells on polymer coated coverslips *via* brightfield and scanning electron microscopy (Figure 4.13). The morphology of MEG-01 cells on PA382 was representative for all polyacrylates except for PA112. The round, suspension cell-like morphology with numerous microvilli on the cells' surfaces resembled in its appearance adherent K562.<sup>137</sup> Most MEG-01 cells cultivated on these polyacrylates did not have any pseudopodia (Figure 4.13). In the case of PA112, the adherent MEG-01 cells were characterised by a “rounded” morphology (similar to the one for PA382) as well as an “outstretched” structure with long pseudopodia forming proplatelets and leading to platelet-like particle formation (Figure 4.13). These adherent cells resemble the mature status of MEG-01 cells on polystyrene (Figure 4.13). Here, rounded cells were not captured by the polymer.

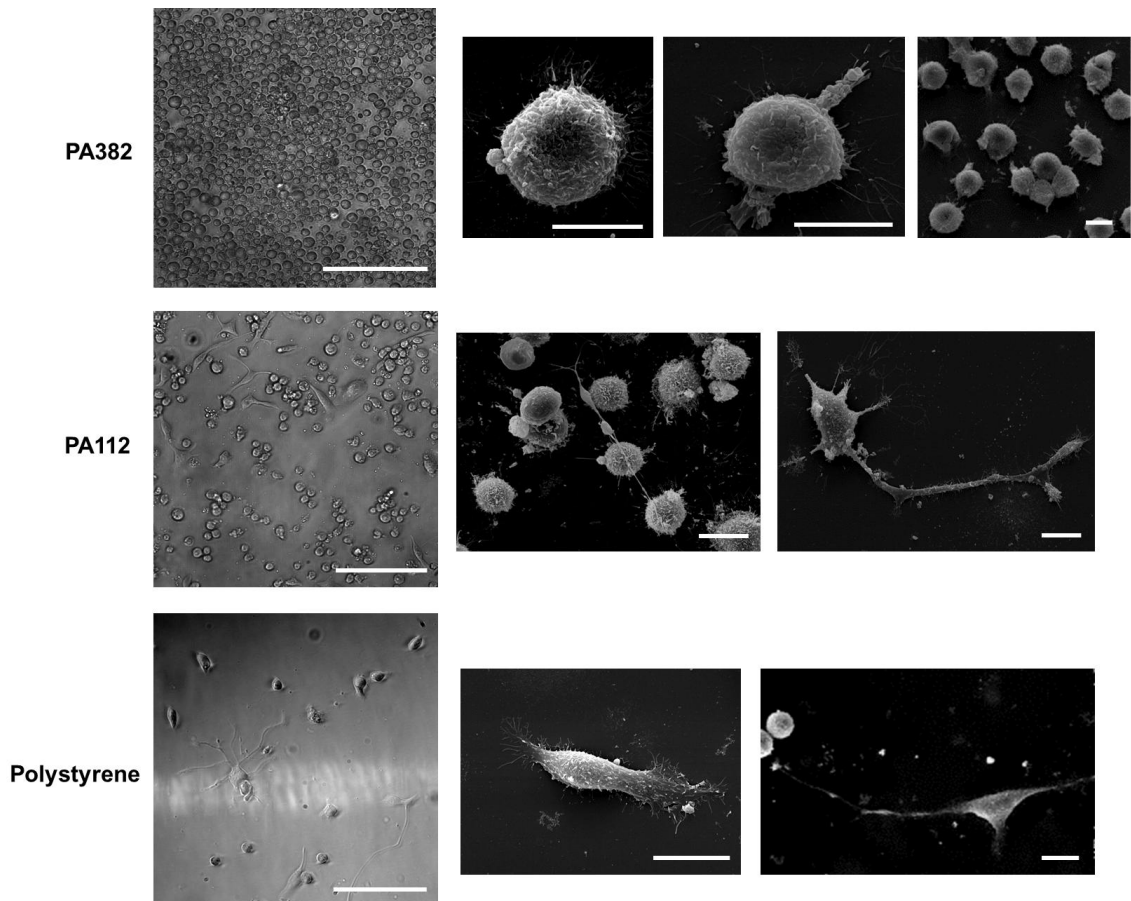


**Figure 4.13:** MEG-01 cell binding on PA382, PA112 and polystyrene after 4 d of incubation. MEG-01 cells adhered on PA382 were small and of round morphology, partly with short pseudopodia extruding. On polystyrene, the MEG-01 cells had lost their round morphology (less suspension cell like) and also showed clear matured cells with long pseudopodia and proplatelets. The cells adhered on PA112 were a mixture of the cells shown for PA382 and polystyrene. Brightfield Images: scale bars = 100  $\mu\text{m}$ ; scanning electron microscopy: scale bars = 10  $\mu\text{m}$ .

To gain a deeper understanding of the binding mechanisms for the identified polyacrylates, protein binding studies were carried out. Polymer coated coverslips that showed successful MEG-01 cell binding were incubated in fully supplemented RPMI medium for 16 h, washed with PBS and the binding proteins were stripped off the polymers by boiling in sodium dodecyl sulfate (SDS). All polymers gave protein bands for the same protein mixture with serum albumin as major component (Figure 4.14). Interestingly in all studies, polystyrene (PS) and PA112 bound less of the

adhered proteins. This suggests that the protein binding content is crucial for the adherence of MEG-01 cells and its morphology – a higher content of protein bound to the polymers led to a round suspension cell like morphology, while the cells had an outstretched morphology in the case of polymers binding less proteins. (as shown in Figure 4.13 and Figure 4.14).

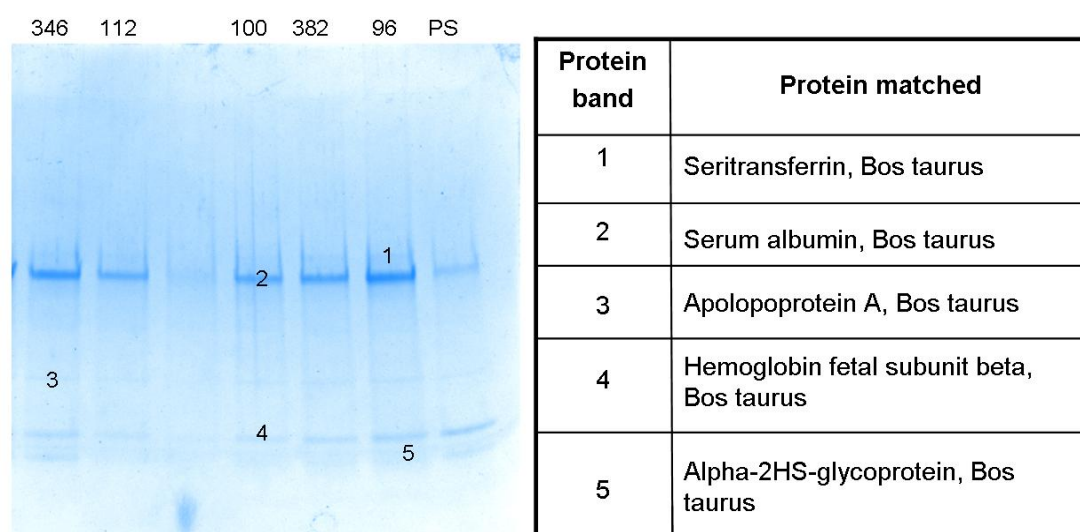


**Figure 4.14:** Representative protein gel used to analyse the “amount” and type of proteins that bound to polymers after 24 h. While all MEG-01 binding polymers bound a large variety of proteins, polystyrene (PS) binds only three different proteins – serum albumin, hemoglobin and alpha-2HS-glycoprotein ( $n = 4$  with 2 replicates).

#### 4.12 Influence on Maturation and Gene Regulation

To investigate if the identified polyacrylates affected the differentiation/ maturation of the adhered cells, flow cytometry studies were carried out. After 4 d incubation of the MEG-01 cell line on the different polymer substrates, the adhered cells were collected and stained with antibodies for the maturation markers CD41 and CD42b, which are characteristic for the cell-specific megakaryocytic progenitor cells and



fully mature megakaryocytes. As control MEG-01 cells that were in suspension and cultivated in polystyrene tissue flasks were used. The ratio of the cells in the different maturation states, analysed by their expression of CD41 and CD42b antigens, did not change in comparison to polystyrene cultivated cells after immobilisation (Table 4.4).<sup>268-269</sup>

**Table 4.4:** Flow Cytometry Studies of polymer bound MEG-01 cells stained with CD41 after 4 d incubation on different polymer substrates. The number given is the percentage of 10000 cells positive for CD41 (standard deviation, n=3 in duplicates).

<b>Substrate</b>	<b>CD41 [%]</b>	<b>CD42b [%]</b>
<b>Polystyrene</b>	16±3	2±1
<b>PA 96</b>	8±6	2±2
<b>PA100</b>	6±4	5±5
<b>PA112</b>	12±4	4±1
<b>PA346</b>	12±3	3±1
<b>PA382</b>	10±3	2±1

To further investigate if polymer immobilisation had an influence on the adhered MEG-01 cells, the miRNA fingerprint of cells cultivated on polystyrene was compared to the miRNA fingerprint of cells cultivated on the polymers PA382 and

PA112.<sup>^</sup> As shown in Figure 4.15, MEG-01 cells cultivated on polystyrene, PA112 and PA382 showed a very good correlation (94% and 70%), proving that the gene regulation was not or only to a minor extent influenced by the immobilisation.

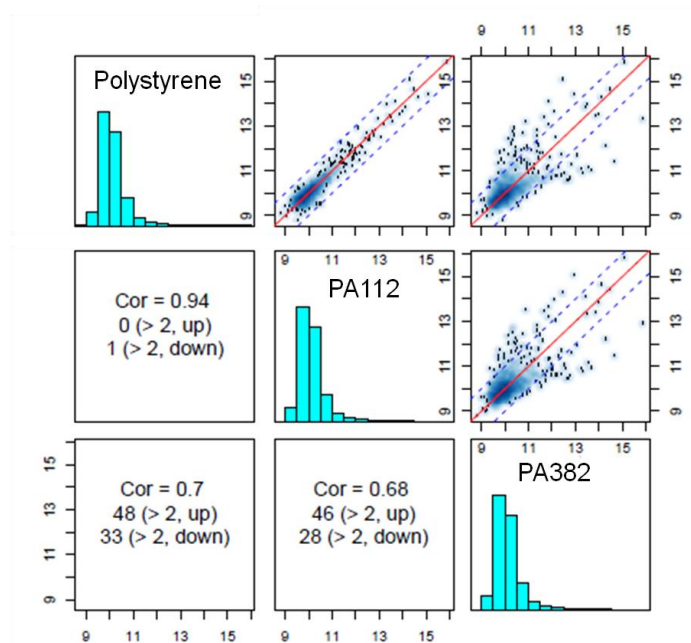


**Figure 4.15:** Pairwise plot ( $\log_2$ ) with sample correlation for polystyrene, PA112 and PA382. Similarities and differences between the three datasets are indicated, showing that between polystyrene and PA112 one single miRNA is changed in regulation (correlation 94%). The difference between PA382 and polystyrene to PA112 gives a correlation of 70% for both samples (polystyrene=81, PA112=74 miRNA changes).

Interestingly, five human miRNAs were found to be highly up-regulated in cells cultivated on PA382 in comparison to polystyrene and PA112 (Table 4.5). Most of these miRNAs are known to regulate genes that are responsible for cellular adhesion, migration and apoptosis. These events are important in the course of the maturation

<sup>^</sup> The miRNA array kits were kindly provided by Dr. Juraj Petrik. The computational analysis of the miRNA arrays was carried out by Samuel Corless in the research group of Dr. Nick Gilbert (University of Edinburgh).

process of the megakaryoblastic cell line MEG-01 and may give a hint how PA382 effects the maturation process which might not be observable *via* flow cytometry within a short incubation time (4 d).

**Table 4.5:** Up-regulated human miRNAs (x5) and their putative targets in MEG-01 cells cultivated on PA382 sampled in comparison to Polystyrene and PA112.

<b>miRNA</b>	<b>Putative Targets<sup>270,271</sup></b>	<b>Target related Regulations<sup>270,271</sup></b>
hsa-miR-129-5p	ETV1, PAPD5, SGCD, RUNX1T1, SOX4	Cell growth, Differentiation, Proliferation, Polyadenylation of miRNA, ECM Structure, Apoptosis
hsa-miR-602	LRPAP1, BCL2L13, C5AR1, KLHK24, CUX1	Apoptosis, Differentiation, Cell Cycle Progression, Chemotaxis
hsa-miR-483-5p	IQCE, ALCAM, SLC25B4, RUSC1, UGT3A1	Solute Carriers, Glycosyltransferases, Cellular Adhesion and Migration
hsa-miR-149-3p	SMARCD1, FOXP4, WDTC1, NFIX, POU2AF1	Cell-type Specific Transcription Factors, Cellular Migration
hsa-miR-1469	BAIAP3, FEZF2	Brain-specific Proteins (Synapsis Formation)

However, for confirmation of the upregulation of the identified genes, further experiments have to be carried out such as qPCR with the specific primers for the miRNA sequences.

#### **4.13 Conclusion for Sorting of Megakaryocytic Cells**

Polymer microarrays were successfully used for the identification of polymers that bind MEG-01 cells. By extending the cellular binding studies to K562 cells, which have both erythroid and megakaryocytic markers, two polymers, PA112 (poly(2-methoxyethyl acrylate-co-(2-*tert*-butylamino)ethyl methacrylate) (70:30)) and PA346 (poly(methyl acrylate-co-(dimethylamino)propyl (methylamino)-2-propanol methacrylate) (70:30)) were identified which are specific for the megakaryocytic lineage. Analysis of MEG-01 cell morphology on the different polymers showed that most polymers bound cells in a round, suspension cell-like form with few and only short pseudopodia. In contrast, PA112 bound cells displaying an “outstretched” morphology with long pseudopodia forming proplatelets as could be seen for mature cells on polystyrene. Analysis of the proteins binding to the artificial polymers indicated a possible link between quantity of bound protein mixture to the cellular morphology. Immobilisation had only a minor influence on the cellular gene regulation as shown by miRNA studies and flow cytometry.

The identified polymers offer the opportunity to enrich and sort megakaryocytic cells from bone marrow suspensions but also to modify the polymeric structure with proliferation factors such as thombopoietin (TPO) for controlling cellular maturation.

## **Chapter 5: Experimental**

### **5.1 General Information**

#### **5.1.1 Equipment**

##### **Instruments for Microarray fabrication**

SciFLEXARRAYER S5 inkjet printer (Scienion AG, Germany)

Microdrop inkjet printer (microdrop Technologies GmbH, Germany)

Qarray<sup>mini</sup> contact printer (Genetix, UK)

Vacuum oven Vacutherm VT6025 (Heraeus, Germany)

Oxygen plasma (Europlasma, Belgium).

##### **Special Microscopes and Scanner**

Philips XL30CP Scanning electron microscope (Koninklijke Philips Electronics N.V., Netherlands)

Veeco Atomic Force Microscope Multimode/Nanoscope IIIa (Veeco, Canada)

Bioanalyzer 4F/4S white light scanner with FIPS software (LaVision BioTech, Germany)

Nikon 50i fluorescence microscope with automated stage and Pathfinder<sup>TM</sup> software (IMSTAR S.A., France).

## **Cell Culture**

Incubator HERAcell 150 (Heraeus, Germany)

Biosafety cabinet HERAsafe KS 18 class II (Heraeus, Germany)

### **5.1.2 Microscope Slides and Coverslips**

Microscope glass slides: 76 x 26 mm (Menzel GmbH Co. KG, Germany)

Round coverslips :13 mm in diameter (Menzel GmbH Co. KG, Germany)

### **5.1.3 Chemicals and Solvents**

All chemicals and solvents unless otherwise stated were purchased from Sigma Aldrich (UK). Collagen Type I (PureCol®) was received from Advanced Biomatrix Inc. (USA). Phosphate buffered saline (PBS, pH 7.4) was purchased from Oxoid (UK). Osmium tetroxide and 0.1 M cacodylate buffer (pH 7.4) containing 2.5% glutaraldehyde were purchased from Electron Microscopy Sciences (USA). Tridecafluoro-1,1,2,2-tetrahydrooctyl-dimethylchlorosilane (FDS) was purchased from abcr GmbH Co. KG (Germany).

### **5.1.3 Polymer Libraries**

The polyacrylate and polyurethane libraries were synthesised in our laboratory as part of previous projects.<sup>272,273</sup> All members of the libraries were characterised by gel

permeation chromatography, contact angle measurements and FT-IR (Mattson Instrument, USA) as previously described.<sup>272,273</sup> Endotoxin tests were not carried out.



## **5.2 Experimental for Chapter 2**

### **5.2.1 Preparation of Acrylate Functionalised Masks**

Microscope glass slides (76 x 26 mm) were cleaned in sodium hydroxide (1 M) for 2 h and afterwards rinsed with water and acetone. As a mask, spots of 2 drops 20% aqueous sucrose solution (w/w) were printed at 400  $\mu\text{m}$  distances onto the slides using a microdrop inkjet printer. The sucrose printed slides were coated with tridecafluoro-1,1,2,2-tetrahydrooctyl-dimethylchlorosilane (FDS, 5  $\mu\text{L}$ ) for 12 h in a sealed box. After removing the sugar spots with water and acetone, the slides were incubated with a solution of 3-(trimethoxysilyl)propyl methacrylate (TMSA, 10  $\mu\text{L}$ ) for 12 h. Finally, the slides were washed with water and acetone and the solutions needed for the *in situ* polymerization were printed on the former sugar sites.

### **5.2.2 Inkjet Printing for In Situ Formation of Polymer Spots**

*In situ* polymerization was achieved by printing two individual acrylate monomer solutions (20% (w/v) in 1-methyl-2-pyrrolidinone (NMP)), the crosslinker 1,4-butanediol diacrylate (30% (w/v) in NMP) and the photoinitiator 1-hydroxycyclohexyl phenyl ketone (30% (w/v) in NMP) on a drop-by-drop basis with a sciFLEXARRAYER S5. After half of the array was printed (3658 spots), the array was cooled on dry ice and irradiated with UV light for 20 min. Thereafter, the print was continued as before and finished with a second UV light application (20 min) under cooling. To ensure hardening of the polyacrylates and to evaporate all solvent traces, the arrays were incubated at 50  $^{\circ}\text{C}$  overnight. Thereafter, the array was rinsed

with ethanol leaving successful polymerized spots on the array and washing away any unpolymerised material.

### ***5.2.3 Preparation of Polymer Coated Coverslips***

Coverslips (13 mm in diameter) were cleaned in sodium hydroxide (1 M) for 16 h and afterwards rinsed with water and acetone. After having been air dried, the coverslips were incubated with a solution of 2% (v/v) TMSA and 0.5% (v/v) ethylenediamine in acetonitrile for 16 h. After washing with acetonitrile and acetone, the coverslips were dried on air and stored until polymer coating at -20 °C. For polymer coating, monomer, crosslinker and photoinitiator solutions in NMP were spread onto coverslips and exposed to UV light (Model B 100AP, Black-Ray) for 30 min. After incubation at 50 °C for 16 h, the coverslips were rinsed with ethanol. Prior cell cultivation, the coverslips were sterilised with UV light for 15 min and washed with PBS.

### ***5.2.4 Scanning Electron Microscopy (SEM) and energy dispersive X-ray spectroscopy (EDX)***

The printed polymer microarrays were gold coated using a Bal-Tec SCD050 sputter coater (Leica Microsystems GmbH, Germany) and secondary electron (SE) images of the microarrays were captured with a Philips XL30CP scanning electron microscope using an accelerating voltage of 20kV.

For the energy dispersive X-ray spectroscopy, a microarray consisting of the monomers 2-hydroxyethyl methacrylate and ethylene glycol methacrylate phosphate was fabricated and carbon coated with a Denton BTT-IV carbon evaporation coater (Denton Vacuum LLC, USA). An X-ray map was collected for carbon, oxygen and the phosphorous over the whole spot area for 60 min to verify its uniformity using the PGT Spirit ED system on the above microscope. For this investigation an accelerating voltage of 10 kV beam was used.

### **5.2.5 Water Contact Angle Measurements**

Water drops of 5  $\mu\text{L}$  in volume were deposited on the substrates using a micro-syringe. Images of the drops were captured with a CCD (Flee 2, Point Grey Research Camera, Canada) camera operating at 60 fps. A white LED backlight with diffuser was used to ensure uniform lighting and good contrast. The drop shape analysis software from First Ten Angstroms (USA) was used to determine the contact angles once the droplets reached a steady state. Assuming drop axisymmetry, the contact angles were measured (n=5).

### **5.2.6 Atomic Force Microscopy**

Polymer coated coverslips were imaged with atomic force microscopy under ambient conditions using a Veeco AFM, Multimode/Nanoscope IIIa equipped with a J-scanner (x-y-range of 140  $\mu\text{m}$ ). The images were recorded in tapping mode using RTESP Veeco cantilevers with a nominal spring constant and a resonance frequency

of 40 N/m and 300 kHz. The set-point amplitude ratio  $rsp = A_{sp} / A_0$  was kept close to 1 (where  $A_{sp}$  is the reduced scanning set-point amplitude and  $A_0$  stands for the free oscillation amplitude). This ensured a “light tapping” where the interaction force between the tip and the substrate was minimized without losing contact. Areas of  $4 \mu\text{m}^2$  were recorded and the root mean square roughness (RMS) was measured across this region. Image processing was conducted with the software Scanning Probe Image Processor (SPIP, Image Metrology, Denmark).

### **5.2.7 Cell Culture**

The hESC line RH1 used in this study was described previously.<sup>94</sup> The cell line was derived under an HFEA license (No. R0136) permitting the use of donated embryos in research, the creation of embryos and the derivation of human embryonic stem cells. Full informed consent for research use was obtained in advance from the donor couple. The RH1 cell line was cultured on growth factor reduced Matrigel<sup>TM</sup> (Becton Dickinson, UK), in chemically defined medium mTESR 1 (Stem Cell Technologies, France) and passaged using a collagenase/ scraping regime. For incubation on the microarrays, RH1 hESC were treated with collagenase for 5 min at 37 °C and the cells manually detached from Matrigel<sup>TM</sup> plates with a scraper. Cell lumps were broken down by pipetting and the cells plated on the sterilized and PBS washed array at a concentration of 1.2 million cells/array. After an incubation time of 4 d, with daily media change, the cells were fixed with paraformaldehyde in PBS (4 %, (v/v)) and the cells stained with DAPI and Oct-4 antibody labeled with FITC.

For the incubation on coverslips, the RH1 cell line was seeded at a concentration of 60 000 cells/coverslip. After approx. 7 d the cells were confluent and were passaged by treatment with trypsin (0.025 % (v/v)) for 2 min and following suspension in mTESRI supplemented with p160-Rho-associated coiled kinase (ROCK) inhibitor (1:10). The cells were seeded at a concentration of 60000 cells/coverslip in mTESRI medium supplemented with ROCK inhibitor. The following daily medium changes were carried out with mTESRI medium without further supplements.

### ***5.2.8 Cell population Doubling Time***

The cell population doubling time was calculated by counting the cells before and after passaging. The cell doubling time was estimated as an exponential function and calculated using an online cell doubling calculator.<sup>274</sup>

### ***5.2.9 Immunocytochemistry of hESCs on Polymer Coverslips***

Cells were stained using a standard immunocytochemistry protocol. Briefly, hESCs on polymers were washed once with PBS and fixed with 4% (v/v) paraformaldehyde in PBS. After permeabilisation with 0.2% (v/v) Igepal (Sigma-Aldrich, USA) and blocking in 10% (v/v) normal rabbit serum (Millipore), cells were incubated with primary antibodies (Oct-4 (1:50, Santa Cruz Biotechnology, USA), Nanog (1:30, R&D systems, USA), for 2-4 hours at room temperature or overnight at 4°C. Visualisation with secondary antibodies was performed using Alexafluor antibodies 488 and 555, (Invitrogen, USA) and nuclei were stained with DAPI. Imaging

analysis was carried out using a fluorescence microscope Leica DM IRB equipped with a DFC 350 FX camera (Leica Microsystems CMS GmbH, Germany)

#### **5.2.10 Flow Cytometry Analysis**

Cells were dissociated by incubation with 0.025% (v/v) trypsin/EDTA for 5-10 min at 37 °C, resuspended in FACS PBS (PBS supplemented with 0.1% (v/v) BSA and 0.1% (v/v) sodium azide) and incubated with preconjugated antibodies (SSEA-4-FITC; SSEA-1-PE (all from BioLegend, USA) and in FACS PBS for 20-40 min. Data were obtained using a FACS calibur and analysed using FlowJo 7.6.3. (TreeStar Inc., USA).

### **5.3 Experimental for Chapter 3**

#### **5.3.1 Preparation of Masked Glass Slides**

Microscope glass slides (76 x 26 mm) were cleaned with sodium hydroxide (1 M) for 2 h and then rinsed with water and acetone. The slides were masked by printing 25 spots (each 3 drops) of 20% aqueous sucrose solution (w/v) 200  $\mu\text{m}$  apart in 3 columns (each column 200  $\mu\text{m}$  apart) using a microdrop inkjet printer (Microdrop Technologies GmbH, Germany). The distance between the single spots allowed the spots to merge together to form a line. The masked slides were treated with (tridecafluoro-1,1,2,2-tetrahydrooctyl) dimethylchlorosilane (5  $\mu\text{L}$ ) for 12 h in a sealed box. After removing the sucrose masking by washing the slides with water and acetone, the exposed slide surfaces were coated with 3-(trimethoxysilyl)propylmethacrylate (10  $\mu\text{L}$ ) for 16 h. Finally, the slides were washed with water and acetone and stored at -20  $^{\circ}\text{C}$  until use.

#### **5.3.2 Inkjet Printed Gradients**

Gradients were generated by printing acrylate monomers (20% (w/v) in NMP), a crosslinker (1,4-butanediol diacrylate, 30% (w/v) in NMP) and the photoinitiator (1-hydroxycyclohexyl phenyl ketone, 30% (w/v) in NMP) on a drop-by-drop basis (sciFLEXARRAYER S5, Scienion AG, Germany). For the printing of 5 mm long and 0.5 mm wide lines, six spots each of 26 drops (400 pL per droplet) were printed 800  $\mu\text{m}$  apart. The drop ratio of Monomer A:Monomer B varied from 19:0 to 15:4, 12:8, 8:12, 4:15 and 0:19, with a final crosslinker concentration per spot of 6% (5

drops) and a final photoinitiator concentration of 2% (2 drops). Depending on the length and width of the gradients, the number of drops of the different components was changed accordingly (SI Table 1).

A fluororous coated slide, (tridecafluoro-1,1,2,2-tetrahydrooctyl) dimethylchlorosilane coated microscope slide) was placed on top of the printed array. Compression allowed the merging of the spots to give the gradient-line prior to UV irradiation (Black Ray® Model B 100,) for 15 min. The slides were kept at 50 °C overnight to ensure complete polymerisation and were then rinsed with ethanol to remove non-polymerised material. For visualisation purposes, a gradient of 2-diethyl amine acrylate and (2-hydroxyethyl methacrylate with 1% (w/v) 5(6)-carboxyfluorescein) was prepared and the fluorescent gradient analysed using a Bioanalyzer 4F scanner.

### **5.3.3 X-Ray Photoelectron Spectroscopy**

XPS analysis of the phosphorous 2p signal intensity was carried out with a VG Sigma Probe spectrometer using Al K $\alpha$  radiation with a 30  $\mu$ m diameter spot (1.5 W), a pass energy of 100 eV and a 0.5 eV step size on a polymer gradient prepared from the monomers 2-hydroxyethyl methacrylate and ethylene glycol methacrylate phosphate.

### **5.3.4 Cell Culture**

*Cell lines:* Human erythroleukaemic cells (K562) and human cervical cancer cells (HeLa) were grown in RPMI 1640 growth medium supplemented with heat



inactivated fetal bovine serum (FBS) (10% v/v), penicillin (100 U mL<sup>-1</sup>), streptomycin (100 mg mL<sup>-1</sup>) and *L*-glutamine (4 mM) at 37 °C with 5% CO<sub>2</sub>. Media, serum and antibiotics were purchased from (Gibco, UK) or (Sigma-Aldrich, UK). Prior to incubation with 5x10<sup>5</sup> cells/array, the gradient polymer microarrays were sterilized with UV light for 15 min. After an incubation time of 3 d, cells were fixed with paraformaldehyde in PBS (4%, (v/v)) and cells stained with propidium iodide (1 µg/mL). In case of OGPCS, the cells were incubated for 18 h on the slides till the slides were fixed and mounted.

*Primary Cells:* OGPCS were obtained by following the protocol described by McCarthy.<sup>170</sup> Forebrains of neonatal rat pups were removed, stripped of meninges and then mechanically and enzymatically dissociated. The resulting cell suspension was plated onto Poly-D-lysine coated Falcon 75 cm<sup>2</sup> cell culture flasks in culture medium consisting of DMEM supplemented with 10% (w/v) FBS with 1% (w/v) penicillin and streptomycin and incubated at 37 °C and 7.5% CO<sub>2</sub>. Culture medium was changed after 24 h and twice weekly thereafter. Prior to incubation on the gradient polymer microarrays (750000 cells/array), the arrays were sterilised by 10 min exposure to UV light on either side. Microglia were incubated on the slides and incubated at 37 °C, 7.5% CO<sub>2</sub> for 18 h before being fixed in 4% (v/v) paraformaldehyde in PBS and stained with Hoechst 33342 (1 µg/mL).

### **5.3.5 Image Acquisition and Analysis**

*K562, HeLa:* Stained cells were imaged using a Leica fluorescence microscope DM IRB equipped with a DFC 350 FX camera (Leica Microsystems CMS GmbH,

Germany). The gradients were divided into seven sections and analyzed with the software ImageJ.<sup>275</sup>

*OGPCS*: Images were taken from the two ends of the gradient lines with a Zeiss observer Microscope (Carl Zeiss Ltd, UK) and the cells and areas counted with the software ImageJ.<sup>275</sup>

### **5.3.6 Modification of Gradients with 6-Aminofluorescein**

Polymer gradients of *N*-acryloxysuccinimide and 2-hydroxyethyl methacrylate were fabricated and after polymerisation, washed with hexane. Gradient derivatisation was achieved by a 2 h incubation with 6-aminofluorescein (300  $\mu$ L, 1 mg/mL in dry DMF). After washing the slide with DMF and water, fluorescence analysis was carried out with a Bioanalyzer 4F scanner.

### **5.3.7 Modification of Gradients with Semaphorin 3F**

Polymer gradients of 2-carboxyethyl methacrylate and *tert*-butyl acrylate or *tert*-butylcyclohexyl acrylate were fabricated and after polymerisation, washed with hexane. Gradient derivatisation was achieved incubating the arrays with 300  $\mu$ L of a mixture of 1-ethyl-3-(3-dimethylaminopropyl) carbodiimide, 0.1 M) and *N*-hydroxysuccinimide (5 mM) in dry DMF for 2 h. This was followed by coupling of Sema3F (100  $\mu$ g/mL) in PBS for 1.5 h.

### ***5.3.8 Protein Gradient Verification: Fluorescence Intensity Measurement***

The fluorescence of each gradient was calculated by measuring the fluorescence at 15 circular areas of interest (AOI, diameter = 50 pixels) along each line from both pre- and post - incubation with semaphorin antibodies using Bioanalyzer 4F. The score from the pre-incubation AOIs could then be subtracted as background to give the fluorescence score for that point.

## **5.4 Experimental for Chapter 4**

### **5.4.1 Platelets and Red Blood Cells**

Two-day-old buffy coat-derived, pooled and leuco-reduced, citrated platelet rich plasma (PRP) was obtained from the Scottish National Blood Transfusion Service (SNBTS). It was stored at 22 °C with agitation. Flow cytometry studies were carried out prior to the microarray tests to ensure minimal activation and consistent platelet contents. Platelet poor plasma (PPP) was prepared by two centrifugations of the PRP samples at 1700 g for each 15 min and collecting the supernatant. Red blood cells were obtained from the SNBTS components processing laboratories using standard blood bank methods. The samples were leuco-reduced on the day of donation and stored in a saline, adenine, glucose, mannitol additive (SAGM) at  $4 \pm 2$  °C. All cell counts and haematocrit determinations were carried out on a Sysmex KX-21 cell counter (Sysmex, UK).

### **5.4.2 Polymer Microarray Fabrication**

#### *Agarose Coating*

Glass slides were cleaned with an oxygen plasma (Europlasma, Belgium) at 20 °C for 5 min and treated with 2 % (w/v) 3-aminopropyltriethoxysilane in acetonitrile for 1 h. Thereafter, the slides were rinsed with acetonitrile, acetone and dried at 100 °C overnight. Agarose coating was achieved by dipping 2/3 of the slides into a 2 % (w/v) aqueous agarose solution at 65 °C. After drying, the slides were used for contact printing.

### *Contact Printing of Polymers and Collagen Coating*

Polyacrylates (PA) and polyurethanes (PU) were contact printed with a Qarrayer<sup>mini</sup> equipped with aQu solid pins (K2785, Genetix). For printing, 1 % (w/v) polymer solutions in *N*-methyl pyrrolidine were used and stamped five times for each spot. The inking time was 200 ms, the stamping time 100 ms. Under these conditions, typical spot diameters of 300 to 320  $\mu\text{m}$  were achieved. The slides were dried under vacuum at 40 °C overnight. The part of the glass slide which was free of agarose, was further dip coated into collagen I solution (3 mg/mL) and left overnight at 4 °C before being air dried.

#### **5.4.3 Static Microarray PRP Studies and Fluorescence Microscopy**

PRP (300  $\mu\text{L}$ ) was directly incubated on the microarray slides for 30 min at room temperature. Thereafter, the slides were washed with PBS and fixed with 1 % paraformaldehyde for a further 30 min. The slides were rinsed in PBS and incubated with a solution of the antibodies CD41-FITC and CD62P-PE (dilution: 1:100 in PBS). After 1 h, the slides were washed with PBS, water and air dried. The fluorescence intensity of each spot was measured with a Bioanalyzer 4F (LaVision, Germany). Images of each polymer spot were captured with a Nikon 50i fluorescence microscope using the Pathfinder<sup>TM</sup> software (IMSTAR S.A., France). For adsorption studies of plasma proteins, PPP was incubated on microarrays for 30 min. The slides were washed twice with PBS and stained with antibodies against fibrinogen (sheep anti human fibrinogen-FITC), von Willebrand factor (vWF, sheep anti human vWF antibody following an incubation with donkey anti-sheep

IgG:Dylight®649) and serum albumin (mouse anti-human serum albumin antibody following an incubation with goat-anti mouse IgG-Dylight®549). All antibodies were used at dilutions of 1:100 in PBS. After washing the slides in PBS and water, the slides were scanned with the Bioanalyzer 4F system.

#### ***5.4.4 Upscale of Polymers on Coverslips***

Glass coverslips of 13 mm diameter were cleaned with tetrahydrofuran (THF) and spin coated with 2 % (w/v) preformed polymer solutions in THF for 2 s at 2000 rpm. The coverslips were dried in a vacuum oven overnight at 40 °C, 200 mbar and irradiated with UV light for 20 min prior use in cell studies. As a control, collagen I and BSA coverslips were prepared by incubating the aqueous protein solutions (3 mg/mL) overnight at 4 °C and left to air dry.

#### ***5.4.5 Scanning Electron Microscopy***

PRP (100 µL) was incubated on 13 mm coverslips coated with the hit polymers from the static microarray experiments for 30 minutes. After washing with PBS, the remaining cells on the coverslips were fixed with 2.5 % glutaraldehyde in 0.1 M cacodylate buffer (pH 7.4) for 2 h. After washing twice with 0.1 M cacodylate buffer, the samples were post-fixed with 1 % osmium tetroxide for 1 h and dehydrated through graded ethanol (50, 70, 90 and 100 %). Finally, the samples were critical point dried in CO<sub>2</sub> and gold coated by sputtering. Images were captured with

a Philips XL30CP scanning electron microscope. For each polymer, five images were taken in random areas of the coverslips in two separate experiments.

#### **5.4.6 Shear Studies on the Cone and Platelet Analyser**

Platelet adhesion on 13 mm polymer coated coverslips was carried out under arterial flow conditions according to the Cone and Plate(let) principal on an Impact-R analyzer (Matis-Medical, Belgium) [22]. A mixture of 0.6 mL PRP and 1 mL of ABO-compatible routine leuco-reduced red blood cells in SAGM was rotated at 10 rpm for 1 min. The resulting mixture had similar levels of platelet counts ( $300 \times 10^3$  cells/ $\mu\text{L}$ ) and haematocrit (35-45 %) as in whole blood samples except for the reduced levels of leucocytes. For the studies, 130  $\mu\text{L}$  of this mixture was placed onto the cone equipped with the polymer coated coverslip and rotated at  $1800 \text{ s}^{-1}$  for 4 min. The coverslips were washed with distilled water and the adhered platelets were stained with 300  $\mu\text{L}$  of May-Grünwald solution for 1 min. The remaining staining solution was removed and the coverslips were air-dried. Seven images of the stained platelets were captured on defined areas. The surface coverage and aggregate size were calculated *via* the Impact R software (Version: 1.28, DiaMed, USA). All samples were run in duplicate and average values obtained ( $n = 10$ ).

#### **5.4.7 Statistics**

For comparing two data sets the two-tailed, unpaired Student's-test was applied. For data sets more than two the one-way analysis of variance (ANOVA) was calculated.

In the calculations, a significant probability of 95 % was accepted as being reasonable (i.e.  $p < 0.05$  is significant).

#### **5.4.8 Megakaryocytic Cell Culture**

The cell strains MEG-01 and K562 were received from the Health Protection Agency's Culture Collection, (London, UK). They were grown in RPMI 1640 medium supplemented with 10 % FBS (Invitrogen, UK), 2mM *L*-Glutamine (100 U/mL of penicillin and 100  $\mu\text{g/mL}$  of streptomycin. The cells were seeded at a concentration of  $3 \times 10^5$  cells/mL and passaged every three days.

#### **5.4.9 Polymer Microarray Studies**

Cells were washed with PBS and diluted with media to a final concentration of  $10^5$  cells/mL. The polymer microarrays were placed in a four well-plate (Nunc, Germany) and 6 mL of the cell solution was gently added into the well. After an incubation period of 4 d, the microarray slides were washed with PBS and fixed with 4 % (v/v) formaldehyde in PBS for 1 h. Then the cells were stained with the nuclear stain Hoechst 33342 at a final concentration of 1  $\mu\text{g/mL}$  in PBS for 30 min. When it was required to stain the cells with further antibodies, the slides were washed with PBS and incubated with the respective antibody solution in PBS for 1 h. At the end the, the microarray was washed with PBS and water and finally air dried. Image capture was carried out *via* a Nikon 50i fluorescence microscope using IMSTAR Pathfinder<sup>TM</sup> software (IMSTAR S.A., France).



#### **5.4.10 Proteinbinding on Polymer SDS-Page and MS analysis**

Polymer coated coverslips (diameter: 13 mm) were incubated for 1 d in RPMI medium supplemented with 10 % FBS, 2mM *L*-Glutamine and 100 U/mL of penicillin and 100 µg/mL of streptomycin (SIGMA-Aldrich, UK). The coverslips were washed twice with PBS and the proteins were eluted by boiling in SDS-sample buffer (0.5 M Tris-HCl (pH 8.8), SDS 4% (w/v), glycerol 20% (v/v), 2-mercaptoethanol 2% (v/v), and bromophenol blue 0.0025%) for 5 min. The proteins were separated on a mini-PROTEAN TGX 4-20% SDS/PAGE 1D gel in TGS buffer (Tris 0.025M, Glycine 0.192M, w/v SDS 0.1%, 200 V, 180 mA, 35 min) stained with Coomassie Blue or ProteoSilver™ silver stain and imaged and processed. Detected protein bands were reduced with 10 mM DTT, 0.2% EDTA in 100 mM ammonium bicarbonate in acetonitrile (AbC) at 56 °C for 30 min followed by alkalation with 50 mM iodoacetamide in 100 mM AbC in the dark at room temperature for 30 min. After washing the mixture was digested in trypsin buffer (13 ng trypsin in 50 mM AbC) at 37 °C for 12 h. The digested mixture was analyzed by LC-MS/MS (Dionex Ultimate 3000; Solvent A: 98% water, 2% acetonitrile (ACN), 0.1% formic acid (FA); Solvent B: 80% ACN, 20% water, 0.1% FA; 100 % A to 100% B in 1 h; MS/MS: Bruker HCT Ultra PTM). The data were analyzed with DataAnalysis v.4.0 SP4, BioTools 3.2 SR1 and compared with a protein database (Mascot version 2.2.07).

#### **5.4.11 Flow Cytometry**

The expression of CD41 (GPIIb/IIIa) and CD42b on MEG-01 cells was measured as described before.<sup>268</sup> Briefly, MEG-01 cells were cultivated on polymer coverslips for 4 d. The adherent cells were washed, detached with trypsin (2 min, 1:100 Trypsin/PBS), washed in medium and PBS (containing 0.1 % BSA) and stained with antibodies against anti-human CD41-FITC and CD42b-Pe for 30 min. Subsequently, the cells were washed in PBS (0.1% BSA) and analysed in a FACSArier2000 (BD, UK). Controls without any antibody and of suspension cells were analysed as well.

#### **5.4.12 miRNA Array Profiling**

The cell line MEG-01 was washed with PBS and diluted with media to a final concentration of  $10^5$  cells/mL and incubated on polymer coated coverslips (PA382, PA112, diameter: 5 cm) or on 6-well polystyrene culture dishes (Nunc, Germany) for 4 d. Thereafter, miRNA was extracted with the miRCURY™ RNA Isolation Kit-Cell and Plant Version 1.1 (Exiqon, Denmark) according to the protocol provided. The cells were counted and about  $10^6$  cells were used for miRNA isolation. After purification with the provided columns and buffers provided, samples were stored at -70 °C until further usage. The quantity of the total RNA was determined with a Nanodrop2000 (Thermo Fisher Scientific Inc., USA) and for each sample 0.5 µg of total RNA were used for labelling with Hy3™ fluorescent label with the miRCURY LNA™ microRNA Array Power Labelling Kit version 3.0 (Exiqon, Denmark) according to the instructions provided. The samples were hybridised to miRNA™ LNA arrays 5<sup>th</sup> generation, human, mouse and rat (Exiqon, Denmark) which contains

control probes and more than 1800 capture probes complementary to human, mouse, rat and their related viral sequences registered in the miRBASE version 14.0 at the Sanger Institute following the procedure described by the manufacturer. After washing, the slides were scanned and image analysis was carried out with Aida Image Analyzer version 4.50 (raytest GmbH, Germany). The quantified signals were background corrected and normalised using a quantile normalisation. The median of each set of identical datapoints (quadruplicates) was calculated to account for the variance within the data. The data was re-normalised using a quantile normalisation, to account for minor changes introduced by using the medians. From this data pairwise comparisons (log<sub>2</sub>-plots) were generated to show the similarities and differences between the samples.

## **Chapter 6: References**

1. D. F. Williams; *Definitions in Biomaterials - Proceedings of a Consensus Conference of the European Society for Biomaterials*, D.F. Williams, Ed.; Elsevier: New York, USA, **1987**.
2. D. F. Williams; On the mechanisms of biocompatibility. *Biomaterials* **2008**, *29*, 2941-2953.
3. R. Langer, D. A. Tirrell; Designing materials for biology and medicine. *Nature* **2004**, *428*, 487-492.
4. M. Yliperttula, B. M. Chung, A. Navaladi *et al.*; High-throughput screening of cell responses to biomaterials. *Eur. J. Pharm. Sci.* **2008**, *35*, 151-160.
5. H. Shin, S. Jo, A. G. Mikos; Biomimetic materials for tissue engineering. *Biomaterials* **2003**, *24*, 4353-4364.
6. C. Chen, J. Peng, H. S. Xia *et al.*; Quantum dots-based immunofluorescence technology for the quantitative determination of HER2 expression in breast cancer. *Biomaterials* **2009**, *30*, 2912-2918.
7. L. DeLaporte, J. C. Rea, L. D. Shea; Design of modular non-viral gene therapy vectors. *Biomaterials* **2006**, *27*, 947-954.
8. D. F. Williams; On the nature of biomaterials. *Biomaterials* **2009**, *30*, 5897-5909.

9. M. B. Gorbet, M. V. Sefton; Biomaterial-associated thrombosis: roles of coagulation factors, complement, platelets, and leukocytes. *Biomaterials* **2004**, *25*, 5681-5703.
10. A. L. Hook, D. G. Anderson, R. Langner *et al.*; High-throughput methods applied in biomaterial development and discovery, *Biomaterials* **2010**, *31*, 187-198.
11. J. J. Diaz-Mochon, G. Tourniaire, M. Bradley; Microarray platforms for enzymatic and cell-based assays. *Chem. Soc. Rev.* **2007**, *36*, 449-457.
12. J. Petrik; Diagnostic applications of microarrays. *Transfus. Med.* **2006** *16*: 233-247.
13. S. P. Fodor, J. L. Read, M. C. Pirrung *et al.*; Light-directed, spatially addressable parallel chemical synthesis. *Science* **1991**, *251*, 767-773.
14. R. J. Lipshutz, D. Morris, M. Chee *et al.*; Using oligonucleotide probe arrays to access genetic diversity. *BioTechniques* **1995**, *19*, 442-447.
15. Affymetrix : [www.affymetric.com](http://www.affymetric.com) Date: 06/2012.
16. ArrayIt: [www.arrayit.com](http://www.arrayit.com), Date: 06/2012.
17. M. Cretich, G. di Carlo, R. Longhi *et al.*; High sensitivity protein assays on microarray silicon slides. *Anal. Chem.* 2009, *81*, 5197-5203.

18. T. Schenk, T. Brandstetter, A. zur Hausen *et al.*; Performance of a polymer-based DNA chip platform in detection and genotyping of human Papillomavirus in clinical samples. *J. Clin. Microbiology*. **2009**, *47*, 1428-1435.
19. N. Zammateo, L. Jeanmart, S. Hamels *et al.*; Comparison between different strategies of covalent attachment of DNA to glass surfaces to build DNA microarrays. *Anal. Biochem*. **2000**, *280*, 143-150.
20. G. Tourniaire, J. Collins, S. Campbell, *et al.*; Polymer microarrays for cellular adhesion. *Chem. Commun*. **2006**, 2118-2120.
21. D. G. Anderson, S. Levenburg, R. Langer; Nanoliter-scale synthesis of arrayed biomaterials and application to human embryonic stem cells. *Nat. Biotechnol*. **2004**, *22*, 863-866.
22. C. S. Chen, M. Mrksich, S. Huang *et al.*; Micropatterned surfaces for control of cell shape, position, and function. *Biotechnol. Prog*. **1998**, *14*, 356-363.
23. B. T. Houseman, J. H. Huh, S. J. Kron *et al.*; Peptide chips for the quantitative evaluation of protein kinase activity. *Nat. Biotechnol*. **2002**, *20*, 270-274.
24. R. Zhang, A. Liberski, R. Sanchez-Martin *et al.*; Microarrays of over 2000 hydrogels - Identification of substrates for cellular trapping and thermally triggered release. *Biomaterials*, **2009**, *30*, 6193-6201.
25. A. Liberski, R. Zhang, M. Bradley; Inkjet fabrication of polymer microarrays and grids-solving the evaporation problem. *Chem. Commun*. **2009**, 334-336.

26. Y. Ito, M. Nogawa, M. Takeda *et al.*; Photo-reactive polyvinylalcohol for photo-immobilised microarray. *Biomaterials* **2005**, *26*, 211-216.
27. Z. Nie, E. Kumacheva; Patterning surfaces with functional polymers, *Nature Materials* **2008**, *7*, 277-290.
28. U. R. Müller; *Microarray technology and its application*, U. R. Müller, D. V. Nicolau, Eds.; Springer: Berlin, Germany, **2005**, 73-88.
29. G. Tournaire, *PhD Thesis*, December **2006**.
30. D. Wu, L. Song, K. Chen *et al.*; Modelling and hydrostatic analysis of contact printing microarrays by quill pins, *Int. J. Mech. Sci.* **2012**, *54*, 206-212.
31. M. K. McQuain, K. Seale, J. Peek *et al.*; Effects of relative humidity and buffer additives on the contact printing of microarrays by quill pins. *Anal. Biochem.* **2003**, *320*, 281-291.
32. J. M. Schwenk, D. Stoll, M. F. Templin *et al.*; Cell microarrays: an emerging technology for the characterization of antibodies. *Biotechniques* **2002**, *Suppl.*, 54-61.
33. R. Rapley, S. Harborn; *Molecular analysis and genome discovery*, J. Burgess, Ed.; John Wiley and Sons Ltd.: Hoboken, USA, **2004**, 127-158.
34. Y. Xia, D. Qin, G. M. Whitesides; Microcontact printing with a cylindrical rolling stamp: A practical step toward automatic manufacturing of patterns with submicrometer-sized features. *Adv. Mater.* **1996**, *8*, 1015-17.

35. S. A. Ruiz, C. S. Chen; Microcontact printing: A tool to pattern. *Soft Matter* **2007**, *3*, 1–11.
36. R. S. Kane, S. Takayama, E. Ostuni, D. E. Ingber and G. M. Whitesides, Patterning proteins and cells using soft lithography. *Biomaterials*, **1999**, *20*, 2363.
37. A. Perl, D. N. Reinhoudt, J. Huskens; Microcontact Printing: Limitations and Achievements. *Adv. Mater.* **2009**, *21*, 2257-2268.
38. Y. Xia, G. M. Whitesides; Extending microcontact printing as a microlithographic technique. *Langmuir* **1997**, *13*, 2059-67.
39. M. J. Doktycz; *Microarray technology and its applications*, U. R. Müller, D.V. Nicolau, Ed.; Springer: Berlin, Germany, **2005**, 63-72.
40. A. Hudd; *The Chemistry of Inkjet Inks*, S. Magdassi, Ed.; World Scientific Publishing Co. Pte. Ltd.: Singapore, **2009**, 3-18.
41. E. A. Roth, T. Xu, M. Das *et al.*; Ink-jet Printing for high throughput cell patterning. *Biomaterials* **2004**, *25*, 3707-3715.
42. T. Xu, J. Jin, C. Gregory *et al.*; Inkjet printing of viable mammalian cells. *Biomaterials* **2005**, *26*, 93-99.
43. <http://www.sciencion.de/index.php?mid=46&vid=&lang=en> Date: 06/2012
44. [http://www.microdrop.de/Microdrop\\_dispenser\\_heads.html](http://www.microdrop.de/Microdrop_dispenser_heads.html) Date: 06/2012



45. P. Calvert; Inkjet printing for materials and devices. *Chem. Mat.* **2001**, *13*, 3299-3305.
46. R. Miki, K. Kadota, H. Bono *et al.*; Delineating developmental and metabolic pathways in vivo by expression profiling using the RIKEN set of 18 816 full-length enriched mouse cDNA arrays. *Proc. Natl. Acad. Sci.* **2001**, *98*, 2199–2204.
47. M. Schena, D. Shalon, R. Heller *et al.*; Parallel human genome analysis: microarray-based expression monitoring of 1000 genes. *Proc. Natl. Acad. Sci.* **1996**, *93*, 10614–10619.
48. C. B. Tempfer, E.-K. Riener, L. A. Hefler *et al.*; DNA microarray-based analysis of single nucleotide polymorphisms may be useful for assessing the risks and benefits of hormone therapy. *Fertil. Steril.* **2004**, *82*, 132-137.
49. F. Gemignani, C. Perra, S. Landi *et al.*; Reliable detection of  $\beta$ -thalassemia and G6PD mutations by a DNA microarray. *Clin. Chem.* **2002**, *48* 2051-2054.
50. S. Honma, V. Chizhikov, N. Santos *et al.*; Development and validation of DNA microarray for genotyping group A rotavirus VP4 (P[4], P[6], P[8], P[9], and P[14]) and VP7 (G1 to G6, G8 to G10, and G12) genes. *J. Clin. Microbiol.* **2007**, *45*, 2641–2648.
51. R. S. Uma, T. Rajkumar; DNA microarray and breast cancer - a review. *Int. J. Hum. Genet.* **2007**, *7*, 49-56.

52. S. vani Guttula, A. Allam, R. S. Gumpeny; Analyzing microarray data of alzheimer's using cluster analysis to identify the biomarker genes. *Int. J. Alzheimers Dis.* **2012**, 2012, 649456.
53. D.A. Hall, J. Ptacek, M. Snyder; Protein microarray technology. *Mech. Ageing Dev.* **2007**, 128, 161-167.
54. P. Bertone, M. Snyder; Advances in functional protein microarray technology *FEBS J.* **2005**, 272, 5400-5411.
55. A. Shreekumar, M. K. Nyati, S. Varambally *et al.*; Profiling of Cancer cells using protein microarrays: discovery of novel radiation-regulated proteins. *Cancer Res.* **2001**, 7585-93.
56. D. A. Hall, H. Zhu, X. Zhu *et al.*; Regulation of gene expression by a metabolic enzyme. *Science* **2004**, 306, 482-484.
57. H. Zhu, M. Bilgin, R. Bangham *et al.*; Global analysis of protein activities using proteome chips. *Science* **2001**, 293, 2101-2105.
58. M. D. Kurkuri, C. Driever, G. Johnson *et al.*; Multifunctional polymer coatings for cell microarray applications. *Biomacromolecules* **2009**, 10, 1163-1172.
59. T. G. Fernandes, M. M. Diog, D. S. Clark *et al.*; High-throughput cellular microarray platforms: applications in drug discovery, toxicology and stem cell research. *Trends Biotechnol.* **2009**, 27, 342-349.

60. ASAHI KASEI KABUSHIKI KAISHA, M. Bradley, G. Tourniaire, Patent GB 2408331: *Arrays for screening polymeric materials* **2003**.
61. A. D. Celiz, A. L. Hook, D. J. Scurr *et al.*; ToF-SIMS imaging of a polymer microarray prepared using ink-jet printing of acrylate monomers. *Surf. Interface Anal.* **2012**, doi: 10.1002/sia.5042.
62. H. Thissen, G. Johnson, G. McFarland *et al.*; Microarrays for the evaluation of cell-biomaterial surface interactions, *Proc. SPIE* **2006**, 6413, 64131-64139.
63. S. Pernagallo, M. Wu, M. P. Gallagher *et al.*; Colonising new frontiers—microarrays reveal biofilm modulating polymers. *J. Mater. Chem.* **2011**, 21, 96-101.
64. R. D. Deegan, O. Bakajin, T. F. Dupont *et al.*; Capillary flow as the cause of ring stains from dried liquid drops. *Nature* **1997**, 389, 827–829.
65. Y. Mei, M. Goldberg, D. Anderson; The development of high-throughput screening approaches for stem cell engineering. *Curr. Opin. Chem. Biol.* **2007**, 11, 388-393.
66. T. Burdon, I. Chambers, C. Stracey *et al.*; A Signaling mechanisms regulating self-renewal and differentiation of pluripotent embryonic stem cells. *Cells Tissues Organs* **1999**, 165, 131–143.
67. G. R. Martin; Isolation of a pluripotent cell line from early embryos cultured in medium conditioned by teratocarcinoma stem cells. *Proc. Natl. Acad. Sci.* **1981**, 78, 7634–7638.

68. M. J. Evans, M. Kaufman; Establishment in culture of pluripotential cells from mouse embryos. *Nature* **1981**, 292, 154–156.
69. O. Lindvall, Z. Kokaia; Stem cells for the treatment of neurological disorders. *Nature* **2006**, 441, 1094-1096.
70. J. Han, K. Sidhu; Embryonic stem cell extracts: use in differentiation and reprogramming. *Regen. Med.* **2011**, 6, 215-27.
71. E. A. Kimbrel, S. J. Lu; Potential clinical applications for human pluripotent stem cell-derived blood components. *Stem Cells Int.* **2011**, 2011, 273076.
72. W. S. Toh, E. H. Lee, T. Cao; Potential of human embryonic stem cells in cartilage tissue engineering and regenerative medicine. *Stem Cell Rev.* **2011** 7, 544-559.
73. S. C. Zhang, M. Wernig, I. D. Duncan *et al.*; *In vitro* differentiation of transplantable neural precursors from human embryonic stem cells. *Nat. Biotechnol.* **2001**, 19, 1129 –1133.
74. J. W. McDonald, X. Z. Liu, Y. Qu *et al.*; Transplanted embryonic stem cells survive, differentiate and promote recovery in injured rat spinal cord. *Nat. Med.* **1999** 5, 1410 –1412.
75. D. S. Krause, N. D. Theise, M. I. Collector *et al.*; Multi-organ, multi-lineage engraftment by a single bone marrow-derived stem cell. *Cell* **2001**, 105, 369–77.

76. S. Smith, W. Neaves, S. Teitelbaum *et al.*; Adult versus embryonic stem cells: treatments. *Science* **2007**, *316*, 1422–1423.
77. K. Okita, T. Ichisaka, S. Yamanaka; Generation of germlinecompetent induced pluripotent stem cells. *Nature* **2007**, *448*, 313–317.
78. M. Baker; Adult cells reprogrammed to pluripotency, without tumors. *Nature Reports Stem Cells*. Retrieved **2007**-12-11.
79. K. Takahashi, S. Yamanaka; Induction of pluripotent stem cells from mouse embryonic and adult fibroblast cultures by defined factors. *Cell* **2006**, *126*, 663–676.
80. K. Takahashi, K. Tanabe, M. Ohnuki *et al.*; Induction of pluripotent stem cells from adult human fibroblasts by defined factors. *Cell* **2007**, *131*, 1–12.
81. H. Niwa, J. Miyazaki, A. G. Smith; Quantitative expression of Oct-3/4 defines differentiation, dedifferentiation or self-renewel of ES cells. *Nat. Genet.* **2000**, *24*, 372–376.
82. H. Niwa; Molecular mechanism to maintain stem cell renewal. *Cell Struct. Funct.* **2001**, *26*, 137–148.
83. I. Chambers, D. Colby, M. Robertson *et al.*; Functional Expression Cloning of Nanog, a Pluripotency Sustaining Factor in Embryonic Stem Cells. *Cell* **2003**, *113*, 643–655, 2003,
84. L. A. Boyer, T. I. Lee, M. F. Cole *et al.*; Core transcriptional regulatory circuitry in human embryonic stem cells. *Cell* **2005**, *122*, 947–956.

85. Y. H. Loh, Q. Wu, J. L. Chew *et al.*; The Oct4 and Nanog transcription network regulates pluripotency in mouse embryonic stem cells. *Nat. Genet.* **2006**, *38*, 431–440.
86. J. Wang, S. Rao, J. Chu *et al.*; A protein interaction network for pluripotency of embryonic stem cells. *Nature* **2006**, *444*, 364–368.
87. M. Richards, C.Y. Fong, W. K. Chan *et al.*; Human feeders support prolonged undifferentiated growth of human inner cell masses and embryonic stem cells. *Nat. Biotechnol.* **2002**, *20*, 933-936.
88. L. Z. Cheng, H. Hammond, Z.H. Ye *et al.*; Human adult marrow cells support prolonged expansion of human embryonic stem cells in culture. *Stem Cells* **2003**, *21*, 131-142.
89. O. Genbacev, A. Krtolica, T. Zdravkovic *et al.*; Serum-free derivation of human embryonic stem cell lines on human placental fibroblast feeders. *Fertil. Steril.*, **2005**, *83*, 1517-1529.
90. J. S. Odorico, D. S. Kaufman, J. S. Thomson; Multilineage Differentiation from Human Embryonic Stem Cell Lines. *Stem Cells* **2001**, *19*, 193-204. 91.
91. P. A. De Sousa, J. Gardner, S. Pelles *et al.*; Clinically failed eggs as a source of normal human embryo stem cells. *Stem Cell Res.* **2009**, *2*, 188 – 197.
92. [http://www.bionews.org.uk/page\\_48620.asp](http://www.bionews.org.uk/page_48620.asp). Date: June. 2012

93. J. M. Cummis, T. M. Breen, K. L. Harrison; A formular for scoring human embryo growth rates in in vitro fertilization: its value in predicting pregnancy and comparison with visual estimates of embryo quality. *J. In Vitro Fertil. Embryo Transfer* **1986**, 3, 284-295.
94. D. K. Gardner, M. Lane, J. Stevens *et al.*; Blastocyst score affects implantation and pregnancy outcome: towards a single blastocyst transfer. *Fertil. Steril.* **2000**, 73, 1155-1158.
95. M. Buehr, S. Meek, K. Blair *et al.*; Capzure of authentic embryonic stem cells from rat blastocysts. *Cell* **2008**, 135, 1287-1298.
96. S. Gavrillov, D. Marolt, N. C. Douglas *et al.*; Derivation of two new human embryonic stem cell lines from nonviable human embryos. *Stem Cell Int.* **2011**, 2011, 1-9.
97. J. A. Thomson, J. Itskovitz-Eldor, S. S. Shapiro *et al.*; Embryonic stem cell lines derived from human blastocysts. *Science* **1998**, 282, 1145-1147.
98. S. V. Diaz Perez, R. Kim, Z. Li *et al.*; Derivation of new human embryonic stem cell lines reveals rapid epigenetic progression *in vitro* that can be prevented by chemical modification of chromatin, *Hum. Mol. Genet.* **2011**, 21, 751-764.
99. Z. F. Fang, F. Jin, H. Gai *et al.*; Human embryonic stem cell lines derived from the Chinese population, *Cell Res.* **2005**, 15, 394-400.
100. X. Zhang, P. Stojkovic, S. Przyborski *et al.*; Derivation of human embryonic stem cells from developing and arrested embryos. *Stem Cells* **2006**, 24, 2669-2676.

101. P. H. Lerou, A. Yabuuchi, H. Huo *et al.*; Human embryonic stem cell derivation from poor-quality embryos. *Nat. Biotechnol.* **2008**, *26*, 212 – 214.
102. <http://www.bdbiosciences.com> Date:06/2012.
103. H. K. Kleinman, M. L. McGarvey, L. A. Liotta *et al.*; Isolation and characterization of type IV procollagen, laminin, and heparan sulfate proteoglycan from the EHS sarcoma. *Biochemistry* **1982**, *21*, 6188.
104. N. Bigdeli, M. Andersson, R. Strehl, K. *et al.*; Adaptation of human embryonic stem cells to feeder-free and matrix-free culture conditions directly on plastic surfaces. *J. Biotechnol.* **2008**, *133*, 146-153.
105. N. Kohen, L. E. Little, K. E. Healy; Characterization of Matrigel interfaces during defined human embryonic stem cell culture. *Biointerphases* **2009**, *4*, 69-79
106. J. Li, J. Bardy, L. Y. W. Yap *et al.*; Impact of vitronectin concentration and surface properties on the stable propagation of human embryonic stem cells. *Biointerphases* **2010**, *5*, 132-142.
107. S. R. Braam, L. Zeinstra, S. Litjens *et al.*; Recombinant Vitronectin Is a functionally defined substrate that supports human embryonic stem cell self-renewal via  $\alpha V\beta 5$  integrin. *Stem Cells* **2008**, *26*, 2257-2265.



108. S. Rodin, A. Domogatskaya, S. Ström *et al.*; Long-term self-renewal of human pluripotent stem cells on human recombinant laminin-511. *Nat. Biotechnol.* **2010**, *28*, 611-617.
109. R. Timpl, H. Rohde, P. G. Robey *et al.*; Laminin – a glycoprotein from basement membranes. *J. Biol. Chem.* **1979**, *254*, 9933-9937.
110. J. R. Klim, L. Li, P. J. Wrighton *et al.*; A defined glycosaminoglycan-binding substratum for human pluripotent stem cells. *Nat. methods* **2010**, *7*, 989-994.
111. Z. Melkounian, J. L. Weber, D. M. Weber *et al.*; Synthetic peptide-acrylate surfaces for long-term self-renewal and cardiomyocyte differentiation of human embryonic stem cells. *Nat. Biotechnol.* **2010**, *28*, 606-610.
112. L. G. Villa-Diaz, H. Nandivada, J. Ding *et al.*; Synthetic polymer coatings for long-term growth of human embryonic stem cells. *Nat. Biotechnol.* **2010**, *28*, 581-583.
113. Y. J. Li, E. H. Chung, R. T. Rodriguez *et al.*; Hydrogels as artificial matrices for human embryonic stem cell self-renewal. *J. Biomed. Mater. Res. A* **2006**, *79*, 1-5.
114. R. Derda, L. Li, B. P. Orner *et al.*; Combinatorial approach to chemically-defined substrates for human embryonic stem cells growth. *ACS Chem. Biol.* **2007**, *2*, 347-355.
115. H. Hakala, K. Rajala, M. Ojala *et al.*; Comparison of Biomaterials and Extracellular Matrices as a Culture Platform for Multiple, Independently derived human embryonic stem cell lines. *Tissue Eng. Part A* **2004**, *15*, 1775-1785.

116. N. Wells, M. A. Baxter, J. E. Turnbull *et al.*; The geometric control of E14 and R1 mouse embryonic stem cell pluripotency by plasma polymer surface chemical gradients. *Biomaterials* **2009**, *30*, 1066-1070.
117. N. T. Kohen, L. E. Little, K. E. Healy, Characterization of Matrigel interfaces during defined human embryonic stem cell culture. *Biointerphases* **2009**, *4*, 69-79.
118. E. Biazar, M. Heidari, A. Asefnezhad *et al.*; The relationship between cellular adhesion and surface roughness in polystyrene modified by microwave plasma radiation. *Int. J. Nanomed.* **2011**, *6*, 631-639.
119. N. R. Washburn, K. M. Yamadah, C. G. Simon Jr. *et al.*; High-throughput investigation of osteoblast response to polymer crystallinity: influence of nanometer-scale roughness on proliferation. *Biomaterials* **2004**, *25*, 1215-1224.
120. Y. Mei, K. Saha, S. R. Bogatyrev *et al.*; Combinatorial development of biomaterials for clonal growth of human pluripotent stem cells. *Nat. Mater.* **2010**, *9*, 768-778.
121. C. Xu, M. S. Inokuma, J. Denham *et al.*; Feeder-free growth of undifferentiated human embryonic stem cells. *Nat. Biotechnol.* **2001**, *19*, 971-974.
122. J. A. Thomson, J. Itskovitz-Eldor, S. S. Shapiro *et al.*; Embryonic stem cell lines derived from human blastocysts. *Science* **1998**, *282*, 1145.
123. I. Chambers, D. Colby, M. Robertson *et al.*; Functional expression cloning of Nanog, a pluripotency sustaining factor in embryonic stem cells. *Cell* **2003**, *113*, 643-655.

124. O. Adewumi, B. Aflatoonian, L. Ahrlund-Richter *et al.*; Characterization of human embryonic stem cell lines by the international stem cell initiative. *Nat. Biotechnol.* **2007**, *25*, 803-816.
125. M. S. Bodnar, J. J. Meneses, R. T. Rodriguez *et al.*; Propagation and maintenance of undifferentiated human embryonic stem cells. *Stem Cells Dev.* **2004**, *13*, 243-253
126. D. Y. Matsuoka, H. Kubota, E. Adachi *et al.*; Insufficient folding of Type IV collagen and formation of abnormal basement membrane-like structure in embryoid bodies derived from Hsp47-Null embryonic stem cells. *Mol. Biol. Cell* **2004**, *15*, 4467-4475.
127. J. Kohn; New approaches to biomaterials design. *Nat. Mater.* **2004**, *3*, 745-747.
128. S. Rana, P. White, M. Bradley; Influence of resin cross-linking on solid-phase chemistry. *J. Comb. Chem.*, **2001**, *3*, 9-15.
129. S. M. Alesso, Z. R. Yu, D. Pears *et al.*; Synthesis of resins *via* multiparallel suspension polymerization. *J. Comb. Chem.*, **2001**, *3*, 631-633.
130. C. G. J. Simon, S. Lin-Gibson; Combinatorial and high-throughput screening of biomaterials. *Adv. Mater.*, **2011**, *23*, 369-387.
131. T. R. Cull, M. J. Goulding, M. Bradley; Liquid crystal libraries-ink-jet formulation and high-throughput analysis, *Adv. Mater.* **2007**, *19*, 2355-2359.

132. M. Yliperttula, B. G. Chung, A. Navaladi *et al.*; High-throughput screening of cell responses to biomaterials. *Eur. J. Pharm. Sci.*, **2008**, *35*, 151-160.
133. J. C. Meredith, A. P. Smith, A. Karim *et al.*; Combinatorial materials science: polymer thin-film dewetting. *Macromolecules* **2000**, *33*, 9747-9756.
134. J. C. Meredith, A. Karim, E. J. Amis; High-throughput measurement of polymer blend phase behavior. *Macromolecules* **2000**, *33*, 5760-5762.
135. J. C. Meredith, J.-L. Sormana, B. G. Keselowsky *et al.*; Combinatorial characterization of cell interactions with polymer surfaces. *J. Biomed. Mater. Res.* **2003**, *66A*, 483-490.
136. A. Hansen, L. McMillan, A. Morrison *et al.*; Polymers for the rapid and effective activation and aggregation of platelets. *Biomaterials* **2011**, *32*, 7034-7041.
137. S. Pernagallo, J. J. Diaz-Mochon, M. Bradley; A cooperative polymer-DNA microarray approach to biomaterial investigation. *Lab Chip* **2009**, *9*, 397-403.
138. Y. Mei, S. Gerecht, M. Taylor *et al.*; Mapping the interactions among biomaterials, adsorbed proteins and human embryonic stem cells. *Adv. Mater.* **2009**, *21*, 2781.
139. J. Yang, F. R. A. J. Rose, N. Gadegaard *et al.*; Porous polymer and cell composites that self-assemble in situ. *Adv. Mater.* **2009**, *21*, 300-304.
140. S. Morgenthaler, C. Zink, N. D. Spencer; Surface-chemical and -morphological gradients *Soft Matter*. **2008**, *4*, 419-434.

141. T. G. Ruardy, J. M. Schakenraad, H. C. van der Mei *et al.*; Preparation and characterization of chemical gradient surfaces and their application for the study of cellular interaction phenomena. *Surf. Sci. Rep.* **1997**, *29*, 3-30.
142. M. Zelzer, R. Majani, J. W. Bradley *et al.*; Investigation of cell-surface interactions using chemical gradients formed from plasma polymers. *Biomaterials* **2008**, *29*, 172-184.
143. K. J. Siow, L. Britcher, S. Kumar *et al.*; Plasma methods for the generation of chemically reactive surfaces for biomolecule immobilization and cell colonization - a review. *Plasma Process. Polym.* **2006**, *3*, 392-418.
144. X. Wang, P. W. Bohn; Anisotropic in-plane gradients of poly(acrylic acid) formed by electropolymerization with spatiotemporal control of the electrochemical potential. *J. Am. Chem. Soc.* **2004**, *126*, 6825-6832.
145. R. H. Terril, K. M. Balss, Y. M. Zhang *et al.*; Dynamic monolayer gradients: active spatiotemporal control of alkanethiol coatings on thin gold films. *J. Am. Chem. Soc.* **2000**, *122*, 988-989.
146. S. M. Rosentreter, R. W. Davenport, J. Löschinger *et al.*; Response of retinal ganglion cell axons to striped linear gradients of repellent guidance molecules. *J. Neurobiol.* **1998**, *37*, 541-62.
147. J. A. Burdick, A. Khademhosseini, R. Langer; Fabrication of gradient hydrogels using a microfluidics/photopolymerization process. *Langmuir* **2004**, *20*, 5153-5156.

148. N. L. Jeon, S. K. W. Dertinger, D. T. Chiu *et al.*; Generation of solution and surface gradients using microfluidic systems. *Langmuir* **2000**, *16*, 8311-8316.
149. J. T. Smith, J. K. Tomfohr, M. C. Wells *et al.*; Measurement of Cell Migration on Surface-Bound Fibronectin Gradients. *Langmuir* **2004**, *20*, 8279-8286.
150. J. H. Lee, H. B. Lee; Platelet adhesion onto wettability gradient surfaces in the absence and presence of plasma proteins. *J. Biomed. Mater. Res.* **1998**, *41*, 304-311.
151. D. E. Robinson, A. Marson, R. D. Short *et al.*; Surface gradient of functional heparin. *Adv. Mater.* **2008**, *20*, 1166-1169.
152. B. Li, Y. Ma, S. Wang *et al.*; A technique for preparing protein gradients on polymeric surfaces: effects on PC12 pheochromocytoma cells. *Biomaterials* **2005**, *26*, 1487-1495.
153. B. P. Harris, J. K. Kutty, E. W. Fritz *et al.*; Photopatterned polymer brushes promoting cell adhesion gradients. *Langmuir* **2006**, *22*, 4467-4471.
154. N. D. Gallant, K. A. Lavery, E. J. Amis *et al.*; Universal gradient substrates for “Click” biofunctionalization. *Adv. Mater.* **2007**, *19*, 965-969.
155. R. Fricke, P. D. Zentis, L. T. Rajappa *et al.*; Axon guidance of rat cortical neurons by microcontact printed gradients. *Biomaterials* **2011**, *32*, 2070-2076.
156. K. Cai, H. Dong, C. Chen *et al.*; Inkjet printing of laminin gradient to investigate endothelial cellular alignment. *Coll. Surf. B : Bioninterf.* **2009**, *72*, 230-235.

157. T. Kraus, R. Stutz, T. E. Balmer *et al.*; Printing chemical gradients. *Langmuir* **2005**, *21*, 7796-7804.
158. S. Ilkhanizadeh, A. I. Teixeira, O. Hermanson; Inkjet printing of macromolecules on hydrogels to steer neural stem cell differentiation. *Biomaterials* **2007**, *28*, 3936-3943.
159. Q. Zheng, J. Lu, H. Chen *et al.*; Application of inkjet printing technique for biological material delivery and antimicrobial assays. *Anal. Biochem.* **2011**, *40*, 171-176.
160. S.-H. Choi, B. Z. Newby; Micrometer-scaled gradient surfaces generated using contact printing of octadecyltrichlorosilane. *Langmuir* **2003**, *19*, 7427-7435.
161. Y. Cai, Y. H. Yun, B. Z. Newby; Generation of contact-printing based poly (ethylene glycol) gradient surfaces with micrometer-sized steps. *Coll. Surf. B : Biointerf.* **2010**, *75*, 115-120.
162. L. Pardo, W. C. Wilson, T. J. Boland; Characterization of patterned selfassembled protein arrays generated by the ink-jet method. *Langmuir* **2003**, *19*, 1462-1466.
163. Y. Wang, J. Bokor, A. Lee; Maskless Lithography Using Drop-On-Demand Inkjet Printing. *Method Proc. of SPIE* **2004**, *5374*, 628-636.
164. M. Bessis, *Studies on Cell Agony and Death: An Attempt at Classification*, in *Ciba Foundation Symposium - Cellular Injury*, A. V. S. de Reuck, J. Knight, Eds.; John Wiley & Sons, Ltd.: Chichester, UK. doi: 10.1002/9780470719336.ch13.

165. C. Debru; A particular form of chemotaxis: necrotaxis. An historical view. *Blood Cells* **1993**, *19*, 5–19.
166. R. Ragot; Negative necrotaxis. *Blood Cells* **1993**, *19*, 81–88.
167. M. Bessis; Necrotaxis. Chemotaxis towards an injured cell. *Antibiot. Chemother.* **1974**, *19*, 369–381.
168. E. L. Becker; Stimulated neutrophil locomotion: chemokinesis and chemotaxis. *Arch. Pathol. Lab. Med.* **1977**, *101*, 509-513.
169. P. C. Wilkinson; How do leucocytes perceive chemical gradients? *FEMS Microbiol. Immunol.* **1990**, *2*, 303-311
170. J. B. McCarthy, S. L. Palm, L. T. Furcht; Migration by haptotaxis of a Schwann cell tumor line to the basement membrane glycoprotein laminin. *J. Cell Biol.* **1983**, *97*, 772–777.
171. S. Cattaruzza, R. Perris; Proteoglycan control of cell movement during wound healing and cancer spreading. *Matrix Biol.* **2005** *24*, 400–417.
172. S. V. Boyden; The chemotactic effect of mixtures of antibody and antigen on polymorphonuclear leucocytes. *J. Exp. Med.* **1962**, *115*, 453-466.
173. S. H. Zigmond; Orientation chamber in chemotaxis. *Methods Enzymol.* **1988** *162*, 65–72.
174. D. Zicha, G. A. Dunn, A. F. Brown; A new direct-viewing chemotaxis chamber. *J. Cell Sci.* **1991**, *99*, 769–775.



175. D. L. Englert, M. D. Manson, A. Jayaraman; Investigation of bacterial chemotaxis in flow-based microfluidic devices. *Nature Prot.* **2010**, *5*, 864–872.
176. S. H. Zigmond, E. F. Foxman, J. E. Segall; Chemotaxis assays for eukaryotic cells. *Curr. Protoc. Cell Biol.* **2001**, 12.1.1–12.1.29.
177. <http://www.millipore.com/cellbiology/cb3/qcmchemotaxis> Date: 06/2012.
178. <http://www.cellbiolabs.com/chemotaxis-assays> Date: 06/2012.
179. [http://www.rndsystems.com/literature\\_chemotaxis.aspx](http://www.rndsystems.com/literature_chemotaxis.aspx) cellbiolab Date: 06/2012.
180. R. P. Kruger, J. Aurandt, K. L. Guan; Semaphorins command cells to move. *Nat Rev. Mol. Cell. Biol.* **2005** *6*, 789-800.
181. E. Koncina, L. Roth, B. Gonthier *et al.*; *Role of semaphorins during axon growth and guidance*. In *Axon growth and guidance*. D. Bagnard, Ed.; Landes Bioscience, Austin, USA, **2007**, 50-64.
182. J. A. Raper; Semaphorins and their receptors in vertebrates and invertebrates. *Curr. Opin. Neurobiol.* **2000**, *10*, 88-94.
183. A. L. Kolodkin; Semaphorins: mediators of repulsive growth cone guidance. *Trends Cell Biol.* **1996**, *6*, 15-22.
184. A. L. Kolodkin, D. J. Matthes, C. S. Goodman; The semaphorin genes encode a family of transmembrane and secreted growth cone guidance molecules. *Cell* **1994**, *75*, 1389–1399.

185. A. W. Püschel; Semaphorins: repulsive guidance molecules show their attractive side. *Nature* **1999**, *2*, 777-778.
186. N. Spassky, F. de Castro, B. Le Bras *et al.*; Directional guidance of oligodendroglial migration by class 3 semaphorins and netrin-I. *J. Neurosci.* **2002**, *22*, 3321-3330.
187. T. Okuno, Y. Nakatsuji, A. Kumanogoh; The role of immune semaphorins in multiple sclerosis. *FEBS Letters* **2011**, *585*, 3829-3835.
188. A. Williams, G. Piaton, M.-S. Aigrot *et al.*; Semaphorin 3A and 3F: key players in myelin repair in multiple sclerosis? *Brain* **2007**, *130*, 2554-2565.
189. Y. A. Syed, E. Hand, W. Moebius *et al.*; Inhibition of CNS Remyelination by the Presence of Semaphorin 3A. *J. Neurosci.* **2011**, *31*, 3719-3728.
190. A. Compston, A. Coles ; Multiple sclerosis. *Lancet* **2008**, *372*, 1502-1517.
191. G. Piaton, M.-S. Aigrot, A. Williams *et al.*; Class 3 semaphorins influence oligodendrocyte precursor recruitment and remyelination in adult central nervous system. *Brain* **2011**, *134*, 1156-1167.
192. S. E. Lind, P. W. Marks, B. M. Ewenstein; *Hemostatic System. In Blood – Principles and Practice of Hematology.* S. E. Lux, T. P. Stossel, Eds.; Lippincott Williams & Wilkins: Philadelphia, USA, **2003**, 959-982.
193. N. Shaw; Textured Collagen, a hemostatic agent. *Oral Surg. Oral Med. Oral Pathol.* **1991**, *72*, 642-645.

194. E. C. Yackel, D. O. Kenyou; The oxidation of cellulose by nitrogen dioxide. *J. Am. Chem. Soc.* **1942**, *64*, 121-125.
195. C. J. Zeebregts, R. H. Heijmen, J. J. van den Dungen *et al.*; Non-suture methods of vascular anastomosis. *Br. J. Surg.* **2003**, *90*, 261-271.
196. D. M. Albala; Fibrin sealants in clinical practice. *Cardiovasc. Surg.* **2003**, *1*, 5-11.
197. M. B. Dowling, R. Kumar, M. A. Keibler *et al.*; A self-assembling hydrophobically modified chitosan capable of reversible hemostatic action. *Biomaterials* **2011**, *32*, 3351-3357.
198. A. S. Herford, L. Akin, M. Cicciu *et al.*; Use of a porcine collagen matrix as an alternative to autogenous tissue for grafting oral soft tissue defects. *J. Oral Maxillofac. Surg.* **2010**, *68*, 1463-1470.
199. T. Baykul, E. G. Alanoglu, G. Kocer; Use of Ankaferd Blood Stopper as a hemostatic agent: a clinical experience. *J. Contemp. Dent. Pract.* **2010**, *11*, E088-94.
200. A. A. M. Todd, A. Gray, E. Pirie *et al.*; *Better Blood Transfusion Level 2-Blood Component Use Self-directed Learning Pack*; J. Fordham, Ed.; Scottish National Blood Transfusion Service, Edinburgh, UK **2006**, 33-45.
201. C. B. Thompson, D. G. Love, P.G. Quinn *et al.*; Platelet size does not correlate with platelet age. *Blood* **1983**, *62*, 487-494.
202. J. Wright; The origin and nature of the blood plates. *Boston Med. Surg. J.* **1906**, *154*, 643-645.

203. E. Battinelli, S. R. Willoughby, T. Foxall *et al.*; Induction of platelet formation from megakaryocytoid cells by nitric oxide. *Proc. Nat. Acad. Sci.* **2001**, 98, 14458-14463.
204. S. Ebbe; Biology of megakaryocytes. *Prog. Hemost. Thromb.* **1976**, 3, 211-229.
205. Y. Nagata, Y. Muro, K. Todokoro; Thrombopoietin-induced polyploidization of bone marrow megakaryocytes is due to a unique regulatory mechanism in late mitosis. *J. Cell. Biol.* **1997**, 139, 449-457.
206. N. Vitrat, K. Cohen-Solal, C. Pique *et al.*; Endomitosis of human megakaryocytes are due to abortive mitosis. *Blood* **1998**, 91, 3711-3723.
207. J. H. Hartwig, J. E. Italiano Jr.; *Life of the blood platelets in Blood – principles and practice of hematology*; R. I. Handin, S. E. Lux, T. P. Stossel, Eds.; Lippincott Williams & Wilkins: Philadelphia, USA, **2003**; 1055-1067.
208. R. M. Kaufmann, R. Airo, S. Pollack *et al.*; Circulating megakaryocytes and platelet release in the lung. *Blood* **1965**, 26, 720- 731.
209. L. A. Harker, C. A. Finch; Thrombokinetis in man. *J. Clin. Invest.* **1969**, 48, 963-974.
210. G. Schmitz, G. Rothe, A. Ruf *et al.*; European Working Group on Clinical Cell Analysis: Consensus protocol for the flow cytometric characterisation of platelet function. *Thromb. Haemost.* **1998**, 79, 885-896.

211. R. J. Haslam; *Signal transduction in platelet activation in thrombosis and haemostasis* M. Verstraete, J. Vermynen, R. Lijnen, J. Arnout, Eds.; Leuven University Press: Leuven, Belgium, **1987**, 147-174.
212. H. Nygren, E. Hrustic, C. Karlsson *et. al.*; Respiratory burst response of peritoneal leukocytes adhering to titanium and stainless steel. *J. Biomed. Mat. Res.* **2001**, *57*, 238-247.
213. J. M. Grunkemeier, W. B. Tsai, C. D. McFarland *et. al.*; The effect of adsorbed "brinogen, "bronectin, von Willebrand factor and vitronectin on the procoagulant state of adherent platelets. *Biomaterials* **2000**, *21*, 2243-2252.
214. O. Behnke, A. Forer; From megakaryocytes to platelets: platelet morphogenesis takes place in the bloodstream. *Eur. J. Haematol. Suppl.* **1998**, *60*, 3-23.
215. C. S. Abrams, S. J. Shattil; Immunological detection of activated platelets in clinical disorders. *Thromb. Haemost.* **1991**, *65*, 467-473.
216. A. D. Michelson, S. J. Shattil; *Platelets. A practical approach*, S.P. Watson, K. S. Authi, Eds.; Oxford University Press: Oxford, UK, **1996**, 111-129.
217. J. Dachary-Prigent, J. M. Paquet, J. M. Freyssinet, *et al.*; Calcium involvement in aminophospholipid exposure and microparticle formation during platelet activation: a study using Ca<sup>2+</sup>-ATPase inhibitors. *Biochemistry* **1995**; *34*; 11625-11634.

218. T. A. Davies, D. Drotts, G. J. Weil *et al.*; Flow cytometric measurements of cytoplasmic calcium changes in human platelets. *Cytometry* **1988**, 9, 138-142.
219. A. Oda, J. F. Daley, C. Cabral *et al.*; Heterogeneity in filamentous actin content among individual human blood platelets. *Blood* **1992**, 79, 920-927.
220. E. Gurdak, J. Booth, C. J. Roberts *et al.*; Influence of collagen denaturation on the nanoscale organization of adsorbed layers. *J. Col. Int. Sci.* **2006**, 302, 475-484.
221. H. Seyednejad, M. Imani, T. Jamieson *et al.*; Topical haemostatic agents, *Br. J. Surg.* **2008**, 95, 1197–1225.
222. W. C. Chapman, P. A. Clavien, J. Fung *et al.*; Effective control of hepatic bleeding with a novel collagen-based composite combined with autologous plasma: results of a randomized controlled trial. *Arch. Surg.* **2000**, 135, 1200–1204.
223. M. Doita, K. Nishida, M. Kurosaka; Radiculopathy due to microfibrillar collagen hemostat mimicking recurrence of disc herniation. *Skeletal Radiol.* **2006**, 35, 953–955.
224. C. Schonauer, E. Tessitore, G. Barbagallo *et al.*; The use of local agents: bone wax, gelatin, collagen, oxidized cellulose. *Eur. Spine J.* **2004**, 13, S89–S96.
225. U. Frost-Arner, W. D. Spotnitz, G. T. Rodeheaver *et al.*; Comparison of the thrombogenicity of internationally available fibrin sealants in an established microsurgical model. *Plast. Reconstr. Surg.* **2001**, 108, 1655–1660.
226. C. Buchta, H. C. Hedrich, M. Macher *et al.*; Biochemical characterization of autologous fibrin sealants produced by CryoSeal and Vivostat in comparison to the

homologous fibrin sealant product Tissucol/Tisseel. *Biomaterials* **2005**, *26*, 6233–6241.

227. H. T. Peng, P. N. Shang; Novel wound sealants: biomaterials and applications. *Expert Rev. Med. Dev.* **2010**, *7*, 639-659.

228. M. Ryou M, C. C. Thompson; Tissue adhesives: a review. *Tech. Gastrointest. Endosc.* **2006**, *8*, 33–37.

229. M. Hino, O. Ishiko, K. I. Honda *et al.*; Transmission of symptomatic parvovirus B19 infection by fibrin sealant used during surgery. *Br. J. Haematol.* **2000**, *108*, 194–195.

230. M. Kanko, T. Liman, S. Topcu; A low-cost and simple method to stop intraoperative leakage-type bleeding: use of the vancomycin-oxidized regenerated cellulose (ORC) sandwich. *J. Invest. Surg.* **2006**, *19*, 323–327.

231. D. Spangler, S. Rothenburger, K. Nguyen *et al.*; *In vitro* antimicrobial activity of oxidized regenerated cellulose against antibiotic-resistant microorganisms. *Surg. Infect.* **2003**, *4*, 255–262.

232. M. F. Ibrahim, C. Aps, C. P. Young; A foreign body reaction to Surgicel mimicking an abscess following cardiac surgery. *Eur. J. Cardiothorac. Surg.* **2002**, *22*, 489–490.

233. S. Dogan, H. Kocaeli, M. Doygun; Oxidised regenerated cellulose as a cause of paraplegia after thoracotomy: case report and review of the literature. *Spinal. Cord.* **2005**, *43*, 445–447.

234. J. John, P. Manoj, S. G. Nair *et al.*; Paraplegia after thoracotomy: an unusual cause. *J. Cardiothorac. Vasc. Anesth.* **2006**, 20, 696–699.
235. J. Galownia, J. Martin, M. E. Davis; Aluminophosphate-based, microporous materials for blood clotting. *Micropor. Mesopor. Mater.* **2006**, 92, 61–63.
236. A. E. Pusateri, A. V. Delgado, E. J. Dick *et al.*; Application of a granular mineral-based hemostatic agent (QuikClot) to reduce blood loss after grade V liver injury in swine. *J. Trauma.* **2004**, 57, 555–562.
237. M. C. Neuffer, J. McDivitt, D. Rose *et al.*; Hemostatic dressings for the first responder: a review. *Mil. Med.* **2004**, 169, 716–720.
238. E. Leikina, M. V. Merts, N. Kuznetsova *et al.*; Type I collagen is thermally unstable at body temperature. *Proc. Nat. Acad. Sci.* **2002**, 99, 1314–1318.
239. A. J. McMichael, P. C. L. Beverly, S. Cobbold *et al.*; *Leukocyte typing III. White cell differentiation antigens*; A. J. McMichael, Ed.; Oxford University Press Inc: Oxford, UK, **1987**.
240. S. C. Hsu-Lin, C. L. Berman, B. C. Furie *et al.*; A platelet membrane protein expressed during platelet activation and secretion. Studies using a monoclonal antibody specific for thrombin-activated platelets. *J. Biol. Chem.* **1984**, 259, 9799–9801.
241. S. L. Goodman; Sheep, pig, and human platelet-material interactions with model cardiovascular biomaterials, *J. Biomed. Mater. Res.* **1999**, 45, 240–250.



242. S. P. Jackson; The growing complexity of platelet aggregation. *Blood* **2007**, *109*, 5087-5095.
243. A. Morrison, V. S. Hornsey, C. V. Prowse *et al.*; Use of the DiaMed Impact R to test platelet function in stored platelet concentrates. *Vox. Sang.* **2007**, *93*, 166-173.
244. A. Morrison, L. McMillan, V. S. Hornsey *et al.*; Stored red-blood-cells inhibit platelet function under physiologic flow. *Vox. Sang.* **2010**, *99*, 362-368.
245. M. Gorbet, M. V. Sefton; Biomaterial-associated thrombosis: roles of coagulation factors, complement, platelets and leukocytes. *Biomaterials* **2004**, *25*, 5681-5703.
246. B. Sivaraman, R. A. Latour; The relationship between platelet adhesion on surfaces and the structure versus the amount of adsorbed fibrinogen. *Biomaterials* **2010**, *31*, 832-839.
247. G. Tourniaire, J. J. Diaz-Mochon, M. Bradley; Fingerprinting polymer microarrays. *Comb. Chem. High Throughput. Screen.* **2009**, *12*, 690-696.
248. H. Ni, C. V. Denis, S. Subbarao *et al.*; Persistence of platelet thrombus formation in arterioles of mice lacking both von Willebrand factor and fibrinogen. *J. Clin. Invest.* **2000**, *106*, 385-392.
249. R. M. Hakim; Complement activation by biomaterials. *Cardiovasc. Pathol.* **1993**, *2*, 187S-97S.

250. M. A. Blajcham, A. H. Oetzge-Anwar; The role of the complement system in hemostasis. *Prog. Hematol.* **1986**, *XIV*, 149-182.
251. T. Sekikawa, S. Iwase, S. Saito *et al.*; JAS-R, a new megakaryo-erythroid leukemic cell line that secretes erythropoietin. *Anticancer Res.* **2006**, *26*, 843-850.
252. K. Ravid, D. L. Beeler, M. S. Rabin *et al.*; Selective targeting of gene products with the megakaryocyte platelet factor 4 promoter (platelet targeting). *Proc. Nat. Acad. Sci. USA* **1991**, *88*, 1521-1525.
253. M. Ogura, Y. Morishima, R. Ohno *et al.*; Establishment of a novel human megakaryoblastic leukemia cell line, MEG-01, with positive Philadelphia chromosome. *Blood* **1985**, *66*, 1384-1392.
254. D. Vittet, M.-N. Mathieu, J.-M. Launay *et al.*; Thrombin inhibits proliferation of the human megakaryoblastic MEG-01 cell line: A possible involvement of a cyclic-AMP dependent mechanism. *J. Cell. Physiol.* **1992**, *150*, 65-72.
255. E. Battinelli, J. Localzo; Nitric oxide induces apoptosis in megakaryocytic cell lines. *Blood*. **2000**, *95*, 3451-3459.
256. C. Lacabartz-Porret, S. Launay, E. Corvazier *et al.*; Biogenesis of endoplasmic reticulum proteins involved in Ca<sup>2+</sup> signaling during megakaryocytic differentiation: an in vitro study. *Biochem. J.* **2000**, *350*, 723-734.

257. C. Mroske, M. H. Plant, D. J. Franks *et al.*; Characterization of prostaglandin endoperoxide H synthase-1 enzyme expression during the differentiation of the megakaryocytic cell line, MEG-01. *Exp. Hematol.* **2000**, *28*, 411-421.
258. Y. Isakari, S. Sogo, T. Ishida *et al.*; Gene Expression Analysis during platelet-like particle production in phorbol myristate acetate-treated MEG-01. *Cells. Biol. Pharm. Bull.* **2009**, *32*, 354-358.
259. L. M. Beaulieu, E. Lin, K. M. Morin *et al.*; Regulatory effects of TLR2 on megakaryocytic cell function. *Blood* **2011**, *117*, 5963-5974.
260. T. P. McDonald, P. S. Sullivan; Megakaryocytic and erythrocytic cell lines share a common precursor cell. *Exp. Hematol.* **1993**, *21*, 1316-1320.
261. X. Xie, R. J. Chan, S. A. Johnson *et al.*; Thrombopoietin promotes mixed lineage and megakaryocytic colony-forming cell growth but inhibits primitive and definitive erythropoiesis in cells isolated from early murine yolk sacs. *Blood* **2003**, *101*, 1329-1335.
262. C. B. Lozzio, B. B. Lozzio; Human chronic myelogenous leukemia cell-line with positive Philadelphia chromosome. *Blood* **1975**, *45*, 321-334.
263. P. A. T. Tetteroo, F. Massaro, A. Mulder *et al.*; Megakaryoblastic differentiation of proerythroblastic K562 cell-line cells. *Leukemia Res.* **1984**, *8*, 197-206.
264. R. Alitalo; Induced differentiation of K562 leukemia cells: a model for studies of gene expression in early megakaryoblasts. *Leukemia Res.* **1990**, *14*, 501-514.

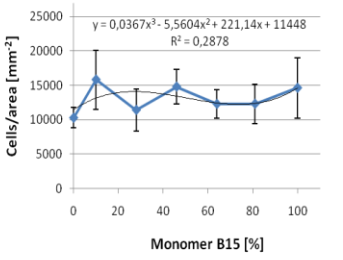
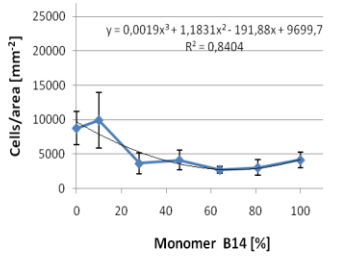
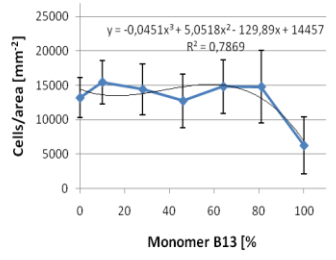
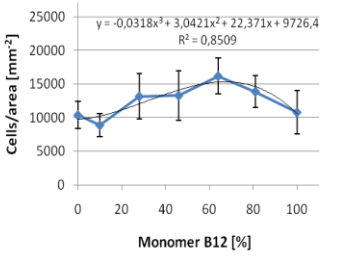
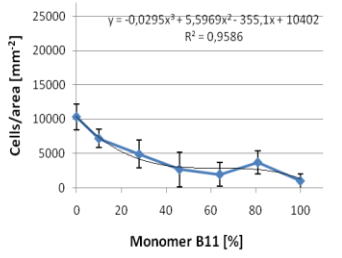
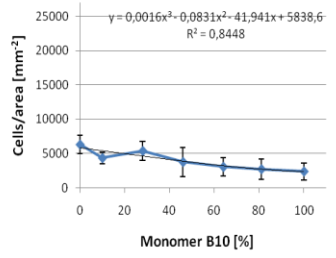
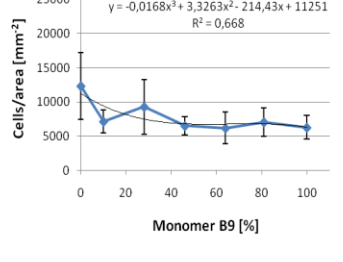
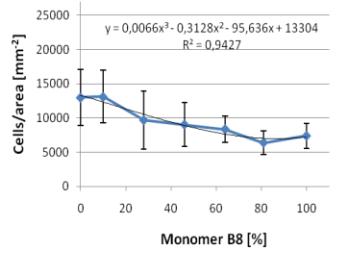
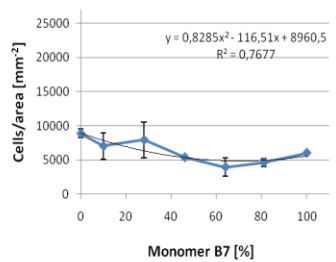
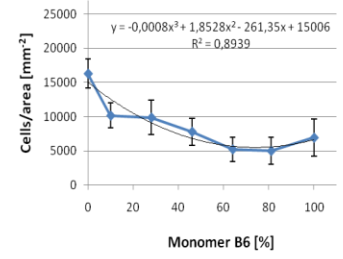
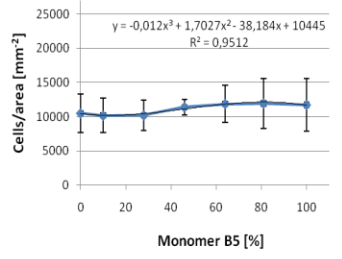
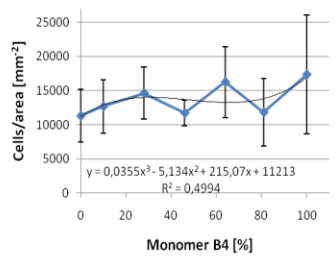
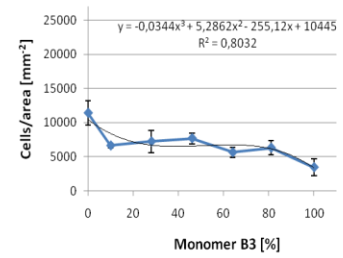
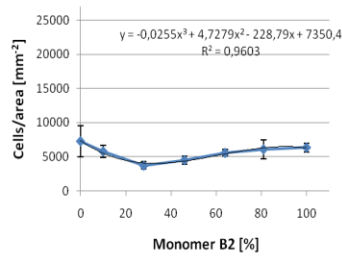
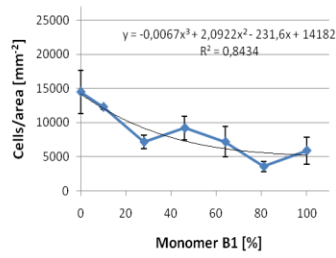
265. L. C. Andersson, M. Jokinen, C. G. Gahmberg; Induction of erythroid differentiation in the human leukaemia cell-line K562. *Nature* **1979**, 278, 364-365.
266. L. Cioe, A. McNab, H. R. Hubbel *et al.*; Differential expression of the globin genes in human leukemia K562(S) cells induced to differentiate by hemin or butyric acid. *Cancer Res.* **1981**, 41, 237-243.
267. X.-F. Huo, J. Yu, H. Peng *et al.*; Differential expression changes in K562 cells during the hemin-induced erythroid differentiation and the phorbol myristate acetate (PMA)-induced megakaryocytic differentiation. *Mol. Cell. Biochem.* **2006**, 292, 155-167.
268. P. G. Genever, D. J. P. Wilkinson, A. J. Patton *et al.*; Expression of a functional *N*-methyl-D-aspartate-type glutamate receptor by bone marrow megakaryocytes. *Blood* **1999**, 93, 2876-2883.
269. R. A. Shivdasani; Lonely in Paris: when one gene copy isn't enough. *J. Clin. Invest.* **2004**, 114, 17-19.
270. X. Wang, I. M. El Naqa; Prediction of both conserved and nonconserved microRNA targets in animals. *Bioinformatics* **2008**, 24, 325-332.
271. X. Wang; miRDB: a microRNA target prediction and functional annotation database with a wiki interface. *RNA* **2008**, 14, 1012-1017.
272. H. Mizomoto, *PhD Thesis*, University of Southampton, Uk, **2005**.

273. J.-F. Thaburet, H. Mizomoto, M. Bradley; High-throughput evaluation of the wettability of polymer libraries. *Macromol. Rapid Commun.* **2004**, *25*, 366–370.

274. [www.doubling-time.com/compute.php](http://www.doubling-time.com/compute.php) Date:06/2012.

275. Image J software: <http://rsb.nih.gov/ij> Date:06/2012

# Appendices



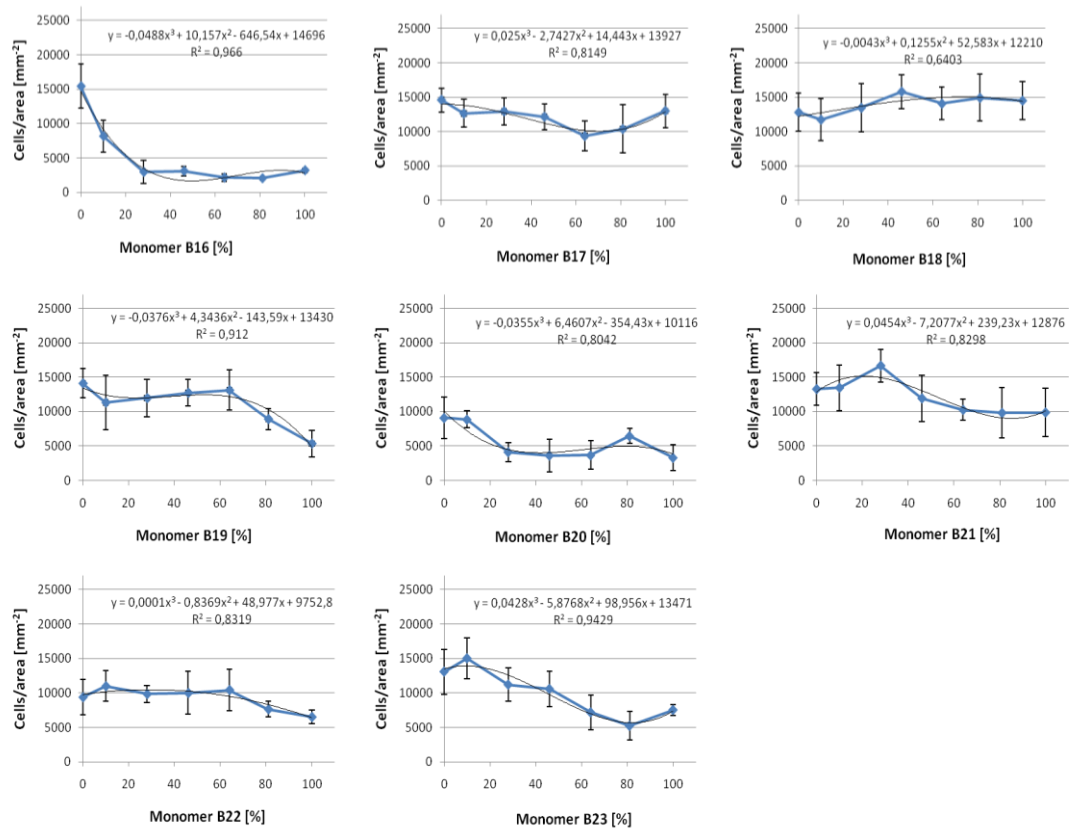
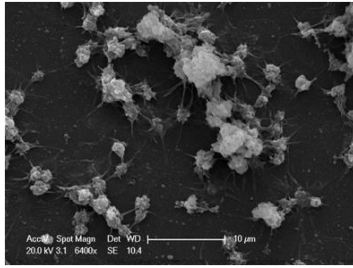
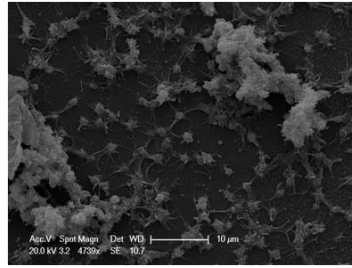


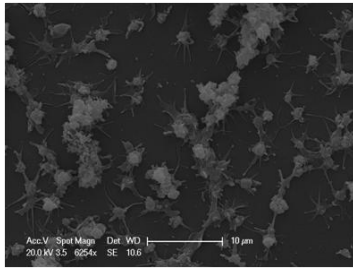
**Figure 1:** Cell binding profile of K562 cells across the polymer gradients as discussed in Chapter 3.



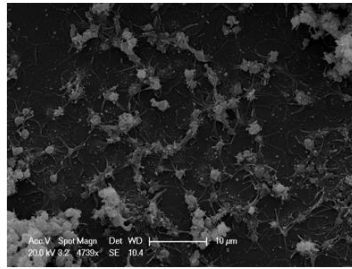
PA100



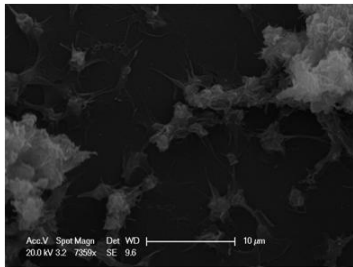
PA345



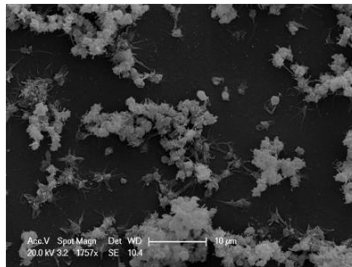
PA346



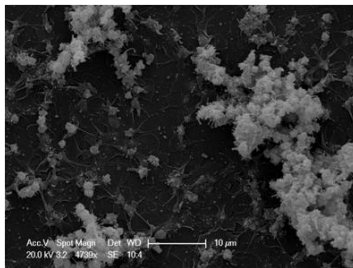
PA363



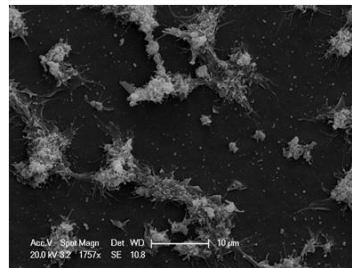
PA364



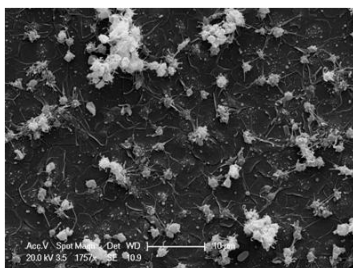
PA371



PA380



PA382



PA393

**Figure 2:** Representative SEM images taken for the different platelet binding polyacrylates as discussed in Chapter 4.



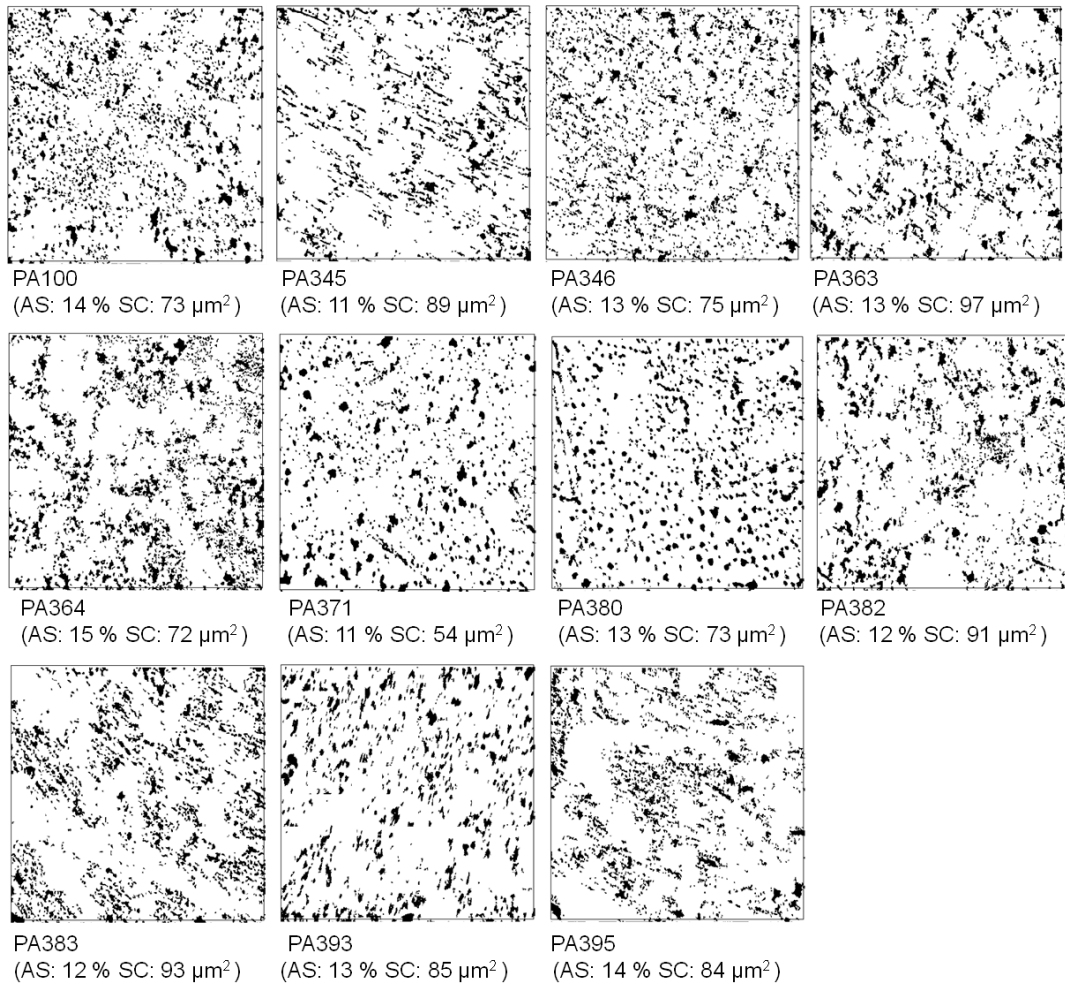


**Figure 3:** Impact *R* test images showing the different surface coverage and aggregation sizes of platelets for the diverse polyacrylates as discussed in Chapter 4. AS – Aggregate Size, SC-Surface coverage.

## Polyacrylate Library

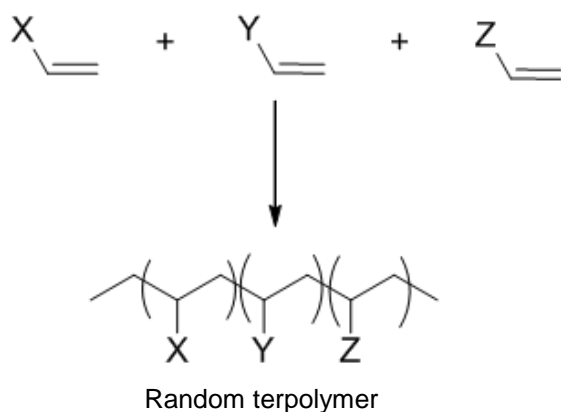


**Figure 4:** Synthesis scheme of polyacrylates.

### Monomer Abbreviations:

St styrene

MMA	methyl methacrylate
Ema	ethyl methacrylate
BMA	butyl methacrylate
MEMA	2-methoxyethylacrylate
MEA	2-methoxyethylacrylate
HEMA	2-hydroxyethyl methacrylate
HPMA	hydroxypropyl methacrylate
HBMA	hydroxybutyl methacrylate
DEAAm	<i>N,N</i> -diethylacrylamide
DMAAm	<i>N,N</i> -dimethylacrylamide
NIPAAm	<i>N</i> -isopropyl acrylamide
DAAA	diacetone acrylamide
DMAAPMAAm	<i>N,N</i> -dimethylaminopropyl acrylamide
DEAEAMA	2-(diethylamino)ethyl methacrylate
DMAEMA	2-(dimethylamino)ethyl methacrylate

DEAEA	2-(diethylamino)ethyl acrylate
DMAEA	2-(dimethylamino)ethyl acrylate
MTEMA	2-(methylthio)ethyl methacrylate
BAEMA	2-(tert-butylamino)ethyl methacrylate
BACOEA	2-[[butylamino)carbonyl]oxy]ethylacrylate
MNPMA	2-methyl-2-nitropropyl methacrylate
DMVBA	<i>N,N</i> -dimethylvinylbenzylamine
VAA	<i>N</i> -vinylacetamide
VI	1-vinylimidazole
VPNO	1-vinyl-2-pyrrolidinone
VP-4	4-vinylpyridine
VP-2	2-vinylpyridine
A-H	acrylic acid
AES-H	mono-2-(acryloyloxy)ethyl succinate
MA-H	methacrylic acid
AAG-H	2-acrylamidoglycolic acid
EGMP-H	ethylene glycol methacrylate phosphate

## Amines for Functionalisation

GMA	glycidyl methacrylate
DnBA	di-n-butylamine
DnHA	di-n-hexylamine
DcHA	dicyclohexylamine
DBnA	dibenzylamine
MnHA	<i>N</i> -methylhexylamine
cHMA	cyclohexanemethylamine
BnMA	<i>N</i> -benzylmethylamine
MAEPy	2-(2-methylaminoethyl)pyridine
Pyrrole	pyrrole
Man	n-methylaniline
TMEDA	<i>N,N,N'</i> -trimethylethylenediamine
DEMEDA	<i>N,N</i> -diethyl- <i>N'</i> -methylethylenediamine
TMPDA	<i>N,N,N'</i> -trimethyl-1,3-propanediamine
Mpi	1-methylpiperazine
TEDETA	<i>N,N,N',N'</i> -tetraethyldiethylenetriamine

**Table 1:** List of polyacrylates in the polyacrylate library used.

Polyacrylate ID number	Polymer Composition			Monomer Ratios			Monomer Type	
	Monomer 1	Monomer 2	Monomer 3	M 1	M 2	M 3	M 2	M 3
1	St	DEAA	-	90	10	-	CON	-
2	St	DEAA	-	70	30	-	CON	-
3	St	DEAA	-	50	50	-	CON	-
4	St	DMAA	-	90	10	-	CON	-
5	St	DMAA	-	70	30	-	CON	-
6	St	DMAA	-	50	50	-	CON	-
7	St	PAA	-	90	10	-	CON	-
8	St	PAA	-	70	30	-	CON	-
9	St	PAA	-	50	50	-	CON	-
10	MMA	DEAA	-	90	10	-	CON	-
11	MMA	DEAA	-	70	30	-	CON	-
12	MMA	DEAA	-	50	50	-	CON	-
13	MMA	DMAA	-	90	10	-	CON	-
14	MMA	DMAA	-	70	30	-	CON	-
15	MMA	DMAA	-	50	50	-	CON	-
16	MMA	PAA	-	90	10	-	CON	-
17	MMA	PAA	-	70	30	-	CON	-
18	MMA	PAA	-	50	50	-	CON	-
19	MEMA	DEAA	-	90	10	-	CON	-
20	MEMA	DEAA	-	70	30	-	CON	-
21	MEMA	DEAA	-	50	50	-	CON	-
22	MEMA	DMAA	-	90	10	-	CON	-

23	MEMA	DMAA	-	70	30	-	CON	-
24	MEMA	DMAA	-	50	50	-	CON	-
25	MEMA	PAA	-	90	10	-	CON	-
26	MEMA	PAA	-	70	30	-	CON	-
27	MEMA	PAA	-	50	50	-	CON	-
28	MEA	DEAA	-	90	10	-	CON	-
29	MEA	DEAA	-	70	30	-	CON	-
30	MEA	DEAA	-	50	50	-	CON	-
31	MEA	DMAA	-	90	10	-	CON	-
32	MEA	DMAA	-	70	30	-	CON	-
33	MEA	DMAA	-	50	50	-	CON	-
34	MEA	PAA	-	90	10	-	CON	-
35	MEA	PAA	-	70	30	-	CON	-
36	MEA	PAA	-	50	50	-	CON	-
37	HEMA	DEAA	-	90	10	-	CON	-
38	HEMA	DEAA	-	70	30	-	CON	-
39	HEMA	DEAA	-	50	50	-	CON	-
40	HEMA	DMAA	-	90	10	-	CON	-
41	HEMA	DMAA	-	70	30	-	CON	-
42	HEMA	DMAA	-	50	50	-	CON	-
43	HEMA	PAA	-	90	10	-	CON	-
44	HEMA	PAA	-	70	30	-	CON	-
45	HEMA	PAA	-	50	50	-	CON	-
46	HPMA	DEAA	-	90	10	-	CON	-
47	HPMA	DEAA	-	70	30	-	CON	-
48	HPMA	DEAA	-	50	50	-	CON	-
49	HPMA	DMAA	-	90	10	-	CON	-

50	HPMA	DMAA	-	70	30	-	CON	-
51	HPMA	DMAA	-	50	50	-	CON	-
52	HPMA	PAA	-	90	10	-	CON	-
53	HPMA	PAA	-	70	30	-	CON	-
54	HPMA	PAA	-	50	50	-	CON	-
55	HBMA	DEAA	-	90	10	-	CON	-
56	HBMA	DEAA	-	70	30	-	CON	-
57	HBMA	DEAA	-	50	50	-	CON	-
58	HBMA	DMAA	-	90	10	-	CON	-
59	HBMA	DMAA	-	70	30	-	CON	-
60	HBMA	DMAA	-	50	50	-	CON	-
61	HBMA	PAA	-	90	10	-	CON	-
62	HBMA	PAA	-	70	30	-	CON	-
63	HBMA	PAA	-	50	50	-	CON	-
96	MEMA	DEAEMA	-	90	10	-	NH2	-
97	MEMA	DEAEMA	-	70	30	-	NH2	-
98	MEMA	DEAEMA	-	50	50	-	NH2	-
99	MEMA	DMAEMA	-	90	10	-	NH2	-
100	MEMA	DMAEMA	-	70	30	-	NH2	-
101	MEMA	DMAEMA	-	50	50	-	NH2	-
102	MEMA	DEAEA	-	90	10	-	NH2	-
103	MEMA	DEAEA	-	70	30	-	NH2	-
104	MEMA	DEAEA	-	50	50	-	NH2	-
105	MEMA	DMAEA	-	90	10	-	NH2	-
106	MEMA	DMAEA	-	70	30	-	NH2	-
107	MEMA	DMAEA	-	50	50	-	NH2	-

108	MEMA	MTEMA	-	90	10	-	RSR	-
109	MEMA	MTEMA	-	70	30	-	RSR	-
110	MEMA	MTEMA	-	50	50	-	RSR	-
111	MEMA	BAEMA	-	90	10	-	NH2	-
112	MEMA	BAEMA	-	70	30	-	NH2	-
113	MEMA	BAEMA	-	50	50	-	NH2	-
114	MEMA	DMAPMAA	-	90	10	-	NH2, CON	-
115	MEMA	DMAPMAA	-	70	30	-	NH2, CON	-
116	MEMA	DMAPMAA	-	50	50	-	NH2, CON	-
117	MEMA	BACOEAE	-	90	10	-	CON	-
118	MEMA	BACOEAE	-	70	30	-	CON	-
119	MEMA	BACOEAE	-	50	50	-	CON	-
120	MEMA	DMVBA	-	90	10	-	NH2	-
121	MEMA	DMVBA	-	70	30	-	NH2	-
122	MEMA	DMVBA	-	50	50	-	NH2	-
123	MEMA	VAA	-	90	10	-	CON	-
124	MEMA	VAA	-	70	30	-	CON	-
125	MEMA	VAA	-	50	50	-	CON	-
126	MEMA	VI	-	90	10	-	Aromatic	-
127	MEMA	VI	-	70	30	-	Aromatic	-
128	MEMA	VI	-	50	50	-	Aromatic	-
129	MEMA	VPNO	-	90	10	-	CON	-
130	MEMA	VPNO	-	70	30	-	CON	-
131	MEMA	VPNO	-	50	50	-	CON	-



132	MEMA	VP-4	-	90	10	-	Aromatic	-
133	MEMA	VP-4	-	70	30	-	Aromatic	-
134	MEMA	VP-4	-	50	50	-	Aromatic	-
135	MEMA	VP-2	-	90	10	-	Aromatic	-
136	MEMA	VP-2	-	70	30	-	Aromatic	-
137	MEMA	VP-2	-	50	50	-	Aromatic	-
138	MEMA	DAAA	-	90	10	-	CON	-
139	MEMA	DAAA	-	70	30	-	CON	-
140	MEMA	DAAA	-	50	50	-	CON	-
141	MEMA	MNPMA	-	90	10	-	Nitro	-
142	MEMA	MNPMA	-	70	30	-	Nitro	-
143	MEMA	MNPMA	-	50	50	-	Nitro	-
150	HEMA	DEAEMA	-	90	10	-	NH2	-
151	HEMA	DEAEMA	-	70	30	-	NH2	-
152	HEMA	DEAEMA	-	50	50	-	NH2	-
153	HEMA	DMAEMA	-	90	10	-	NH2	-
154	HEMA	DMAEMA	-	70	30	-	NH2	-
155	HEMA	DMAEMA	-	50	50	-	NH2	-
156	HEMA	DEAEA	-	90	10	-	NH2	-
157	HEMA	DEAEA	-	70	30	-	NH2	-
158	HEMA	DEAEA	-	50	50	-	NH2	-
159	HEMA	DMAEA	-	90	10	-	NH2	-
160	HEMA	DMAEA	-	70	30	-	NH2	-
161	HEMA	DMAEA	-	50	50	-	NH2	-
162	HEMA	MTEMA	-	90	10	-	RSR	-
163	HEMA	MTEMA	-	70	30	-	RSR	-

164	HEMA	MTEMA	-	50	50	-	RSR	-
165	HEMA	BAEMA	-	90	10	-	NH2	-
166	HEMA	BAEMA	-	70	30	-	NH2	-
167	HEMA	BAEMA	-	50	50	-	NH2	-
168	HEMA	DMAPMAA	-	90	10	-	NH2, CON	-
169	HEMA	DMAPMAA	-	70	30	-	NH2, CON	-
170	HEMA	DMAPMAA	-	50	50	-	NH2, CON	-
171	HEMA	BACOEAE	-	90	10	-	CON	-
172	HEMA	BACOEAE	-	70	30	-	CON	-
173	HEMA	BACOEAE	-	50	50	-	CON	-
174	HEMA	DMVBA	-	90	10	-	NH2	-
175	HEMA	DMVBA	-	70	30	-	NH2	-
176	HEMA	DMVBA	-	50	50	-	NH2	-
177	HEMA	VAA	-	90	10	-	CON	-
178	HEMA	VAA	-	70	30	-	CON	-
179	HEMA	VAA	-	50	50	-	CON	-
180	HEMA	VI	-	90	10	-	Aromatic	-
181	HEMA	VI	-	70	30	-	Aromatic	-
182	HEMA	VI	-	50	50	-	Aromatic	-
183	HEMA	VPNO	-	90	10	-	CON	-
184	HEMA	VPNO	-	70	30	-	CON	-
185	HEMA	VPNO	-	50	50	-	CON	-
186	HEMA	VP-4	-	90	10	-	Aromatic	-
187	HEMA	VP-4	-	70	30	-	Aromatic	-

188	HEMA	VP-4	-	50	50	-	Aromatic	-
-----	------	------	---	----	----	---	----------	---

189	HEMA	VP-2	-	90	10	-	Aromatic	-
190	HEMA	VP-2	-	70	30	-	Aromatic	-
191	HEMA	VP-2	-	50	50	-	Aromatic	-
192	HEMA	DAAA	-	90	10	-	CON	-
193	HEMA	DAAA	-	70	30	-	CON	-
194	HEMA	DAAA	-	50	50	-	CON	-
195	HEMA	MNPMA	-	90	10	-	Nitro	-
196	HEMA	MNPMA	-	70	30	-	Nitro	-
197	HEMA	MNPMA	-	50	50	-	Nitro	-
198	MMA	A-H	-	90	10	-	COOH	-
199	MMA	A-H	-	70	30	-	COOH	-
200	MMA	A-H	-	50	50	-	COOH	-
201	MMA	AES-H	-	90	10	-	COOH	-
202	MMA	AES-H	-	70	30	-	COOH	-
203	MMA	AES-H	-	50	50	-	COOH	-
204	MMA	MA-H	-	90	10	-	COOH	-
205	MMA	MA-H	-	70	30	-	COOH	-
206	MMA	MA-H	-	50	50	-	COOH	-
207	MMA	AAG-H	-	90	10	-	COOH	-
208	MMA	AAG-H	-	70	30	-	COOH	-
209	MMA	AAG-H	-	50	50	-	COOH	-
210	MMA	EGMP-H	-	90	10	-	COOH	-
211	MMA	EGMP-H	-	70	30	-	COOH	-
212	MMA	EGMP-H	-	50	50	-	COOH	-
213	MEMA	A-H	-	90	10	-	COOH	-

214	MEMA	A-H	-	70	30	-	COOH	-
215	MEMA	A-H	-	50	50	-	COOH	-
216	MEMA	AES-H	-	90	10	-	COOH	-
217	MEMA	AES-H	-	70	30	-	COOH	-
218	MEMA	AES-H	-	50	50	-	COOH	-
219	MEMA	MA-H	-	90	10	-	COOH	-
220	MEMA	MA-H	-	70	30	-	COOH	-
221	MEMA	MA-H	-	50	50	-	COOH	-
222	MEMA	AAG-H	-	90	10	-	COOH	-
223	MEMA	AAG-H	-	70	30	-	COOH	-
224	MEMA	AAG-H	-	50	50	-	COOH	-
225	MEMA	EGMP-H	-	90	10	-	COOH	-
226	MEMA	EGMP-H	-	70	30	-	COOH	-
227	MEMA	EGMP-H	-	50	50	-	COOH	-
228	MMA	A-H	DEAEMA	70	20	10	COOH	NH2
229	MMA	A-H	DEAEMA	70	15	15	COOH	NH2
230	MMA	A-H	DEAEMA	70	10	20	COOH	NH2
231	MMA	A-H	DEAEA	70	20	10	COOH	NH2
232	MMA	A-H	DEAEA	70	15	15	COOH	NH2
233	MMA	A-H	DEAEA	70	10	20	COOH	NH2
234	MMA	MA-H	DEAEMA	70	20	10	COOH	NH2
235	MMA	MA-H	DEAEMA	70	15	15	COOH	NH2
236	MMA	MA-H	DEAEMA	70	10	20	COOH	NH2
237	MMA	MA-H	DEAEA	70	20	10	COOH	NH2
238	MMA	MA-H	DEAEA	70	15	15	COOH	NH2
239	MMA	MA-H	DEAEA	70	10	20	COOH	NH2
240	MEMA	A-H	DEAEMA	70	20	10	COOH	NH2

241	MEMA	A-H	DEAEMA	70	15	15	COOH	NH2
242	MEMA	A-H	DEAEMA	70	10	20	COOH	NH2
243	MEMA	A-H	DEAEA	70	20	10	COOH	NH2
244	MEMA	A-H	DEAEA	70	15	15	COOH	NH2
245	MEMA	A-H	DEAEA	70	10	20	COOH	NH2
246	MEMA	MA-H	DEAEMA	70	20	10	COOH	NH2
247	MEMA	MA-H	DEAEMA	70	15	15	COOH	NH2
248	MEMA	MA-H	DEAEMA	70	10	20	COOH	NH2
249	MEMA	MA-H	DEAEA	70	20	10	COOH	NH2
250	MEMA	MA-H	DEAEA	70	15	15	COOH	NH2
251	MEMA	MA-H	DEAEA	70	10	20	COOH	NH2
252	MEMA	GMA	-	90	10	-	Epoxy	-
253	MEMA	GMA	-	70	30	-	Epoxy	-
254	MEMA	GMA	-	50	50	-	Epoxy	-
255	MEMA	GMA	DnBA	90	10	-	OH	NH2
256	MEMA	GMA	DnBA	70	30	-	OH	NH2
257	MEMA	GMA	DnBA	50	50	-	OH	NH2
258	MEMA	GMA	DnHA	90	10	-	OH	NH2
259	MEMA	GMA	DnHA	70	30	-	OH	NH2
260	MEMA	GMA	DnHA	50	50	-	OH	NH2
261	MEMA	GMA	DcHA	90	10	-	OH	NH2
262	MEMA	GMA	DcHA	70	30	-	OH	NH2
263	MEMA	GMA	DcHA	50	50	-	OH	NH2
264	MEMA	GMA	DBnA	90	10	-	OH	NH2
265	MEMA	GMA	DBnA	70	30	-	OH	NH2
266	MEMA	GMA	DBnA	50	50	-	OH	NH2
267	MEMA	GMA	MnHA	90	10	-	OH	NH2

268	MEMA	GMA	MnHA	70	30	-	OH	NH2
269	MEMA	GMA	MnHA	50	50	-	OH	NH2
270	MEMA	GMA	cHMA	90	10	-	OH	NH2
271	MEMA	GMA	cHMA	70	30	-	OH	NH2
272	MEMA	GMA	cHMA	50	50	-	OH	NH2
273	MEMA	GMA	BnMA	90	10	-	OH	NH2
274	MEMA	GMA	BnMA	70	30	-	OH	NH2
275	MEMA	GMA	BnMA	50	50	-	OH	NH2
276	MEMA	GMA	MAEPy	90	10	-	OH	NH2
277	MEMA	GMA	MAEPy	70	30	-	OH	NH2
278	MEMA	GMA	MAEPy	50	50	-	OH	NH2
279	MEMA	GMA	Pyrl	90	10	-	OH	NH2
280	MEMA	GMA	Pyrl	70	30	-	OH	NH2
281	MEMA	GMA	Pyrl	50	50	-	OH	NH2
282	MEMA	GMA	2-MAPy	90	10	-	OH	NH2
283	MEMA	GMA	2-MAPy	70	30	-	OH	NH2
284	MEMA	GMA	2-MAPy	50	50	-	OH	NH2
285	MEMA	GMA	MAn	90	10	-	OH	NH2
286	MEMA	GMA	MAn	70	30	-	OH	NH2
287	MEMA	GMA	MAn	50	50	-	OH	NH2
288	MEMA	GMA	TMEDA	90	10	-	OH	NH2
289	MEMA	GMA	TMEDA	70	30	-	OH	NH2
290	MEMA	GMA	TMEDA	50	50	-	OH	NH2
291	MEMA	GMA	DEMEDA	90	10	-	OH	NH2
292	MEMA	GMA	DEMEDA	70	30	-	OH	NH2
293	MEMA	GMA	DEMEDA	50	50	-	OH	NH2
294	MEMA	GMA	TMPDA	90	10	-	OH	NH2

295	MEMA	GMA	TMPDA	70	30	-	OH	NH2
296	MEMA	GMA	TMPDA	50	50	-	OH	NH2
297	MEMA	GMA	Mpi	90	10	-	OH	NH2
298	MEMA	GMA	Mpi	70	30	-	OH	NH2
299	MEMA	GMA	Mpi	50	50	-	OH	NH2
300	MEMA	GMA	TEDETA	90	10	-	OH	NH2
301	MEMA	GMA	TEDETA	70	30	-	OH	NH2
302	MEMA	GMA	TEDETA	50	50	-	OH	NH2
303	MMA	GMA	-	90	10	-	Epoxy	-
304	MMA	GMA	-	70	30	-	Epoxy	-
305	MMA	GMA	-	50	50	-	Epoxy	-
306	MMA	GMA	DnBA	90	10	-	OH	NH2
307	MMA	GMA	DnBA	70	30	-	OH	NH2
308	MMA	GMA	DnBA	50	50	-	OH	NH2
309	MMA	GMA	DnHA	90	10	-	OH	NH2
310	MMA	GMA	DnHA	70	30	-	OH	NH2
311	MMA	GMA	DnHA	50	50	-	OH	NH2
312	MMA	GMA	DcHA	90	10	-	OH	NH2
313	MMA	GMA	DcHA	70	30	-	OH	NH2
314	MMA	GMA	DcHA	50	50	-	OH	NH2
315	MMA	GMA	DBnA	90	10	-	OH	NH2
316	MMA	GMA	DBnA	70	30	-	OH	NH2
317	MMA	GMA	DBnA	50	50	-	OH	NH2
318	MMA	GMA	MnHA	90	10	-	OH	NH2
319	MMA	GMA	MnHA	70	30	-	OH	NH2
320	MMA	GMA	MnHA	50	50	-	OH	NH2
321	MMA	GMA	cHMA	90	10	-	OH	NH2

322	MMA	GMA	cHMA	70	30	-	OH	NH2
323	MMA	GMA	cHMA	50	50	-	OH	NH2
324	MMA	GMA	BnMA	90	10	-	OH	NH2
325	MMA	GMA	BnMA	70	30	-	OH	NH2
326	MMA	GMA	BnMA	50	50	-	OH	NH2
327	MMA	GMA	MAEPy	90	10	-	OH	NH2
328	MMA	GMA	MAEPy	70	30	-	OH	NH2
329	MMA	GMA	MAEPy	50	50	-	OH	NH2
330	MMA	GMA	Pyrlc	90	10	-	OH	NH2
331	MMA	GMA	Pyrlc	70	30	-	OH	NH2
332	MMA	GMA	Pyrlc	50	50	-	OH	NH2
333	MMA	GMA	2-MAPy	90	10	-	OH	NH2
334	MMA	GMA	2-MAPy	70	30	-	OH	NH2
335	MMA	GMA	2-MAPy	50	50	-	OH	NH2
336	MMA	GMA	MAn	90	10	-	OH	NH2
337	MMA	GMA	MAn	70	30	-	OH	NH2
338	MMA	GMA	MAn	50	50	-	OH	NH2
339	MMA	GMA	TMEDA	90	10	-	OH	NH2
340	MMA	GMA	TMEDA	70	30	-	OH	NH2
341	MMA	GMA	TMEDA	50	50	-	OH	NH2
342	MMA	GMA	DEMEDA	90	10	-	OH	NH2
343	MMA	GMA	DEMEDA	70	30	-	OH	NH2
344	MMA	GMA	DEMEDA	50	50	-	OH	NH2
345	MMA	GMA	TMPDA	90	10	-	OH	NH2
346	MMA	GMA	TMPDA	70	30	-	OH	NH2
347	MMA	GMA	TMPDA	50	50	-	OH	NH2
348	MMA	GMA	Mpi	90	10	-	OH	NH2



349	MMA	GMA	Mpi	70	30	-	OH	NH2
350	MMA	GMA	Mpi	50	50	-	OH	NH2
351	MMA	GMA	TEDETA	90	10	-	OH	NH2
352	MMA	GMA	TEDETA	70	30	-	OH	NH2
353	MMA	GMA	TEDETA	50	50	-	OH	NH2
354	MMA	DEAEMA	-	90	10	-	NH2	-
355	MMA	DEAEMA	-	70	30	-	NH2	-
356	MMA	DEAEMA	-	50	50	-	NH2	-
357	MMA	DMAEMA	-	90	10	-	NH2	-
358	MMA	DMAEMA	-	70	30	-	NH2	-
359	MMA	DMAEMA	-	50	50	-	NH2	-
360	MMA	DEAEA	-	90	10	-	NH2	-
361	MMA	DEAEA	-	70	30	-	NH2	-
362	MMA	DEAEA	-	50	50	-	NH2	-
363	MMA	DMAEA	-	90	10	-	NH2	-
364	MMA	DMAEA	-	70	30	-	NH2	-
365	MMA	DMAEA	-	50	50	-	NH2	-
366	HPMA	DEAEMA	-	90	10	-	NH2	-
367	HPMA	DEAEMA	-	70	30	-	NH2	-
368	HPMA	DEAEMA	-	50	50	-	NH2	-
369	HPMA	DMAEMA	-	90	10	-	NH2	-
370	HPMA	DMAEMA	-	70	30	-	NH2	-
371	HPMA	DMAEMA	-	50	50	-	NH2	-
372	HPMA	DEAEA	-	90	10	-	NH2	-
373	HPMA	DEAEA	-	70	30	-	NH2	-
374	HPMA	DEAEA	-	50	50	-	NH2	-
375	HPMA	DMAEA	-	90	10	-	NH2	-

376	HPMA	DMAEA	-	70	30	-	NH2	-
377	HPMA	DMAEA	-	50	50	-	NH2	-
378	HBMA	DEAEMA	-	90	10	-	NH2	-
379	HBMA	DEAEMA	-	70	30	-	NH2	-
380	HBMA	DEAEMA	-	50	50	-	NH2	-
381	HBMA	DMAEMA	-	90	10	-	NH2	-
382	HBMA	DMAEMA	-	70	30	-	NH2	-
383	HBMA	DMAEMA	-	50	50	-	NH2	-
384	HBMA	DEAEA	-	90	10	-	NH2	-
385	HBMA	DEAEA	-	70	30	-	NH2	-
386	HBMA	DEAEA	-	50	50	-	NH2	-
387	HBMA	DMAEA	-	90	10	-	NH2	-
388	HBMA	DMAEA	-	70	30	-	NH2	-
389	HBMA	DMAEA	-	50	50	-	NH2	-
390	EMA	DEAEMA	-	90	10	-	NH2	-
391	EMA	DEAEMA	-	70	30	-	NH2	-
392	EMA	DEAEMA	-	50	50	-	NH2	-
393	EMA	DMAEMA	-	90	10	-	NH2	-
394	EMA	DMAEMA	-	70	30	-	NH2	-
395	EMA	DMAEMA	-	50	50	-	NH2	-
396	EMA	DEAEA	-	90	10	-	NH2	-
397	EMA	DEAEA	-	70	30	-	NH2	-
398	EMA	DEAEA	-	50	50	-	NH2	-
399	EMA	DMAEA	-	90	10	-	NH2	-
400	EMA	DMAEA	-	70	30	-	NH2	-
401	EMA	DMAEA	-	50	50	-	NH2	-
402	BMA	DEAEMA	-	90	10	-	NH2	-

403	BMA	DEAEMA	-	70	30	-	NH2	-
404	BMA	DEAEMA	-	50	50	-	NH2	-
405	BMA	DMAEMA	-	90	10	-	NH2	-
406	BMA	DMAEMA	-	70	30	-	NH2	-
407	BMA	DMAEMA	-	50	50	-	NH2	-
408	BMA	DEAEA	-	90	10	-	NH2	-
409	BMA	DEAEA	-	70	30	-	NH2	-
410	BMA	DEAEA	-	50	50	-	NH2	-
411	BMA	DMAEA	-	90	10	-	NH2	-
412	BMA	DMAEA	-	70	30	-	NH2	-
413	BMA	DMAEA	-	50	50	-	NH2	-
414	MEMA	DEAEMA	MA	40	30	30	NH2	MA
415	MEMA	DEAEMA	MA	60	10	30	NH2	MA
416	MEMA	DEAEMA	MA	60	30	10	NH2	MA
417	MEMA	DEAEMA	MA	80	10	10	NH2	MA
418	MEMA	DEAEA	MA	40	30	30	NH2	MA
419	MEMA	DEAEA	MA	60	10	30	NH2	MA
420	MEMA	DEAEA	MA	60	30	10	NH2	MA
421	MEMA	DEAEA	MA	80	10	10	NH2	MA
422	MEMA	DEAEMA	BMA	40	30	30	NH2	BMA
423	MEMA	DEAEMA	BMA	60	10	30	NH2	BMA
424	MEMA	DEAEMA	BMA	60	30	10	NH2	BMA
425	MEMA	DEAEMA	BMA	80	10	10	NH2	BMA
426	MEMA	DEAEA	BMA	40	30	30	NH2	BMA
427	MEMA	DEAEA	BMA	60	10	30	NH2	BMA
428	MEMA	DEAEA	BMA	60	30	10	NH2	BMA
429	MEMA	DEAEA	BMA	80	10	10	NH2	BMA

430	MEMA	DEAEMA	MEA	40	30	30	NH2	MEA
431	MEMA	DEAEMA	MEA	60	10	30	NH2	MEA
432	MEMA	DEAEMA	MEA	60	30	10	NH2	MEA
433	MEMA	DEAEMA	MEA	80	10	10	NH2	MEA
434	MEMA	DEAEA	MEA	40	30	30	NH2	MEA
435	MEMA	DEAEA	MEA	60	10	30	NH2	MEA
436	MEMA	DEAEA	MEA	60	30	10	NH2	MEA
437	MEMA	DEAEA	MEA	80	10	10	NH2	MEA
438	MEMA	DEAEMA	DEGMEMA	40	30	30	NH2	DEGMEMA
439	MEMA	DEAEMA	DEGMEMA	60	10	30	NH2	DEGMEMA
440	MEMA	DEAEMA	DEGMEMA	60	30	10	NH2	DEGMEMA
441	MEMA	DEAEMA	DEGMEMA	80	10	10	NH2	DEGMEMA
442	MEMA	DEAEA	DEGMEMA	40	30	30	NH2	DEGMEMA
443	MEMA	DEAEA	DEGMEMA	60	10	30	NH2	DEGMEMA
444	MEMA	DEAEA	DEGMEMA	60	30	10	NH2	DEGMEMA
445	MEMA	DEAEA	DEGMEMA	80	10	10	NH2	DEGMEMA
446	MEMA	DEAEMA	THFFA	40	30	30	NH2	THFFA
447	MEMA	DEAEMA	THFFA	60	10	30	NH2	THFFA
448	MEMA	DEAEMA	THFFA	60	30	10	NH2	THFFA
449	MEMA	DEAEMA	THFFA	80	10	10	NH2	THFFA
450	MEMA	DEAEA	THFFA	40	30	30	NH2	THFFA
451	MEMA	DEAEA	THFFA	60	10	30	NH2	THFFA
452	MEMA	DEAEA	THFFA	60	30	10	NH2	THFFA
453	MEMA	DEAEA	THFFA	80	10	10	NH2	THFFA
454	MEMA	DEAEMA	THFFMA	40	30	30	NH2	THFFMA
455	MEMA	DEAEMA	THFFMA	60	10	30	NH2	THFFMA
456	MEMA	DEAEMA	THFFMA	60	30	10	NH2	THFFMA

457	MEMA	DEAEMA	THFFMA	80	10	10	NH2	THFFMA
458	MEMA	DEAEA	THFFMA	40	30	30	NH2	THFFMA
459	MEMA	DEAEA	THFFMA	60	10	30	NH2	THFFMA
460	MEMA	DEAEA	THFFMA	60	30	10	NH2	THFFMA
461	MEMA	DEAEA	THFFMA	80	10	10	NH2	THFFMA
462	MEMA	DEAEMA	HEA	40	30	30	NH2	HEA
463	MEMA	DEAEMA	HEA	60	10	30	NH2	HEA
464	MEMA	DEAEMA	HEA	60	30	10	NH2	HEA
465	MEMA	DEAEMA	HEA	80	10	10	NH2	HEA
466	MEMA	DEAEA	HEA	40	30	30	NH2	HEA
467	MEMA	DEAEA	HEA	60	10	30	NH2	HEA
468	MEMA	DEAEA	HEA	60	30	10	NH2	HEA
469	MEMA	DEAEA	HEA	80	10	10	NH2	HEA
470	MEMA	DEAEMA	HEMA	40	30	30	NH2	OH
471	MEMA	DEAEMA	HEMA	60	10	30	NH2	OH
472	MEMA	DEAEMA	HEMA	60	30	10	NH2	OH
473	MEMA	DEAEMA	HEMA	80	10	10	NH2	OH
474	MEMA	DEAEA	HEMA	40	30	30	NH2	OH
475	MEMA	DEAEA	HEMA	60	10	30	NH2	OH
476	MEMA	DEAEA	HEMA	60	30	10	NH2	OH
477	MEMA	DEAEA	HEMA	80	10	10	NH2	OH
478	MEMA	DEAEMA	A-H	40	30	30	NH2	COOH
479	MEMA	DEAEMA	A-H	60	10	30	NH2	COOH
480	MEMA	DEAEMA	A-H	60	30	10	NH2	COOH
481	MEMA	DEAEMA	A-H	80	10	10	NH2	COOH
482	MEMA	DEAEA	A-H	40	30	30	NH2	COOH
483	MEMA	DEAEA	A-H	60	10	30	NH2	COOH

484	MEMA	DEAEA	A-H	60	30	10	NH <sub>2</sub>	COOH
485	MEMA	DEAEA	A-H	80	10	10	NH <sub>2</sub>	COOH
486	MEMA	DEAEMA	MA-H	40	30	30	NH <sub>2</sub>	COOH
487	MEMA	DEAEMA	MA-H	60	10	30	NH <sub>2</sub>	COOH
488	MEMA	DEAEMA	MA-H	60	30	10	NH <sub>2</sub>	COOH
489	MEMA	DEAEMA	MA-H	80	10	10	NH <sub>2</sub>	COOH
490	MEMA	DEAEA	MA-H	40	30	30	NH <sub>2</sub>	COOH
491	MEMA	DEAEA	MA-H	60	10	30	NH <sub>2</sub>	COOH
492	MEMA	DEAEA	MA-H	60	30	10	NH <sub>2</sub>	COOH
493	MEMA	DEAEA	MA-H	80	10	10	NH <sub>2</sub>	COOH
494	MEMA	DEAEMA	DMAA	40	30	30	NH <sub>2</sub>	CON
495	MEMA	DEAEMA	DMAA	60	10	30	NH <sub>2</sub>	CON
496	MEMA	DEAEMA	DMAA	60	30	10	NH <sub>2</sub>	CON
497	MEMA	DEAEMA	DMAA	80	10	10	NH <sub>2</sub>	CON
498	MEMA	DEAEA	DMAA	40	30	30	NH <sub>2</sub>	CON
499	MEMA	DEAEA	DMAA	60	10	30	NH <sub>2</sub>	CON
500	MEMA	DEAEA	DMAA	60	30	10	NH <sub>2</sub>	CON
501	MEMA	DEAEA	DMAA	80	10	10	NH <sub>2</sub>	CON
502	MEMA	DEAEMA	DAAA	40	30	30	NH <sub>2</sub>	CON
503	MEMA	DEAEMA	DAAA	60	10	30	NH <sub>2</sub>	CON
504	MEMA	DEAEMA	DAAA	60	30	10	NH <sub>2</sub>	CON
505	MEMA	DEAEMA	DAAA	80	10	10	NH <sub>2</sub>	CON
506	MEMA	DEAEA	DAAA	40	30	30	NH <sub>2</sub>	CON
507	MEMA	DEAEA	DAAA	60	10	30	NH <sub>2</sub>	CON
508	MEMA	DEAEA	DAAA	60	30	10	NH <sub>2</sub>	CON
509	MEMA	DEAEA	DAAA	80	10	10	NH <sub>2</sub>	CON
510	MEMA	DEAEMA	MMA	40	30	30	NH <sub>2</sub>	CH <sub>3</sub>

511	MEMA	DEAEMA	MMA	60	10	30	NH2	CH <sub>3</sub>
512	MEMA	DEAEMA	MMA	60	30	10	NH2	CH <sub>3</sub>
513	MEMA	DEAEMA	MMA	80	10	10	NH2	CH <sub>3</sub>
514	MEMA	DEAEA	MMA	40	30	30	NH2	CH <sub>3</sub>
515	MEMA	DEAEA	MMA	60	10	30	NH2	CH <sub>3</sub>
516	MEMA	DEAEA	MMA	60	30	10	NH2	CH <sub>3</sub>
517	MEMA	DEAEA	MMA	80	10	10	NH2	CH <sub>3</sub>
518	MEMA	DEAEMA	St	40	30	30	NH2	Aromatic
519	MEMA	DEAEMA	St	60	10	30	NH2	Aromatic
520	MEMA	DEAEMA	St	60	30	10	NH2	Aromatic
521	MEMA	DEAEMA	St	80	10	10	NH2	Aromatic
522	MEMA	DEAEA	St	40	30	30	NH2	Aromatic
523	MEMA	DEAEA	St	60	10	30	NH2	Aromatic
524	MEMA	DEAEA	St	60	30	10	NH2	Aromatic
525	MEMA	DEAEMA	-	85	15	-	NH2	-
526	MEMA	DEAEMA	-	80	20	-	NH2	-
527	MEMA	DEAEMA	-	75	25	-	NH2	-
528	MEMA	DEAEMA	-	70	30	-	NH2	-
529	MEMA	DEAEMA	-	65	35	-	NH2	-
530	MEMA	DEAEMA	-	60	40	-	NH2	-
531	MEMA	DEAEMA	-	55	45	-	NH2	-
532	MEMA	A-H	DEAEMA	85	5	10	COOH	NH2
533	MEMA	A-H	DEAEMA	80	5	15	COOH	NH2
534	MEMA	A-H	DEAEMA	75	5	20	COOH	NH2
535	MEMA	A-H	DEAEMA	70	5	25	COOH	NH2
536	MEMA	A-H	DEAEMA	65	5	30	COOH	NH2
537	MEMA	A-H	DEAEMA	60	5	35	COOH	NH2

538	MEMA	A-H	DEAEMA	55	5	40	COOH	NH2
539	MEMA	A-H	DEAEMA	50	5	45	COOH	NH2
540	MEMA	A-H	DEAEMA	75	10	15	COOH	NH2
541	MEMA	A-H	DEAEMA	70	10	20	COOH	NH2
542	MEMA	A-H	DEAEMA	65	10	25	COOH	NH2
543	MEMA	A-H	DEAEMA	55	10	35	COOH	NH2
544	MEMA	A-H	DEAEMA	50	10	40	COOH	NH2
545	MEMA	A-H	DEAEMA	65	15	20	COOH	NH2
546	MEMA	A-H	DEAEMA	60	15	25	COOH	NH2
547	MEMA	A-H	DEAEMA	55	15	30	COOH	NH2
548	MEMA	A-H	DEAEMA	50	15	35	COOH	NH2
549	MEMA	A-H	DEAEMA	55	20	25	COOH	NH2
550	MEMA	A-H	DEAEMA	50	20	30	COOH	NH2
551	MEMA	A-H	DEAEMA	90	5	5	COOH	NH2
552	MEMA	A-H	DEAEMA	80	15	5	COOH	NH2
553	MEMA	A-H	DEAEMA	70	25	5	COOH	NH2
554	MEMA	A-H	DEAEMA	60	35	5	COOH	NH2
555	MEMA	A-H	DEAEMA	50	45	5	COOH	NH2
556	MEMA	A-H	DEAEMA	50	40	10	COOH	NH2
557	MEMA	A-H	DEAEMA	60	25	15	COOH	NH2
558	MEMA	A-H	DEAEMA	50	35	15	COOH	NH2
559	MEMA	A-H	DEAEMA	60	20	20	COOH	NH2
560	MEMA	A-H	DEAEMA	50	30	20	COOH	NH2
561	MEMA	A-H	DEAEMA	50	25	25	COOH	NH2



## Polyurethane Library

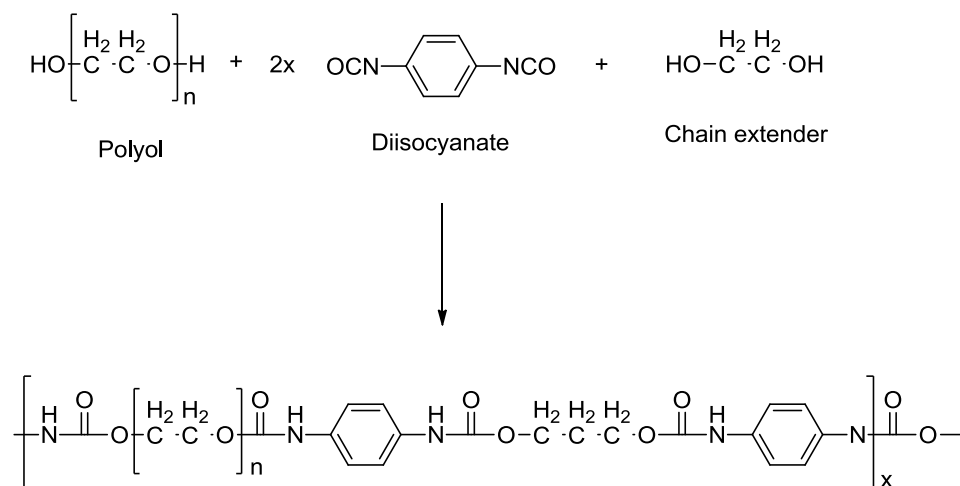


**Figure 5:** Synthesis scheme for polyurethanes.

### Monomer Abbreviations:

#### Polyol:

Peg	poly(ethylene glycol)
PPG	poly(propylene glycol)
PTMG	poly(tetramethylene glycol)
PHNAD	poly[1,6-hexanediol/neopentyl glycol-alt-adipic acid] diol
PHNGAD	poly[1,6-hexanediol/neopentyl glycol/diethylene glycol-alt-adipic acid] diol

#### Diisocyanate (Dis):

BICH	1,3-bis(isocyanatomethyl)cyclohexane
MDI	4,4'-methylenebis(phenylisocyanate)
HDI	1,6-diisocyanohexane
HMDI	4,4'-methylenebis(cyclohexylisocyanate)

PDI	1,4-diisocyanobenzene
TDI	4-methyl-1,3-phenylene diisocyanate

**Chain Extender (Ext.):**

ED	ethylene diamine
BD	1,4-butanediol
EG	ethylene glycol
PG	propylene glycol
DMAPD	3-dimethylamino-1,2-propanediol
DEAPD	3-diethylamino-1,2-propanediol
DHM	diethyl bis(hydroxymethyl)malonate
NMPD	2-nitro-2-methyl-1,3-propanediol
OFHD	2,2,3,3,4,4,5,5-octafluoro-1,6-hexanediol

**Table 2:** List of polyurethanes in the polyurethane library used.

Polyurethane ID number	Polymer structure				Monomer Ratios [mol]	
	Diol	Mn	DIS	Extender	M 1	M 2
1	PEG	2000	HDI	-	48,5	51,5
1	PEG	2000	HDI	-	48,5	51,5
2	PEG	900	HDI	-	48,5	51,5
3	PEG	400	HDI	-	48,5	51,5
4	PPG	2000	HDI	-	48,5	51,5
5	PTMG	2000	HDI	-	48,5	51,5
5	PTMG	2000	HDI	-	48,5	51,5
6	PEG	2000	BICH	-	48,5	51,5
7	PEG	900	BICH	-	48,5	51,5
8	PEG	400	BICH	-	48,5	51,5
8	PEG	400	BICH	-	48,5	51,5
8	PEG	400	BICH	-	48,5	51,5
9	PPG	2000	BICH	-	48,5	51,5
10	PTMG	2000	BICH	-	48,5	51,5
11	PEG	2000	TDI	-	48,5	51,5
12	PEG	900	TDI	-	48,5	51,5
13	PEG	400	TDI	-	48,5	51,5
13	PEG	400	TDI	-	48,5	51,5
14	PPG	2000	TDI	-	48,5	51,5
15	PTMG	2000	TDI	-	48,5	51,5
15	PTMG	2000	TDI	-	48,5	51,5
16	PEG	2000	MDI	-	48,5	51,5
17	PEG	900	MDI	-	48,5	51,5
18	PEG	400	MDI	-	48,5	51,5

18	PEG	400	MDI	-	48,5	51,5
18	PEG	400	MDI	-	48,5	51,5
19	PPG	2000	MDI	-	48,5	51,5
19	PPG	2000	MDI	-	48,5	51,5
20	PTMG	2000	MDI	-	48,5	51,5
20	PTMG	2000	MDI	-	48,5	51,5
21	PEG	2000	PDI	-	48,5	51,5
22	PEG	900	PDI	-	48,5	51,5
23	PEG	400	PDI	-	48,5	51,5
24	PPG	2000	PDI	-	48,5	51,5
25	PTMG	2000	PDI	-	48,5	51,5
26	PEG	2000	HMDI	-	48,5	51,5
26	PEG	2000	HMDI	-	48,5	51,5
27	PEG	900	HMDI	-	48,5	51,5
28	PEG	400	HMDI	-	48,5	51,5
29	PPG	2000	HMDI	-	48,5	51,5
30	PTMG	2000	HMDI	-	48,5	51,5
31	PEG	2000	HDI	BD	0,25	0,52
33	PEG	900	HDI	BD	0,25	0,52
35	PEG	400	HDI	BD	0,25	0,52
37	PPG	2000	HDI	BD	0,25	0,52
38	PPG	2000	HDI	ED	0,25	0,52
39	PTMG	2000	HDI	BD	0,25	0,52
40	PTMG	2000	HDI	ED	0,25	0,52
41	PEG	2000	BICH	BD	0,25	0,52
43	PEG	900	BICH	BD	0,25	0,52
44	PEG	900	BICH	ED	0,25	0,52

45	PEG	400	BICH	BD	0,25	0,52
46	PEG	400	BICH	ED	0,25	0,52
47	PPG	2000	BICH	BD	0,25	0,52
48	PPG	2000	BICH	ED	0,25	0,52
49	PTMG	2000	BICH	BD	0,25	0,52
49	PTMG	2000	BICH	BD	0,25	0,52
50	PTMG	2000	BICH	ED	0,25	0,52
51	PEG	2000	TDI	BD	0,25	0,52
53	PEG	900	TDI	BD	0,25	0,52
55	PEG	400	TDI	BD	0,25	0,52
57	PPG	2000	TDI	BD	0,25	0,52
59	PTMG	2000	TDI	BD	0,25	0,52
61	PEG	2000	MDI	BD	0,25	0,52
63	PEG	900	MDI	BD	0,25	0,52
65	PEG	400	MDI	BD	0,25	0,52
67	PPG	2000	MDI	BD	0,25	0,52
69	PTMG	2000	MDI	BD	0,25	0,52
71	PEG	2000	PDI	BD	0,25	0,52
73	PEG	900	PDI	BD	0,25	0,52
77	PPG	2000	PDI	BD	0,25	0,52
79	PTMG	2000	PDI	BD	0,25	0,52
81	PEG	2000	HMDI	BD	0,25	0,52
83	PEG	900	HMDI	BD	0,25	0,52
85	PEG	400	HMDI	BD	0,25	0,52
87	PPG	2000	HMDI	BD	0,25	0,52
87	PPG	2000	HMDI	BD	0,25	0,52
89	PTMG	2000	HMDI	BD	0,25	0,52

39DE	PTMG	2000	HDI	DEAPD	0,25	0,52
39DM	PTMG	2000	HDI	DMAPD	0,25	0,52
49DM	PTMG	2000	BICH	DMAPD	0,25	0,52
49DE	PTMG	2000	BICH	DEAPD	0,25	0,52
91	PTMG	650	HDI	BD	0,485	0,515
92	PTMG	1000	HDI	BD	0,485	0,515
93	PTMG	650	BICH	BD	0,485	0,515
94	PTMG	1000	BICH	BD	0,485	0,515
94	PTMG	1000	BICH	BD	0,485	0,515
95	PTMG	650	MDI	BD	0,485	0,515
95	PTMG	650	MDI	BD	0,485	0,515
96	PTMG	1000	MDI	BD	0,485	0,515
97	PHNGAD	1800	BICH	DMAPD	0,25	0,52
98	PHNGAD	1800	BICH	DEAPD	0,25	0,52
99	PTMG	650	HDI	DMAPD	0,25	0,52
100	PTMG	1000	HDI	DMAPD	0,25	0,52
100	PTMG	1000	HDI	DMAPD	0,25	0,52
101	PTMG	650	BICH	DMAPD	0,25	0,52
102	PTMG	1000	BICH	DMAPD	0,25	0,52
102	PTMG	1000	BICH	DMAPD	0,25	0,52
103	PHNGAD	1800	MDI	DMAPD	0,25	0,52
103	PHNGAD	1800	MDI	DMAPD	0,25	0,52
104	PHNGAD	1800	MDI	DEAPD	0,25	0,52
104	PHNGAD	1800	MDI	DEAPD	0,25	0,52
105	PHNGAD	1800	HDI	DMAPD	0,25	0,52
105	PHNGAD	1800	HDI	DMAPD	0,25	0,52
106	PHNGAD	1800	HDI	DEAPD	0,25	0,52

107	PTMG	650	HDI	DEAPD	0,25	0,52
108	PTMG	1000	HDI	DEAPD	0,25	0,52
109	PTMG	650	BICH	DEAPD	0,25	0,52
110	PTMG	1000	BICH	DEAPD	0,25	0,52
111	PTMG	650	MDI	DEAPD	0,25	0,52
112	PTMG	1000	MDI	DEAPD	0,25	0,52
113	PTMG	2000	MDI	DEAPD	0,25	0,52
114	PPG	425	HDI	BD	0,485	0,515
115	PPG	1000	HDI	BD	0,485	0,515
116	PPG	425	BICH	BD	0,485	0,515
117	PPG	1000	BICH	BD	0,485	0,515
118	PPG	425	MDI	DMAPD	0,25	0,52
118	PPG	425	MDI	DMAPD	0,25	0,52
119	PPG	1000	MDI	DMAPD	0,25	0,52
120	PPG	425	BICH	DEAPD	0,25	0,52
121	PPG	1000	BICH	DEAPD	0,25	0,52
122	PPG	2000	BICH	DEAPD	0,25	0,52
123	PPG	2000	MDI	DMAPD	0,25	0,52
123	PPG	2000	MDI	DMAPD	0,25	0,52
124	PPG	2000	TDI	DMAPD	0,25	0,52
125	PPG	1000	TDI	DMAPD	0,25	0,52
125	PPG	1000	TDI	DMAPD	0,25	0,52
126	PPG	425	TDI	DMAPD	0,25	0,52
127	PPG	1000	BICH	DMAPD	0,25	0,52
128	PPG	2000	BICH	DMAPD	0,25	0,52
129	PPG	425	BICH	DMAPD	0,25	0,52
130	PTMG	650	TDI	DMAPD	0,25	0,52

131	PTMG	1000	TDI	DMAPD	0,25	0,52
132	PHNGAD	1800	BICH	BD	0,25	0,52
132	PHNGAD	1800	BICH	BD	0,25	0,52
133	PHNGAD	1800	HDI	BD	0,25	0,52
134	PHNGAD	1800	MDI	BD	0,25	0,52
134	PHNGAD	1800	MDI	BD	0,25	0,52
135	PTMG	250	BICH	DMAPD	0,25	0,52
136	PTMG	250	BICH	DEAPD	0,25	0,52
137	PTMG	250	BICH	BD	0,25	0,52
138	PTMG	250	BICH	EG	0,25	0,52
139	PTMG	650	BICH	EG	0,25	0,52
140	PTMG	1000	BICH	EG	0,25	0,52
141	PTMG	2000	BICH	EG	0,25	0,52
142	PTMG	250	BICH	PG	0,25	0,52
143	PTMG	650	BICH	PG	0,25	0,52
144	PTMG	1000	BICH	PG	0,25	0,52
145	PTMG	2000	BICH	PG	0,25	0,52
146	PTMG	250	HDI	DMAPD	0,25	0,52
147	PTMG	250	HDI	DEAPD	0,25	0,52
148	PTMG	250	HDI	BD	0,25	0,52
149	PTMG	250	HDI	EG	0,25	0,52
150	PTMG	650	HDI	EG	0,25	0,52
151	PTMG	1000	HDI	EG	0,25	0,52
152	PTMG	2000	HDI	EG	0,25	0,52
153	PTMG	250	HDI	PG	0,25	0,52
154	PTMG	650	HDI	PG	0,25	0,52
155	PTMG	1000	HDI	PG	0,25	0,52



156	PTMG	2000	HDI	PG	0,25	0,52
157	PTMG	250	MDI	DMAPD	0,25	0,52
158	PTMG	250	MDI	OFHD	0,25	0,52
159	PTMG	250	MDI	BD	0,25	0,52
160	PTMG	250	MDI	EG	0,25	0,52
161	PTMG	650	MDI	EG	0,25	0,52
162	PTMG	1000	MDI	EG	0,25	0,52
163	PTMG	2000	MDI	EG	0,25	0,52
164	PTMG	250	MDI	PG	0,25	0,52
165	PTMG	650	MDI	PG	0,25	0,52
166	PTMG	1000	MDI	PG	0,25	0,52
167	PTMG	2000	MDI	PG	0,25	0,52
168	PTMG	250	BICH	none	48,5	51,5
169	PTMG	650	BICH	none	48,5	51,5
170	PTMG	1000	BICH	none	48,5	51,5
171	PTMG	250	HDI	none	48,5	51,5
172	PTMG	650	HDI	none	48,5	51,5
173	PTMG	1000	HDI	none	48,5	51,5
174	PTMG	250	MDI	none	48,5	51,5
175	PTMG	650	MDI	none	48,5	51,5
176	PTMG	1000	MDI	none	48,5	51,5
177	PTMG	250	HDI	NMPD	0,25	0,52
178	PTMG	1000	HDI	NMPD	0,25	0,52
179	PTMG	2000	HDI	NMPD	0,25	0,52
180	PTMG	1000	BICH	NMPD	0,25	0,52
181	PTMG	2000	BICH	NMPD	0,25	0,52
182	PTMG	650	MDI	NMPD	0,25	0,52

183	PTMG	1000	MDI	NMPD	0,25	0,52
184	PTMG	2000	MDI	NMPD	0,25	0,52
185	PHNAD	900	MDI	OFHD	0,17	0,52
185	PHNAD	900	MDI	OFHD	0,17	0,52
186	PTMG	650	BICH	OFHD	0,25	0,52
187	PTMG	1000	BICH	OFHD	0,25	0,52
188	PTMG	2000	BICH	OFHD	0,25	0,52
189	PPG	1000	BICH	OFHD	0,17	0,52
190	PTMG	650	HDI	OFHD	0,25	0,52
190	PTMG	650	HDI	OFHD	0,25	0,52
191	PTMG	1000	HDI	OFHD	0,25	0,52
192	PTMG	2000	HDI	OFHD	0,25	0,52
193	PPG	1000	MDI	DMAPD	0,17	0,52
194	PTMG	650	MDI	OFHD	0,25	0,52
195	PTMG	1000	MDI	OFHD	0,25	0,52
196	PTMG	2000	MDI	OFHD	0,25	0,52
197	PTMG	650	BICH	DHM	0,25	0,52
198	PTMG	1000	BICH	DHM	0,25	0,52
199	PTMG	2000	BICH	DHM	0,25	0,52
200	PTMG	650	HDI	DHM	0,25	0,52
201	PTMG	1000	HDI	DHM	0,25	0,52
202	PTMG	2000	HDI	DHM	0,25	0,52
203	PTMG	650	MDI	DHM	0,25	0,52
204	PTMG	1000	MDI	DHM	0,25	0,52
205	PTMG	2000	MDI	DHM	0,25	0,52
206	PPG	1000	HDI	OFHD	0,25	0,52
207	PPG	1000	BICH	OFHD	0,25	0,52

208	PPG	1000	MDI	OFHD	0,25	0,52
209	PPG	1000	HDI	PG	0,25	0,52
210	PPG	1000	BICH	PG	0,25	0,52
211	PPG	1000	MDI	PG	0,25	0,52
212	PHNAD	900	HDI	PG	0,25	0,52
213	PHNAD	900	BICH	PG	0,25	0,52
214	PHNAD	900	MDI	PG	0,25	0,52
215	PHNAD	900	HDI	BD	0,25	0,52
216	PHNAD	900	BICH	BD	0,25	0,52
217	PHNAD	900	MDI	BD	0,25	0,52
218	PHNAD	900	HDI	DMAPD	0,25	0,52
219	PHNAD	900	BICH	DMAPD	0,25	0,52
220	PHNAD	900	MDI	DMAPD	0,25	0,52
220	PHNAD	900	MDI	DMAPD	0,25	0,52
221	PHNAD	900	HDI	OFHD	0,25	0,52
222	PHNAD	900	BICH	OFHD	0,25	0,52
223	PHNAD	900	MDI	OFHD	0,25	0,52
223	PHNAD	900	MDI	OFHD	0,25	0,52
224	PHNAD	900	HDI	none	48,5	51,5
225	PHNAD	900	BICH	none	48,5	51,5
226	PHNAD	900	MDI	none	48,5	51,5
227	PPG-PEG	1900	HDI	none	48,5	51,5
228	PPG-PEG	1900	BICH	none	48,5	51,5
229	PPG-PEG	1900	MDI	none	48,5	51,5
230	PPG-PEG	1900	HDI	BD	0,25	0,52
231	PPG-PEG	1900	BICH	BD	0,25	0,52
231	PPG-PEG	1900	BICH	BD	0,25	0,52

232	PPG-PEG	1900	MDI	BD	0,25	0,52
233	PPG-PEG	1900	HDI	OFHD	0,25	0,52
234	PPG-PEG	1900	BICH	OFHD	0,25	0,52
235	PPG-PEG	1900	MDI	OFHD	0,25	0,52
236	PPG-PEG	1900	HDI	PG	0,25	0,52
237	PPG-PEG	1900	BICH	PG	0,25	0,52
238	PPG-PEG	1900	MDI	PG	0,25	0,52
239	PPG-PEG	1900	HDI	DMAPD	0,25	0,52
240	PPG-PEG	1900	BICH	DMAPD	0,25	0,52
241	PPG-PEG	1900	MDI	DMAPD	0,25	0,52
242	PPG-PEG	1900	HDI	EG	0,25	0,52
243	PPG-PEG	1900	BICH	EG	0,25	0,52
244	PPG-PEG	1900	MDI	EG	0,25	0,52
245	PHNGAD	1800	HDI	OFHD	0,25	0,52
246	PHNGAD	1800	BICH	OFHD	0,25	0,52
247	PHNGAD	1800	MDI	OFHD	0,25	0,52
248	PHNGAD	1800	BICH	DMAPD	0,25	0,52
249	PHNGAD	1800	HDI	none	48,5	51,5
250	PHNGAD	1800	BICH	none	48,5	51,5
251	PHNGAD	1800	MDI	none	48,5	51,5
252	PHNGAD	1800	HDI	DHM	0,25	0,52
253	PPG-PEG	1900	MDI	DMAPD	0,17	0,52
254	PHNGAD	1800	BICH	BD	0,17	0,52
255	PPG-PEG	1900	MDI	BD	0,17	0,52
256	PPG	425	MDI	none	48,5	51,5
256	PPG	425	MDI	none	48,5	51,5
257	PTMG	1000	BICH	DMAPD	0,17	0,52

258	PTMG	1000	BICH	OFHD	0,17	0,52
259	PTMG	2000	BICH	DMAPD	0,17	0,52
260	PTMG	2000	BICH	OFHD	0,17	0,52
261	PTMG	1000	BICH	BD	0,17	0,52
262	PTMG	2000	BICH	BD	0,17	0,52
263	PTMG	1000	HDI	OFHD	0,17	0,52
264	PTMG	1000	HDI	DMAPD	0,17	0,52
265	PPG-PEG	1900	BICH	OFHD	0,17	0,52
266	PPG-PEG	1900	BICH	DMAPD	0,17	0,52
267	PPG-PEG	1900	BICH	BD	0,17	0,52
268	PTMG	1000	MDI	DMAPD	0,25	0,52
269	PPG	2000	MDI	DEAPD	0,25	0,52
270	PTMG	2000	MDI	DMAPD	0,25	0,52
271	PEG	400	MDI	DMAPD	0,25	0,52
272	PEG	400	MDI	none	0,58	0,42
273	PPG	425	MDI	DMAPD	0,25	0,52
274	PPG	425	MDI	none	48,5	51,5
275	PEG	400	MDI	none	48,5	51,5
276	PTMG	1000	MDI	OFHD	0,17	0,52
277	PTMG	2000	MDI	OFHD	0,17	0,52
278	PPG-PEG	1900	MDI	OFHD	0,17	0,52

### ***Published Papers***

A. Hansen, L. McMillan, A. Morrison, J. Petrik, M. Bradley; Polymers for the rapid and effective activation and aggregation of platelets. *Biomaterials* **2011**, 32, 7034-7041.

A. Hansen, R. Zhang, M. Bradley; Fabrication of arrays of polymer gradients using inkjet printing. *Macromol. Rapid Commun.* **2012**, DOI: 10.1002/marc.201200193.

Reprint was granted by the publishers.

---